The University Of Sheffield.

INVESTIGATING THE MECHANISMS RESPONSIBLE FOR THE ANTI-TUMOUR EFFECT OF ZOLEDRONIC ACID IN MYELOMA IN VIVO

2009-10

Gurubalan Jayadevan

Prof. Peter Croucher

Dr. Michelle Anne Lawson

MPhil to PhD/MD Transfer Report
The Medical School

JAYADEVAN GURUBALAN

Project Title
Investigating the mechanisms responsible for the anti-tumour effect of zoledronic acid in multiple myeloma *in vivo*

Name of the Supervisor

Prof. Peter Croucher

Name of the Co-Supervisor

Dr. Michelle Anne Lawson

Approval to submit transfer report

Signature of the supervisor(s) indicating he/she has read and approves the submission of the transfer report

Statement of Probity

I confirm that I shall abide by the University of Sheffield's regulations on plagiarism and that all written work shall be my own and will not have been PLAGIARISED from other paper-based or electronic sources. Where used, material gathered from other sources will be clearly cited in the text.

Signature: Date: 4th Oct 2010

Name: Gurubalan Jayadevan

Acknowledgement

"No duty is more urgent than that of returning thanks"

-Unknown

In debt of gratitude: to my supervisor Prof. Peter Croucher and my co-supervisor Dr. Michelle Anne Lawson for giving me the opportunity to do a PhD under their guidance and support. I'm extremely thankful to Dr. Allan J Williams for his friendly help and advice throughout this work. A special thanks to Julia Hough for all the histology work. I would like to thank all my colleagues for welcoming and accepting me as one among their own for which I'm eternally grateful. I would like to thank my sponsor Novartis Pharma AG, Basel, Switzerland for funding this project and the University of Sheffield for the international student fee waiver.

Summary

Background: Multiple Myeloma is an incurable B lymphocyte malignancy characterised by the development of multiple osteolytic lesions. Alteration of the normal remodelling process by the tumour cell has been implicated in the pathogenesis of the bone lesions. Anti-resorptive agent like bisphosphonates has been shown to be effective in the treatment of myeloma bone disease. In addition, there is also increasing evidence of reduction in tumour burden in bone following zoledronic acid treatment. However, the mechanism responsible remains unclear. We hypothesise that blocking bone resorption with zoledronic acid will prevent colonisation of myeloma cells and stop activation of resident cells from developing into overt myeloma colonies. We aim to study the effects of inhibition of osteoclastic resorption by zoledronic acid, on the early events of colonisation and survival of the myeloma cell in the bone marrow microenvironment by using Multiphoton Microscopy. This technique will help to identify and measure individual tumour cell as they arrive and colonise the bone.

Methods: C57BL/KaLwRij mice were pre-treated with zoledronic acid one week prior to 5T33MM-GFP cell injection and sacrificed after 18 hr, 72 hr and 4 week. MicroCT, ELISA for bone markers and static bone histomorphometry was used to assess the effect of zoledronic acid on inhibition of bone resorption. Individual GFP positive tumour cells in bone were identified by Zeiss 510 META Multiphoton microscope and quantified using Volocity software.

Results: Treatment with zoledronic acid was associated with reduction in biochemical markers of bone turnover and decrease in osteoclast no. and surface occupancy on the trabecular bone and the consequence was an increase in bone volume. Secondly, there was no significant difference in the number of GFP positive tumour cell in the femur between the mice treated with zoledronic acid and the untreated control after 18hrs of tumour cell injection.

Discussion & Conclusion: Zoledronic acid treatment in 5T33MM models showed effective suppression of osteoclastic bone resorption after 7 days following treatment. Multiphoton microscopy has the ability to identify individual GFP positive tumour cell in the proximal tibial metaphysis. Treatment with zoledronic acid 1 week prior to tumour cell injection did not show any significant reduction in the number of myeloma cells colonising the tibia 18 hr after tumour cell injection in 5T33MM model. Although 1 week post treatment regimen with clinical dose of zoledronic acid was effective in inhibiting osteoclastic bone resorption, it was not sufficient to inhibit the homing of myeloma tumour cell to the femur. Further studies are required to look into longer timepoints and larger study group for a better understanding on the effect of osteoclastic bone resorption in myeloma cell homing to bone.

Table of Contents

List of Figures

List of Abbreviation

BM	Bone Marrow
BMD	Bone Mineral Density
BMEC	Bone Marrow Endothelial Cell
BMM	Bone Marrow Microenvironment
BMP	Bone Morphogenetic Protein
BMSC	Bone Marrow Stromal Cell
BV/TV	Percentage Bone Volume
CAM	Cell Adhesion Molecule
Ct. V	Cortical Volume
CTX	Carboxy Terminal Telopeptide
CXCL12	Chemokine (C-X-C motif) Ligand 12/Stromal-Cell Derived Factor 1
CXCR4	Chemokine (C-X-C motif) Receptor Type 4
DKK	Dickkopf
Ec	Endocortical
EDTA	Ethylenediaminetetracetic Acid
ELISA	Enzyme Linked Immunosorbent Assay
GC	Germinal Center
GFP	Green Fluorescent Protein
HGF	Hepatocyte Growth Factor
HUVEC	Human Umbilical Vascular Endothelial Cell
IGF	Insulin like Growth Factor
IL	Interleukin
IMS	Industrial Methylated Spirit
JK	Janus Kinase
MAPK	Mitogen-activated protein kinase
MCP	Monocyte Chemoattractant Protein
M-CSF	Macrophage Colony Stimulating Factor
MGUS	Monoclonal Gammopathy of Undetermined Significance
MIP	Macrophage Inflammatory Protein
MM	Multiple Myeloma
N. Ob	Number of Osteoblast
N. Oc	Number of Osteoclast
N.Oc/Ec.Pm	No. of Osteoclast per mm of endocortical bone
N.Oc/Trab.Pm	No. of Osteoclast per mm of trabecular bone

NF-κB	Nuclear Factor Kappa B
NPT	Sodium Dependant Phosphate Transporter
NZM Mice	New Zealand Mixed Mice
OAF	Osteoclast Activating Factor
OB	Osteoblast
OC	Osteoclast
OCT	Optimal Cutting Temperature
ODF	Osteoclast Differentiation Factor
OPG	Osteoprotegerin
PBS	Phosphate Buffered Saline
PDGF	Platelet Derived Growth Factor
PI-3 K	Phosphatidylinositol-3 Kinase
PINP	Procollagen I N-Terminal Peptide
RANK	Receptor for Activation of Nuclear Factor Kappa B
RANKL	Receptor for Activation of Nuclear Factor Kappa B Ligand
ROI	Region of Interest
RT	Room Temperature
SDF	Stromal Derived Factor
SM	Smouldering Myeloma
SMI	Structural Model Index
STAT3	Signal Transducer and Activator of Transcription 3
TGF β	Transforming Growth Factor β
Trab. N	Trabecular Number
Trab. Pf	Trabecular Pattern Factor
Trab. Th	Trabecular Thickness
TRAP	Tartrate Resistant Acid Phosphatase
uPA	Urokinase-type Plasminogen Activator
uPAR	Urokinase-type Plasminogen Activator Receptor
VCAM	Vascular Cell Adhesion Molecule
VLA	Very Late Antigen
VOI	Volume of Interest
ZOL	Zoledronic Acid

Chapter 1

General Introduction

1.1 Multiple Myeloma

Multiple Myeloma (MM) is a malignancy of the bone marrow (BM) where the antibody producing plasma cells grow without restrain and cause impaired hematopoiesis and severe bone disease. It is a rare cancer and accounts for 1 % of all cancers excluding Non-Melanoma skin cancers, 10% of all hematological malignancies and has caused 2660 deaths in UK in 2008 according to CancerResearchUK. The annual incidence was 4040 in the UK in 2007. Myeloma bone disease mainly includes multiple osteolytic lesions (which causes bone pain and pathological fractures), hypercalcaemia, elevated serum levels of monoclonal immunoglobulin protein (paraproteinemia) and osteoporosis (Bataille *et al.* 1991; Taube *et al.* 1992).

1.1.1 Normal Plasma cell and Myeloma cell development

Immature B cells produced from the BM migrate from the local site to germinal centers of peripheral lymphoid tissue such as lymph nodes, spleen and Peyer's patches and undergo somatic hypermutation following antigenic stimulation to form mature memory B cells. They then migrate to the BM and differentiate into long-lived plasma cells (Hallek *et al.* 1998). However, in case of MM there is evidence of extensive somatic hypermutation of the variable region (V_H gene) in the long-lived plasma cells resulting in clonal expansion of idiotype specific B cells both in the peripheral blood and the BM compartment (Fig.1).(Durie 1988; Vescio *et al.* 1995)

1.1.2 Karyotypic Abnormalities

Chromosomal abnormalities have been attributed to cause MM. The most common karyotypic abnormalities include deletion of chromosome 13 (Monosomy 13) and 14q32 (IgH locus) translocation (Avet-Loiseau *et al.* 2002). Other abnormalities include trisomies of chromosome 3, 5, 7, 9, 11, 15 and 19, translocation 11q13 (bcl-1 locus), interstitial deletion of 13q14 and 8q24 (Hallek *et al.* 1998). Similar Karyotypic instabilities have also been observed in monoclonal gammopathy of undetermined significance (MGUS), a premalignant asymptomatic condition that may progress to overt myeloma (Drach *et al.* 1995; Zandecki *et al.* 1995).

1.2 Biology of Multiple Myeloma

1.2.1 Homing of myeloma cell

The interaction between the myeloma plasma cell and the BM microenvironment (BMM) has been associated with the homing and survival of myeloma cells in the BM. Stromal dependency of myeloma cell is seen during the early and the main course of the disease, while in the latter stages of the disease myeloma cells become stromal independent and migrate to extramedullary sites (Van Riet *et al.* 1998; Damaj *et al.* 2004).

Several studies have indicated that myeloma cells show immunophenotypic and histological similarities to normal B lymphocytes at a particular stage of differentiation (Kubagawa *et al.* 1979). It is the intrinsic feature of B cells to migrate to the BM following maturation to long-lived plasma cells. B cells express

a diverse range of adhesion molecules during their maturation phase allowing them to migrate into different compartments. This is coordinated by chemokines which play a critical role in guiding the plasma cell to specific

Figure 1: Myeloma cell development.

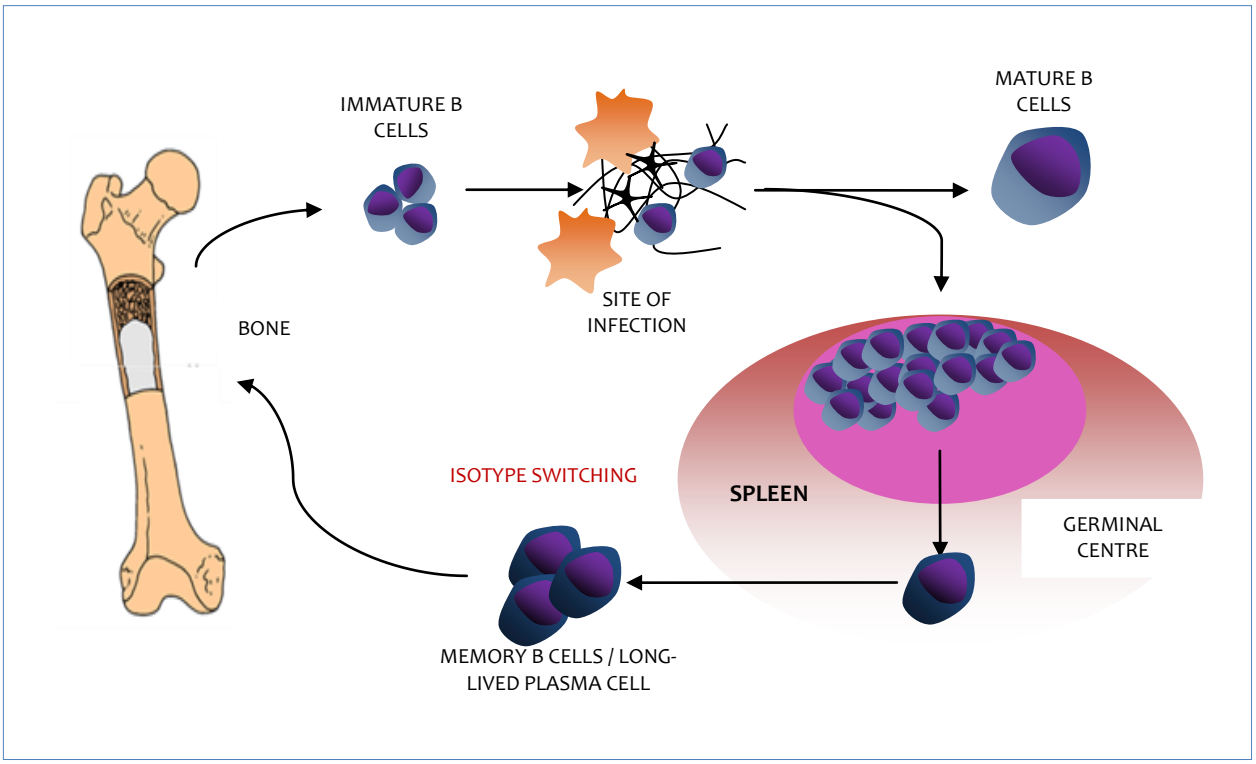

Immature B cells from the BM migrate to the site of infection and upon antigenic stimulation transforms to mature B cell; the plasmablasts and memory B cells. The plasmablast transforms to short lived plasma cells where they eventually terminate, while the memory B cells migrates to the GC and upon antigenic stimulation mediated isotype switching becomes long lived plasma cells. However, in multiple myeloma mutation of the certain oncogene causes malignant transformation (isotype switching and extensive somatic hypermutation of the V_H gene) of the long lived plasma cells which matures into myeloma cell in the germinal centre of the spleen and homes to the BM. (Hallek *et al.* 1998)

BM niches (Dittel *et al.* 1993; Kaisho *et al.* 1994; Koenig *et al.* 2002). As myeloma cells are malignant clones of plasma cells the BM stromal dependency for the initial homing and survival might be a feature acquired from their non-malignant counterpart. CXCR4, a chemokine receptor expression in plasma cells is enhanced during the post GC phase where the plasma cells migrate to the BMM as they express CXCL12 (also known as stromal derived factor-1 [SDF-1]), the unique ligand for CXCR4. This acts as a chemotactic factor not only for haematopoietic progenitor cells but also other cells including MM cell (Aiuti *et al.* 1997; Kawabata *et al.* 1999; Fooksman *et al.* 2010). Interestingly, Ericson and colleagues (2003) demonstrated the selective inability of plasma cells to home to BM in NZM lupus mice deficient in CXCL12 (Erickson *et al.* 2003). However the first step of homing involves the adhesion of the myeloma cell to the luminal bone marrow endothelial cells (BMEC) (Vanderkerken *et al.* 2000). Expression of a diverse range of chemokines like SDF-1 and Monocyte

chemoattractant protein-1 (MCP-1) play a critical role in the initial attraction of the myeloma cell to the BMEC. MCP-1 expression by the BMEC causes the initial attraction of the circulating myeloma cell (CCR2 receptor expressed in myeloma cell) to adhere to the vascular endothelium of the BM while SDF-1 secreted by the BMSC binds with the CXCR4 receptor expressed on the myeloma cells (Uchiyama *et al.* 1992; Sanz-Rodriguez *et al.* 2001; Vanderkerken *et al.* 2002; Alsayed *et al.* 2007). Various adhesion molecules like VLA-4, VLA-5, CD44v, ICAM 1-3 and cadherins, which are expressed on B cells during the early and the late stages of development are also expressed on the myeloma cell (Asosingh *et al.* 2001; Van Driel *et al.* 2002; Menu *et al.* 2004). Several studies have demonstrated that SDF-1/CXCR4 interaction results in upregulation of integrins α4β1 (VLA-4) expression in myeloma cells, which promotes adhesion to fibronectin and VCAM-1 (Sanz-Rodriguez *et al.* 2001; Parmo-Cabañas *et al.* 2004). Asosingh and colleagues (2000) demonstrated that *in vivo* 5TMM cells express multiple splicing variants of CD44, which includes CD44v6, CD44v7, CD44v9 and CD44v10. These molecules play a critical role in the adhesion of myeloma cells to the BMM and also serve as prognostic indicators for the stage of the disease (Stauder *et al.* 1996; Asosingh *et al.* 2001; Van Driel *et al.* 2002).

Invasion of the basement membrane follows the initial attraction and adhesion of the myeloma cell to the BM sinusoids. The process of invasion involves degradation of the basement membrane by proteolysis by proteolytic enzymes secreted by the myeloma cell. Myeloma cells were shown to produce several matrix metalloproteinase's (MMP's), which include MMP-8, MMP-9, and MMP-13 (Barille *et al.* 1997; Wahlgren *et al.* 2001; Parmo-Cabañas *et al.* 2006). 5TMM cells were shown to produce MMP-9 and this was shown to be upregulated by interaction with BMEC (Van Valckenborgh *et al.* 2002; Menu *et al.* 2004; Vande Broek *et al.* 2004). Urokinase-type plasminogen activator (uPA) is a serine protease, which converts plasminogen to its active form plasmin. Plasmin plays a very important role in activating MMP and extracellular matrix degradation (Wong *et al.* 1992; Carmeliet *et al.* 1997; Noel *et al.* 1997; Lijnen *et al.* 1998). Primary myeloma cells and certain myeloma cell lines were shown to express both uPA and uPAR (Hjertner *et al.* 2000).

1.2.2 **Survival and Colonization of Myeloma cell in the Marrow Environment**

The interaction between the myeloma cell and the BMM is thought to provide the necessary survival signals for the proliferation of myeloma cell. The invasion of the myeloma cell through the BMEC and the basement membrane exposes the myeloma cell to cells of the BMM, which include bone cells (osteoclasts and osteoblasts), hematopoietic cells and the bone marrow stromal cells (BMSC).

Interaction of Myeloma cell with BMSC

BMM provides several cytokines and chemokines upon interaction with the myeloma cell which helps in its growth and protects them from apoptosis. Various adhesion molecules like VLA-4 and ICAM-1 mediate the adhesion of myeloma cell to the BMSC ((Uchiyama *et al.* 1992; Uchiyama *et al.* 1993). Evidence shows that myeloma cell adhesion to BMSC results in expression of IL-6 by both the myeloma and the BMSC, which

supplies survival and proliferative signals and confers drug resistance to myeloma cells by paracrine and autocrine mechanisms (Uchiyama *et al.* 1993; Chauhan *et al.* 1996). Adhesion of myeloma cell with BMSC triggers the activation of nuclear factor kappa B (NFκB) pathway which further enhances adhesion by upregulating the adhesion molecules in both the cells. Moreover, they upregulate IL-6 expression in BMSCs via the NFκB dependant pathway (Hideshima *et al.* 2001). IL-6 was shown to trigger phosphorylation of the signal transducer and activation of transcription 3 (STAT3) pathway via Janus-kinase 1 (JK-1), activation of Ras/mitogen-activated protein kinase (MAPK) pathway and the phosphatidylinositol-3 kinase (PI-3K) pathway which results in the production of anti-apoptotic and proliferative signals for myeloma cells (Ogata *et al.* 1997; Hideshima *et al.* 2001; Brocke-Heidrich *et al.* 2004; van de Donk *et al.* 2005). However, IL-6 blockade did not evoke a substantial anti-myeloma effect and myeloma cells were found to survive when co-cultured with BMSCs (Trikha *et al.* 2003; Chatterjee *et al.* 2004). These results suggest that interaction between the myeloma cell and the BMM additionally stimulates IL-6 independent mechanisms for the survival of the myeloma cell. Chatterjee and colleagues (2004) demonstrated that BMSC interaction with myeloma cells stimulates Ras/MAPK pathway in myeloma cells which are independent of IL-6R blockade (Chatterjee *et al.* 2004).

Insulin like growth factor-I (IGF) is another important chemokine produced by the BMSC upon interaction with the myeloma cell. It was shown to have a synergistic effect on myeloma cell survival and proliferation through an IL-6 independent mechanism by activating both MAPK and PI-3K pathway (Ferlin *et al.* 2000). Various other cytokines have been identified that play an important role in the anti-apoptotic effect which include interleukin (IL)-1α, IL-1β, basic fibroblast growth factor (bFGF), hepatocyte growth factor (HGF) and vascular endothelial growth factor (VEGF) (Mitsiades *et al.* 2007). Although interaction with BMSC either by direct adhesion mediated interaction or production of chemokines and cytokines was shown to activate a number of different pathways in the myeloma cell they all converge to a common downstream event enhancing anti-apoptotic and degradation of the pro-apoptotic signals which confers survival advantage to the myeloma cell in the BMM.

Interaction with BMEC & Neovascularisation

Tumour angiogenesis is an important event responsible for the growth and expansion in solid tumours. Myeloma cells produce several pro-angiogenic and angiogenic molecules like VEGF, bFGF, transforming growth factor-β (TGFβ), platelet derived growth factor (PDGF), HGF and IL1 both by autocrine and paracrine mechanism upon interaction with BMSC and BMEC (Vacca *et al.* 1999; Gupta *et al.* 2001; Ria *et al.* 2003; Hideshima *et al.* 2007). All these factors are involved in the growth and differentiation of vascular endothelial cell and recruit new vessels in the BMM. *Vacca et al*.(2003) demonstrated that myeloma BMECs express various adhesion molecules and receptors which confers them high angiogenic and vasculogenic ability compared to HUVEC (Vacca *et al.* 2003). Furthermore, adhesive interaction of BMEC with the myeloma

cell enhances the invasiveness of myeloma cell by stimulating the production of MMPs (especially MMP-2 & MMP-9) which in turn release bone growth factors which favours myeloma growth (Vande Broek *et al.* 2004).

Figure 2: Myeloma cell interaction with the bone marrow microenvironment

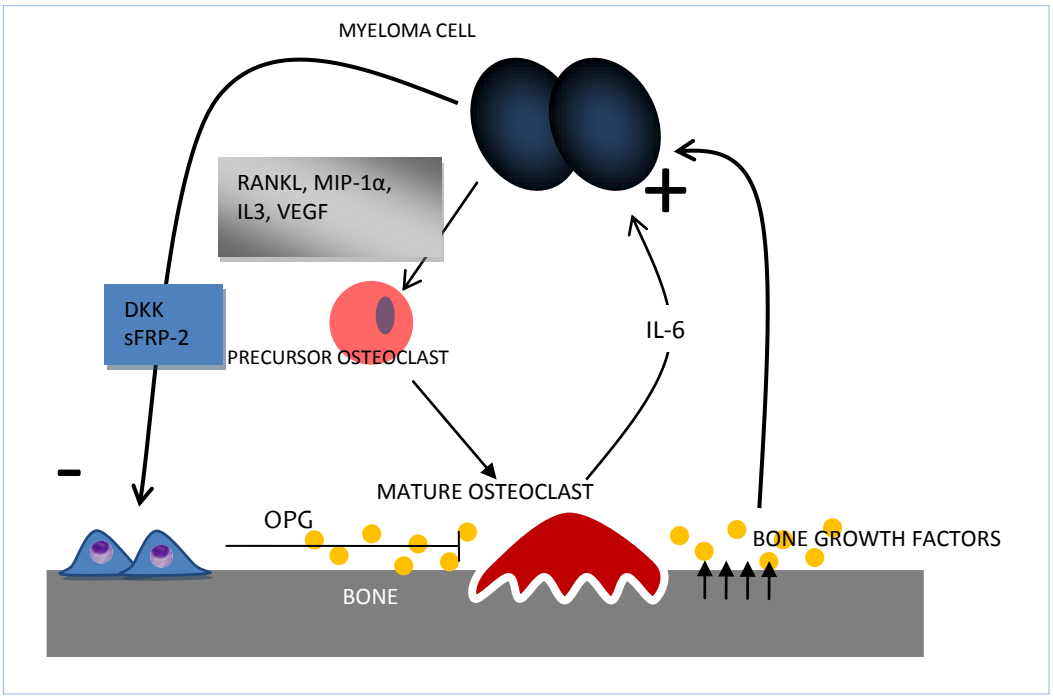

Cell-cell interaction between the myeloma cells and the osteoclast, osteoblast and BMSC play a vital role in the development of osteolytic lesion. The activation of precursor osteoclast into mature and functionally active osteoclast releases factors like IL6 and other bone derived tumour growth factors in the BM niche which supports the proliferation and survival of myeloma cell in the bone. Myeloma cells also inhibit osteoblast mediated release of OPG which further activates osteoclast activation (loss of OPG mediated osteoclast inactivation).

Interaction with osteoblast

Barille *et al.* (1995) showed that certain myeloma cell lines upon interaction with osteoblasts via direct cell-cell contact caused release of IL-6 which in turn enhanced the survival potential of the myeloma cells (Barille *et al.* 1995; Franchimont *et al.* 2000). However, at present the direct role of osteoblasts on the myeloma cell survival is not known. Interestingly, myeloma cells have an inhibitory effect on osteoblastogenesis both by direct adhesive interaction with the osteoblast progenitors, causing down regulation of *RUNX2* transcription factor which plays an important role in osteoblast differentiation, and by the production of soluble Wnt inhibitory factors like dickkopf 1 (DKK1) and frizzled ring protein 2 (FRP2) (Tian *et al.* 2003; Thomas *et al.* 2004; Giuliani *et al.* 2005; Oshima *et al.* 2005; Giuliani *et al.* 2006; Chim *et al.* 2007; Komori 2010). As osteoblasts also regulate the expression of receptor for activation of nuclear factor kappa B ligand (RANKL) and osteoprotegerin (OPG), which are positive and negative mediators of osteoclast differentiation respectively,

this shows that myeloma cells in addition to their direct effect on ostoeclastogenesis, also regulate osteoclasts indirectly through osteoblast inhibition (Glass Ii *et al.* 2005; Spencer *et al.* 2006).

1.2.3 **Development of Myeloma Bone Disease**

Bone disease in multiple myeloma is not merely a functional consequence of the disease on the BMM, it is an ongoing process which promotes myeloma cell survival and tumour growth. Interaction of myeloma cells with the BMSCs results in the production of several osteoclast activating factors (OAFs) which include RANKL, macrophage inflammatory protein-1α (MIP), VEGF, IL-6 and tumour necrosis factor (TNFα) (Lacey *et al.* 1998; Fuller *et al.* 2002; Henriksen *et al.* 2003; Heider *et al.* 2004). RANKL is a TNF-related activation-induced cytokine which binds to the RANK receptor on osteoclasts and is involved in the activation and differentiation of precursor osteoclasts into mature and functionally active osteoclasts (Lacey *et al.* 1998). In normal conditions RANKL is secreted by osteoblasts, BMSCs and BMECs. The extent of osteoclast activation and consequent bone resorption is limited by the production of OPG, a soluble decoy receptor antagonist for RANKL, mainly produced by osteoblasts and BMSCs (Kong *et al.* 1999). However, in MM there is upregulation of RANKL expression by both myeloma cells and the BMSCs (Croucher *et al.* 2001; Giuliani *et al.* 2001). Moreover, myeloma cells were shown to inhibit OPG synthesis by osteoblasts and BMSCs both *in vitro* and *in vivo* (Pearse *et al.* 2001). Additionally, Standal *et al.* (2002) showed myeloma cells by their transmembrane heparin sulphate proteoglycan syndecan -I binds, internalises and degrades circulating OPG (Standal *et al.* 2002). Thus in MM, the RANKL/OPG balance is disrupted resulting in enhanced osteoclastic activity and subsequent increase in bone resorption.

Myeloma cells also produce MIP-1α that directly acts through the receptors CCR1, CCR5 and CCR9 expressed on the osteoclast. They promote osteoclast maturation and differentiation both independently of RANKL and also support RANKL and IL-6 induced osteoclast activation (Choi *et al.* 2000). Studies have shown that MIP-1α mRNA levels from the BM plasma and serum levels of MIP-1α protein corresponds to the severity of the bone disease in myeloma patients (Choi *et al.* 2000; Terpos *et al.* 2003). Furthermore neutralizing antibody to MIP-1α and antisense blocking showed inhibition of osteoclast activation and reduction of bone disease in a myeloma mouse model (Choi *et al.* 2000; Choi *et al.* 2001). VEGF is another angiogenic cytokine produced by myeloma cells, BMSCs and BMECs and it plays a critical role in osteoclast activation, maturation and migration (Henriksen *et al.* 2003; Yang *et al.* 2008). Lee and colleagues (2003) showed IL-3 produced by myeloma cells activates osteoclast along with RANKL and MIP-1α and was consistently found elevated in MM patients (Lee *et al.* 2004). Recently T lymphocytes in the BM plasma of multiple myeloma patients were shown to produce IL-3 and were involved in ostoeclastogenesis (Giuliani *et al.* 2006). A number of other cytokines like IL-6, TNF-α, IL-1β were also shown to be consistently elevated in MM patients with bone disease (MBD). However a definitive role in the pathophysiology of MBD is not clear and warrants further investigation.

Interaction with osteoclast

As already mentioned, myeloma cells produce several cytokines and growth factors for the activation and maturation of osteoclast in the BMM. Abe *et al.* (2004) demonstrated that binding of myeloma cells to osteoclasts through cell surface receptors enhances the release of IL-6 from osteoclasts and also promotes myeloma cell survival. Anti-IL-6 neutralizing antibody was not able to fully abrogate the osteoclast mediated survival in myeloma as it is more dependent on a direct physical contact with the osteoclast. Furthermore, the same group also showed that myeloma-osteoclast interactions have a more potent growth promoting effect than myeloma-BMSC interactions (Abe *et al.* 2004). Two other molecules, *B cell activating factor* (BAFF) and *a proliferation inducing ligand* (APRIL), produced by osteoclasts were shown to promote growth and anti-apoptosis in certain myeloma cell lines (Moreaux *et al.* 2004; Abe *et al.* 2006).

Bone derived growth factors

During osteoclastic bone resorption several growth factors and cytokines are released from the bone tissue into the surrounding BMM. These include factors like IGF, TGF-β, bFGF and PDGF (Mohan *et al.* 1991). Additionally there is also release of calcium (Ca^{2+}) and phosphate (PO_4) due to the breakdown of hydroxyapatite crystals, a major component of the bone mineral matrix (Yoneda *et al.* 2005). The role of IGF, TGF-β, bFGF and PDGF in myeloma cell survival, proliferation and drug resistance is already discussed above. Following resorption there is abundant release of these bone derived factors into the resorption pit under the osteoclast and into the BM. This makes the BM niche a very fertile environment for cells to grow. Yamaguchi *et al.* (2002) showed that certain myeloma cells express calcium sensing receptors (CaR) and shows proliferative effect when stimulated with Ca^{2+} (Yamaguchi *et al.* 2002). The copious release of growth factors supports the survival and proliferation of myeloma cell which in turn activates more osteoclast thereby establishing a vicious cycle leading to continuous bone damage and subsequent tumour expansion (Fig. 2). The use of osteoclast inhibitors such as bisphosphonates have shown a prompt reduction in tumour burden *in vivo* in myeloma preclinical models and clinical trials (Croucher *et al.* 2003; Sordillo *et al.* 2003; Vanderkerken *et al.* 2003; Avilés *et al.* 2007; Morgan *et al.* 2010). However the mechanism is not clearly understood yet.

1.3 Zoledronic acid

Zoledronic acid is a nitrogen containing bisphosphonate (NBP) widely used over the past 10 years as an osteotrophic agent in the treatment of osteolytic bone diseases like Pagets disease, osteoporosis and also in malignancy associated osteolysis and hypercalcaemia. Bisphosphonates (BP) are a class of compounds that are synthetic analogues of the inorganic pyrophosphates where the central oxygen atom (P-O-P) is replaced by carbon atom (P-C-P) (Fig.3A & 3B). The substitution of the central oxygen moiety to the backbone of the naturally occurring inorganic pyrophosphate has made BPs a more stable, resistant to degradation, biologically active and water soluble compound (Green 2005). The P-C-P backbone motif of the BP acts as a bone hook binding to the hydroxyapatite of the bone. This affinity of the BPs is because of their intrinsic property to bind

divalent cations such as Ca^{2+}. Substitution of the R_1 side chain with a hydroxyl (-OH) or primary amino ($-NH_2$) group will increase their binding affinity to bone because it permits a tridentate conformation which binds with Ca^{2+} ions more effectively than substitutions with chlorine (Cl^-) or hydrogen (H) ion which allows only a bidentate conformation (Fig. 3C) (van Beek *et al.* 1998; Rogers *et al.* 2000; Reszka *et al.* 2003; Papapoulos 2006). Although the whole molecular structure is essential for the biological potency of these drugs, the structure of the R2 side chains significantly alter their anti-resorptive potency (van Beek *et al.* 1998; Rogers *et al.* 1999).

Zoledronic acid (manufactured and marketed by Novartis *pharma* in the name of Zometa/ Aclasta/ Reclast) has a heterocyclic imidazole ring with two nitrogen atoms at its R_2 moiety and a hydroxyl (–OH) group at its R_1. It is currently the most potent BP with the highest osteoclast inhibitory effect and the broadest clinical application (Green 2005). It was initially approved for the treatment of bone disease in multiple myeloma and other solid tumours. Recently, due to increasing evidence of reduction in skeletal related events and anti-tumour effect in phase III clinical trials, it is currently under evaluation for considering early integration in anti-cancer treatment regimens for multiple myeloma (Morgan *et al.* 2010).

Figure 3: Chemistry of Bisphosphonates.

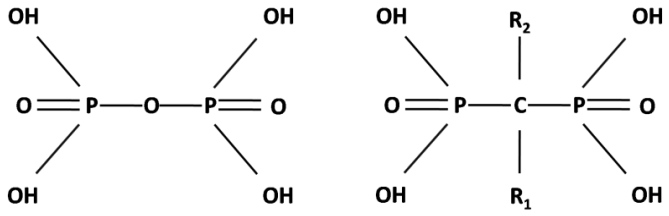

A. Pyrophosphate B. Bisphosphonate

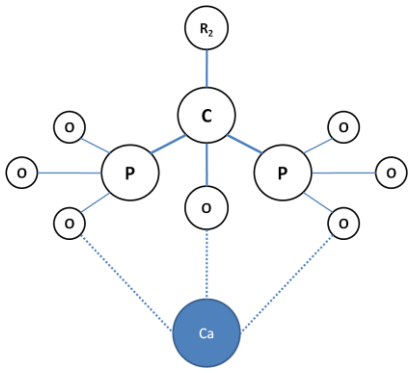

C. Tridentate Configuration in NBPs

Fig. 3A and 3B shows the comparison between pyrophosphate and **BP** compound. Fig. 3C shows the tridentate configuration of BP with Ca^{2+} ion. The substitution of OH group at R1 allows a tight binding with the exposed Ca^{2+} ion at sites of active resorption. The presence of an additional OH group at R1 contributes to one more covalent bond between the BP and calcium in the hydroxyapatite bone matrix.

1.3.1 Zoledronic acid mechanism in the treatment of myeloma bone disease

Zoledronic acid is an effective anti-resorptive agent inhibiting osteoclastic bone resorption thereby preventing bone damage. Although all classes of bisphosphonates target osteoclasts the selective activity differs between the group of compounds classified as Non-NBPs (e.g. Clodronate & Etidronate) and the NBP's (e.g. Zoledronic Acid & Risedronate) (Rogers *et al.* 2000). The intrinsic property of BPs to have a high affinity to mineralized bone matrix, favours the rapid relocation of these molecules from the circulation to areas of active bone remodelling, which has rendered them to have a very short plasma half-life and hence low plasma circulating levels (Sato *et al.* 1991; Masarachia *et al.* 1996; Chen *et al.* 2002; Green 2003). NBPs are internalised into osteoclasts during bone resorption by fluid phase endocytosis (Thompson *et al.* 2006). Sato *et al.* (1991) showed evidence of intracellular accumulation of radio-labelled ALN in various subcellular compartments in rat osteoclasts *in vivo.*

NBPs inhibit an enzyme in the mevalonate pathway in the osteoclast and other cells that can actively uptake NBP's (Amin *et al.* 1992; Luckman *et al.* 1998). NBPs inhibit geranyl diphosphate and farnesyl diphosphate synthase (FPPS) which plays a critical role in the conversion of isopentenyl diphosphate into farnesyl diphosphate (FPP) of the mevalonate pathway (Fig. 4) (van Beek *et al.* 1999; Bergstrom *et al.* 2000; Dunford *et al.* 2001). Inhibition of FPPS results in loss of prenylation of important signalling proteins like Ras, Rho, Rac and hence defective cell signalling, cellular functioning and osteoclast inactivation and apoptosis (Rogers *et al.* 1999; Rogers *et al.* 2000; Mönkkönen *et al.* 2007; Russell *et al.* 2008).

Recently, evidence suggests potent NBPs like zoledronic acid produce a cytotoxic analogue of ATP known as *AppppI* (triphosphoric acid 1-adenosin- 5'–yl ester 3-(3-methyl-but-3-enyl) ester). *AppppI* in both *in vitro* and *in vivo* conditions can induce osteoclast apoptosis by blocking mitochondrial ATP/ADP translocase (Monkkonen *et al.* 2006; Mönkkönen *et al.* 2007).

Figure 4: Mechanism of action of zoledronic acid in osteoclast.

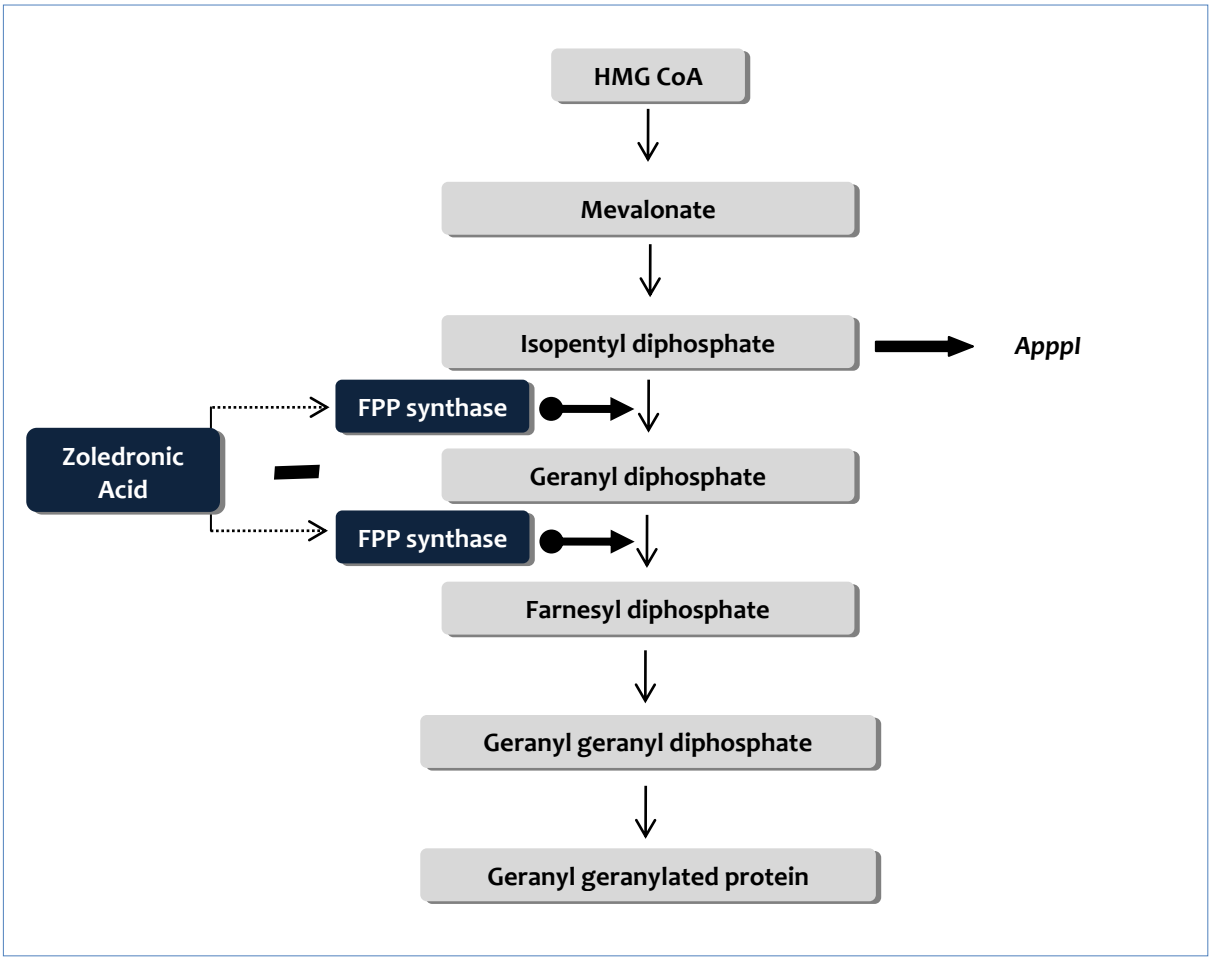

Schematic diagram shows the MOA of zoledronic acid in the osteoclast. Zoledronic acid bound to the bone is released into the resorption pit as result of substances released by the osteoclast. The released zoledronic acid is internalised by the osteoclast by fluid phase endocytosis. They inhibit the enzyme farnesyl diphosphate synthase which in turn inhibits the synthesis of geranyl diphosphate and farnesyl diphosphate which are necessary for protein prenylation and the production of intracellular signalling proteins like Ras, Rac & Rho. Further the accumulation of Isopentyl diphosphate also results in production of *ApppI* which is toxic for the osteoclast.

1.3.2 **Anti-myeloma effects of zoledronic acid**

Several preclinical studies have established BPs as an attractive therapeutic agent for the treatment of tumour induced bone diseases, but emerging evidence suggest that BPs may have a role well beyond being a mere osteolysis inhibitor. In addition to inhibiting tumour induced osteolysis, BPs have a remarkable effect on skeletal tumour burden and survival in several preclinical cancer models and clinical trials of bone metastasis (Green *et al.* 2002; Croucher *et al.* 2003; Green 2003; Clezardin 2005; Clezardin *et al.* 2005; Avilés *et al.* 2007; Saad 2008; Morgan *et al.* 2010).

Evidence in preclinical models of myeloma

Yaccoby and colleagues (2002) demonstrated that zoledronic acid treatment resulted in the reduction of established myeloma growth in human bones implanted in SCID-hu mice (Severe combined immune-deficient mice implanted with human bone). The reduction in tumour development was shown as reduction in serum hu-paraprotein (*hIg*) compared with untreated controls. Furthermore, zoledronic acid pre-treated mice when injected with tumour cells showed no increase in serum *hIg*. Interestingly extramedullary tumour growths in myeloma were insensitive to the inhibitory effects of bisphosphonates (Yaccoby *et al.* 2002). In the 5T2MM murine myeloma model, zoledronic acid (120 µg/kg) treatment with established tumour resulted in a reduction of tumour induced osteolytic lesions. In addition, zoledronic acid treated mice exhibited reduced tumour area, reduction in microvessel density in areas of tumour development in bone, reduction in serum paraprotein levels and prolongation of disease free survival compared with untreated controls (Croucher *et al.* 2003). Recently other NBPs such as Pamidronate and Risedronate showed similar result in 5T2MM model (Libouban *et al.* 2003; Lawson *et al.* 2008; Guenther *et al.* 2010).

Evidence in myeloma clinical trials

A number of clinical trials have shown zoledronic acid to exert an anti-tumour effect not only in multiple myeloma but also in breast cancer, prostate cancer and renal cell carcinoma (Smith 2003; Dabaja *et al.* 2004; Gnant *et al.* 2010). Avilés *et al.* (2007) showed zoledronic acid treatment improved the event free survival (EFS) and overall survival (OS) in advanced myeloma patients upto 80% compared to 52% and 48% respectively in the control group (Avilés *et al.* 2007). Further, zoledronic acid treatment along with standard chemotherapy for metastatic prostate cancer showed more than 50% reduction in prostate specific antigen (PSA), a diagnostic marker for prostate cancer progression levels suggesting a possible anti-tumour effect (Dabaja *et al.* 2004; Vordos *et al.* 2004). Monthly doses of zoledronic acid prolonged bone metastasis free survival in patients with advanced metastatic solid tumours with no evidence of bone metastases at the time of treatment (Mystakidou *et al.* 2005). Moreover, zoledronic acid combination therapy in early breast cancer chemotherapy also showed improvement in the disease free and overall survival by 32% (Gnant *et al.* 2010). In a recently conducted phase III clinical trial (myeloma IX study) for MM involving 1960 patients, zoledronic acid treatment with the standard chemotherapy showed 16% increase in the OS and 12% increase in the progression free survival (PFS) compared with oral clodronate (Morgan *et al.* 2010).

1.3.3 **Mechanisms of the anti-myeloma effect with zoledronic acid**

There is clear evidence that zoledronic acid either independently or in combination with other chemotherapeutic agents, in addition to its anti-resorptive property, also exhibits some disease modifying activity in myeloma and other solid tumour with bone involvement.

Direct toxicity

Several *in vitro* studies have shown that zoledronic acid and certain NBPs have a cytostatic and pro-apoptotic effect on primary human myeloma cells and various myeloma cell lines by inhibiting proliferation and inducing apoptosis. The concentration at which a maximum inhibitory effect seen was between 10-100 µM concentrations of zoledronic acid (Shipman *et al.* 1997; Aparicio *et al.* 1998; Derenne *et al.* 1999; Croucher *et al.* 2003; Baulch-Brown *et al.* 2007). Accumulating evidence suggests that NBPs induce inhibitory and apoptotic effects in tumour cell lines by inhibiting the mevalonate pathway similar to the effect on osteoclasts (Diel 2000). Loss of protein prenylation of small GTPases such as Ras, Rap1A and Rho results in defective downstream signalling which causes the apoptotic effects in tumour cells. The administration of farnesol (FOH) and geranylgeraniol (GGOH) have been shown to partially prevent the inhibitory effects of BPs (Shipman *et al.* 1998; Iguchi *et al.* 2003). In a study reported by Benford *et al*. (2001) the NBP induced apoptotic effect on osteoclasts was due to caspase-3 activation which caused the loss of mitochondrial membrane potential (Benford *et al.* 2001). Down-regulation of anti-apoptotic proteins of the *bcl-2* family of apoptotic genes (*Bcl-xL, Bcl-W*) has been attributed to mitochondrial release of cytochrome c which activates caspase 3 (Fig 5) (Senaratne *et al.* 2002). Studies by Senaratne *et al.* (2002) demonstrated that NBPs down regulate bcl-2 induced apoptosis in breast cancer cell lines. Similar results were produced by Aparicio *et al.* (1998) when forced bcl-2 expression protected IM-9 cells from the zoledronic acid induced apoptotic effects but not the cytostatic effect (Aparicio *et al.* 1998). Interestingly, inhibiting the mevalonate pathway using a HMG CoA reductase inhibitor (fluvastatin) did not affect the Bcl-2 family protein; instead it inhibited anti-apoptotic Mcl-1 and phosphor-Rb (Baulch-Brown *et al.* 2007). However, the *in vivo BMM* is far more complicated with complex cellular interactions and cell signalling. Moreover the concentration at which the cytoreductive effects of BPs described in the *in vitro* setting is much higher to the peak plasma concentration of the drug. BPs owing to their high bone binding affinity rapidly translocates from the plasma and concentrates into areas of active bone resorption. Alendronate, another BP (ALN) has been shown to reach a local concentration in the range of 0.1-1 mM. Though the local concentration at the osteoclast-bone interface is well above the anti-tumour threshold, it still remains unclear whether it would reach the tumour cells in the BMM (Sato *et al.* 1991; Clezardin *et al.* 2005).

Figure 5: Mechanism of cytotoxic effect of zoledronic acid on myeloma cell.

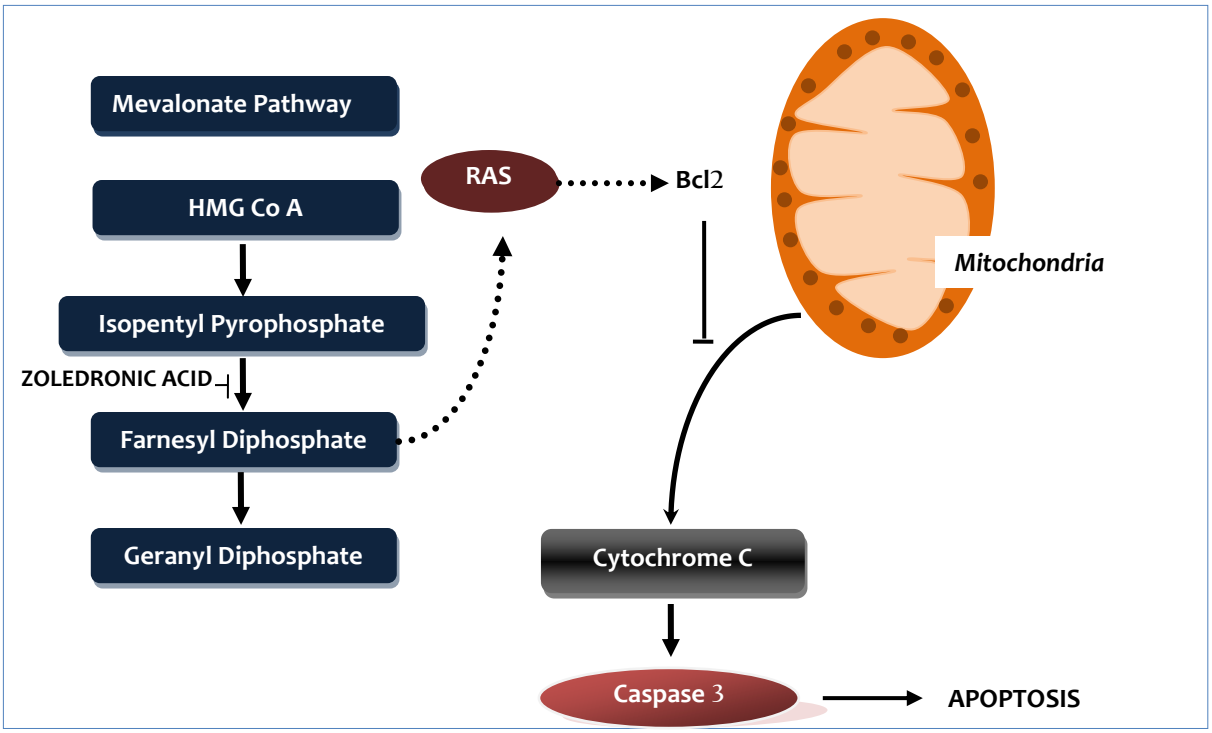

Loss of protein prenylation of important intracellular signalling protein like Ras, Rac and Rho causes down regulation of anti-apoptotic *bcl2* which triggers the release of mitochondrial cytochrome 3 which induces apoptosis by the activation of caspase 3 pathway

Indirect effect by inhibiting osteoclast and subsequent resorption

The selective inhibitory activity of BPs on most cancer metastases to bone suggests that the anti-tumour effect observed might be secondary to osteoclastic inactivation and subsequent resorption. Bone is a complex environment rich in various growth factors including IGF,TGF-β, PDGF, bFGF, IL-6 and bone morphogenetic protein (BMP) which makes it a fertile environment for tumour cell survival and colonisation. Following osteoclastic resorption, these growth factors are released in the bone microenvironment which facilitates tumour cell survival and growth. The tumour cells in turn stimulates the production of factors stimulating osteoclastogenesis and bone resorption, establishing a vicious cycle between the tumour cells and the cellular components of the bone (Yoneda *et al.* 2005). BPs are potent inhibitors of bone resorption and in turn inhibit the release of factors which facilitates tumour cell survival thereby reducing tumour cell colonisation and eventually skeletal tumour burden (Fig. 6). As described earlier, specific osteoclastogenesis inhibitors such as Fc.OPG and recombinant RANK-Fc also exhibit the same anti-tumour effects seen in bone which further supports the theory that it is an indirect effect (Yaccoby *et al.* 2002; Vanderkerken *et al.* 2003).

Figure 6: Indirect anti-myeloma effect of zoledronic acid

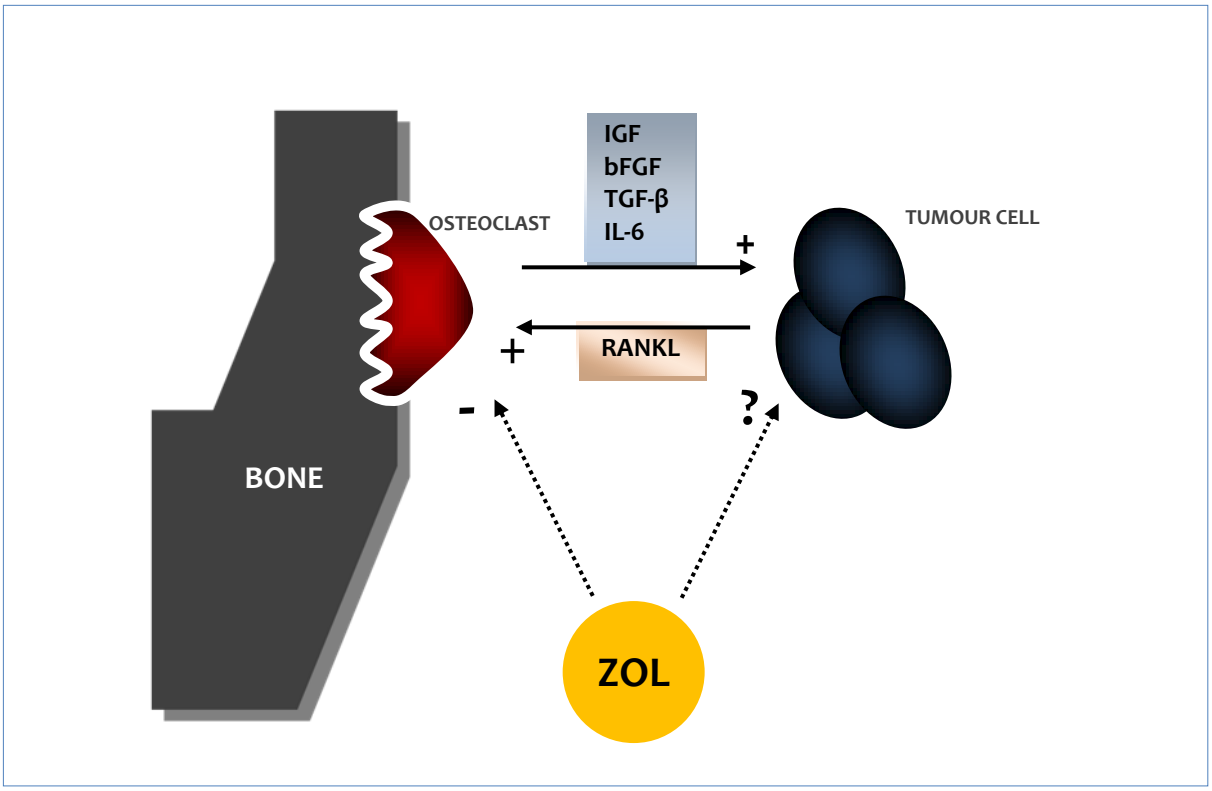

Inhibition of osteoclastogenesis by zoledronic acid in turn inhibits the release of osteoclast derived and bone derived myeloma growth factor such as IL-6, TGF-β, bFGF, IGF release in the BMM. The inhibition of survival signals has a negative influence on the myeloma cell growth which in turn has a negative effect on the tumour cell derived osteoclast activation thereby breaking the vicious cycle.

1.4 Aims and Objectives

Myeloma cell homing to the bone marrow depends on the growth factors in the BMM for colonisation and survival. Evidence that zoledronic acid prolongs the incidence of myeloma bone disease and event free survival suggests that zoledronic acid interferes with early cell colonisation events. Therefore, blocking the release of the bone derived growth factors by inhibiting osteoclastic resorption may alter the BM niche to be unfavourable for the colonisation and survival of the myeloma cell. Based on these we hypothesized that **blocking bone resorption with zoledronic acid will prevent the colonisation of myeloma cells and stop the activation of the resident cells from developing into overt myeloma colonies.** To address this question we have developed a novel technique using multiphoton microscopy to visualise and quantitate fluorescent labelled tumour cells in the bone marrow. Zoledronic acid, a potent osteoclast inhibitor will be used to inhibit osteoclastic bone resorption. Its effect on the tumour cell colonisation and survival will then be assessed using multiphoton microscopy. This will enable visualisation of individual tumour cells in BMM in 3D. The 5T33 murine model of myeloma (5T33MM) will be used as cells can be manipulated to express green fluorescent protein

(GFP) and they home to bone in a similar manner to 5T2MM model that closely resembles the human disease condition (Vanderkerken *et al.* 1997).

Our aims are:

1. To determine whether blocking bone resorption with zoledronic acid reduces the initial colonisation of bone by myeloma cells.
2. To determine whether blocking bone resorption with zoledronic acid prevents the development of myeloma colonies.

To achieve this we initially have to effectively suppress osteoclastic bone resorption with zoledronic acid in C57BL/KaLwRij mice, used in the 5T33MM and 5T2MM model. Then assess the effect of inhibiting osteoclastic bone resorption on the colonisation and survival of 5T33MM cells in the bone. Our objectives are:

1. To determine the time taken by zoledronic acid to effectively suppress osteoclastic bone resorption in C57BL/KaLwRij mice.
2. To visualise 5T33MM-GFP cells in the long bones using multiphoton microscopy.
3. To determine if zoledronic acid inhibits the number of tumour cells homing and colonising the bone and has an effect on tumour cell location in the bone.

Chapter 2

Materials & Methods

2.1 Cell Culture

5T33MM murine myeloma cells (*in vitro*) labelled with GFP (5T33MM-GFP) and wildtype (5T33MM-WT) were provided by Dr. K. Vanderkerken (Vrije Universiteit Brussel, Belgium). The cells were passaged in RPMI 1640 media with Glutamax (GIBCO-Invitrogen 1870-010) supplemented with 10% foetal calf serum (FCS), 1% Penicillin-streptomycin (Pen-strep) (100 units/ml of penicillin and 100 µg/ml of streptomycin), 1 mM sodium pyruvate and 100 mM non-essential amino acid (NEAA). The cells were incubated in a 5% CO_2 incubator at 37°C with 95% humidity with culture medium changed every 3-4 day in a T75 flask.

2.2 Animal Work

C57BL/KaLwRij mice were purchased from Harlan (Netherlands) and were bred and housed in the University of Sheffield Biological Services. Animal work was approved by the local ethical committee and by the UK Home Office Regulations. Animal works was performed by Dr. Michelle Anne Lawson and Dr. Allan J Williams under project licence number: 40/2901.

2.3 Cell Counting

Cell counting was done using a Neubauer haemocytometer. Cells were stained with 0.4% trypan blue dye (1:1 ratio). 10 µl of cell suspension was mixed with 10 µl of trypan blue and cell counted using the haemocytometer. The no. of cell per ml was calculated using the formula

$$\text{Cell count} \times \text{dilution factor} \times 10^4 \text{ cells/ml}$$

2.4 Flow Cytometry

CD11a and GFP profiling of 5T33MM cells

CD11a and GFP profiling was done on the *in vitro* 5T33MM cells to determine the proportion of GFP and CD11a positive cells for phenotypic characterisation and to be injected into the mice. Flow cytometry was done using a FACSCalibur flow cytometer (Becton Dickinson, Oxford UK). For GFP profiling, a volume containing 10^6 cells were centrifuged at 1500RPM for 5 min at RT and resuspended in 500µl of PBS (1X concentration, neutral pH) and counted in the flow cytometer for upto a 100,000 events. The parameters used for GFP calculation is given in *appendix 1*. GFP positive 5T33MM were seen in the FL1 channel and 5T33MM-WT were used as negative control.

For CD11a profiling of 5T33MM, 10^6/100 µl of cells were incubated for 45 min with 1.25 µl of anti-CD11a (0.2 mg/ml, PE rat anti-mouse CD11a antibody, Clone 2D7, rat IgG2a, BD Pharmingen), 1.25 µl isotype control (0.2 mg/ml, PE rat IgG2a, BD Pharmingen) or no antibody. Cells were then washed for 3 times using PBS/10% FCS centrifuging at 1500 RPM for 5 min at RT. After washing, the cells are resuspended in 500 µl PBS / 1% BSA and counted on the flow cytometer. GFP and CD11a positive cells were detected in FL1 and FL2 channels

respectively. Compensatory gating of 4% FL2 in FL1 and 14% of FL1 in FL2 was used. The parameters used are given in detail in *Appendix 2.*

2.5 Micro-Computed Tomography (µCT) scanning and analysis

µCT was performed using SkyScan 1172 Desktop X-ray tomographer manufactured by SkyScan N.V. Aartsalaar, Belgium. Complete quantitative analysis on the morphology of the trabecular and cortical bones of the right tibia was done using a medium sized 2000 X 1048 pixel camera and an x-ray source powered by 50 kV and 200 µA electric current. A 0.5 mm aluminium filter was used to filter the low energy radiations. The proximal end of the left tibia was scanned at 4.3 µm pixels for every 0.7° rotation of 180°. A typical scan using the above parameters took 11 minutes.

Figure 7: µCT analysis of the right tibia.

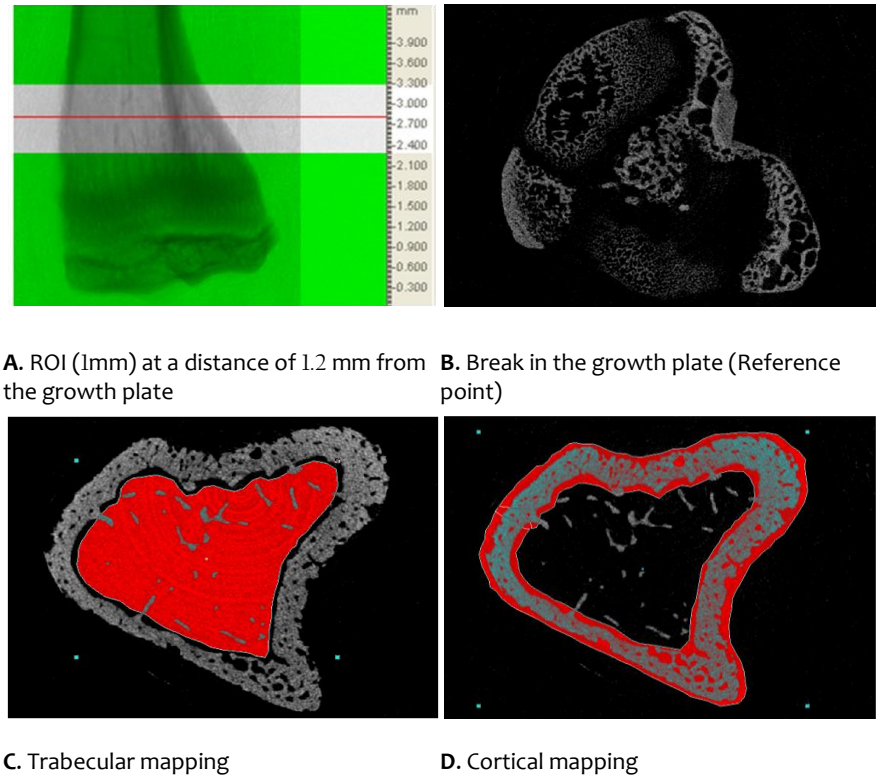

A. ROI (1mm) at a distance of 1.2 mm from the growth plate

B. Break in the growth plate (Reference point)

C. Trabecular mapping

D. Cortical mapping

Figure 7A shows the region of interest on the proximal end of right tibial which is analysed for cortical and trabecular parameters. Figure 7B shows the reference point which is the proximal break in the growth plate. The ROI is chosen at a fixed distance (1.2 mm) for this point for analyses. Figure 7C shows the trabecular mapping drawn inside the bone using drawing tools in the software to include the trabecular bone. Fig 7D shows cortical mapping in red which includes cortical bone.

The scanned images were reconstructed using NRecon software ver. 1.6.1.1 within a dynamic range of 0 to 0.16 and a ring artefact reduction factor of 1%. The reconstructed images were analysed using CTAn ver. 1.9.1.1. Analysis was done on the cross-sectional images of the tibiae at a distance of 1.2mm (offset) from the

distal break in the growth plate (reference point). The distal break in the growth plate was used as a standard reference point for both cortical and trabecular analysis. The analysis was done on a fixed region extending for 1 mm. The trabecular bone was carefully traced on all cross-sectional image of the tibia, not to include cortical bone for the entire ROI. Similarly cortical bone was also analyzed. Figure 7c & 7Dshows the trabecular and cortical bone traced out in the cross-section of tibia. Analysis was done in batches using BatMan (Batch Manager) software and measured the following parameters: trabecular bone volume (%BV/TV), trabecular thickness (Tb. Th), trabecular number (Tb. N), trabecular pattern factor (Tb. Pf), structural model index (SMI) and cortical bone volume (Ct.V). For trabecular analysis the binarised images were thresholded between 90-255 and cortical bones between 100-255.

For µCT scanning of the L3 lumbar vertebrae, due to the asymmetrical nature of the vertebrae the scans were done for 0.7° rotation for 360°s. µCT analysis on the trabecular bone of the L3 lumbar vertebrae was done a fixed volume cylindrical VOI of diameter 0.77 extending between the upper and lower growth plate.

Figure 8: µCT analysis of the lumbar vertebrae.

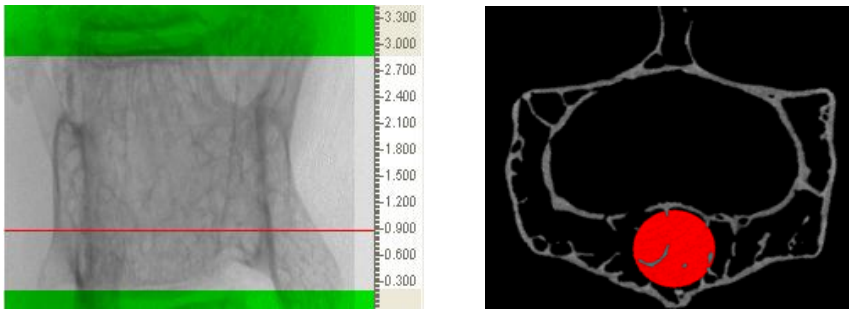

A. ROI for trabecular analysis extending between the ends of growth plates.

B. Isovolumetric cylindrical ROI used for the trabecular analysis of the vertebral body

Fig.8A shows the ROI extending between the growth plates on either sides of the vertebral body upon which trabecular analysis was made. Fig. 8B shows the isovolumetric cylindrical ROI of diameter 0.77 used for trabecular mapping inside the vertebral body for analysis.

2.6 Histological Analysis

Decalcification

After µCT analysis, bones were decalcified for histomorphometric analysis. Decalcification was done using Ethylenediamine tetra Acetic Acid (EDTA, Fischer Scientific) at RT for a period of 4 weeks. The bones were decalcified in volumes of EDTA approximately 20 times the volume of the bones with the solution changed once a week. Once decalcified, the bone tissues were loaded onto labelled tissue cassettes and washed in running tap water for 60 min.

Processing and Wax Embedding

Tissue processing was done using a Leica TP1020 automated carousel tissue processor. The bones were dehydrated using alcohol and infiltrated with paraffin wax (Surgipath). The processed tissues were then embedded in paraffin wax using metal moulds where the tibiae samples were placed diagonally with the crest facing down, and then warm melted paraffin was added to the moulds and was allowed to cool.

Section cutting and Staining

Wax embedded tissue blocks were cut using Leica RM2135 rotary microtome. The microtome was set to cut sections at 3 µm thickness. Initially the wax moulds were slowly trimmed until it cuts through the bone and the marrow is exposed. Chattering was prevented by cooling the exposed tissue surface on ice. Two 3 µm serial sections were cut and floated onto a water bath maintained at 45°C, these were mounted on a Superfrost Plus slide labelled appropriately and then dried overnight in a 37°C incubator. The slides were stored at 4°C until staining.

Tartrate Resistant Acid Phosphatase Staining

Before staining the slides were dewaxed and dried. The slides were dipped in 2 coplin jars of xylene for 5 min in each to remove the paraffin. After dewaxing, they were dipped consecutively in two jars containing 99% and one jar each containing 95% and 70% industrial Methylated spirit (IMS) for 5 min in each for removing the xylene. The slides were then cleared of IMS and rehydrated by rinsing them in tap water.

A standard Napthol AS-BI phosphate post coupling method was used for TRAP staining using hexazonium pararosaniline. To prepare the 1.2% acetic acid solution 6ml of absolute acetic acid (Analar Chemicals) was dissolved in 494ml of distilled water. Acetate buffer (0.2M) was made by dissolving sodium acetate trihydrate (Sigma S-9513) in 200ml of distilled water and the pH was corrected to 5.2 by adding 50ml of 1.2% acetic acid. Sodium tartrate (4.6gm Sigma S-4797) was added to produce acetate tartrate buffer and warmed to 37°C for 2-4 hrs. The dewaxed slides were incubated in the warm buffer for 5 min at RT.

Solution A was prepared by dissolving 0.02 g of Napthol AS-BI phosphate (Sigma N-2250) in 1 ml of dimethyl formamide and the resultant solution mixed with 50 ml of acetate tartrate buffer. The slides were then incubated in solution A for 30 min at RT.

4% sodium nitrate solution was prepared by adding 80 mg of sodium nitrate (Sigma S-2252) in 2 ml of distilled water. 2 ml of pararosaniline (Sigma P-3750) was added to this 4% sodium nitrate solution to form hexazonium pararosaniline. Solution B was prepared by adding 2.5 ml of hexazonium pararosaniline /sodium nitrate to 50 ml of pre-warmed acetate tartrate buffer. Solution B had to be prepared fresh and the slides were incubated for 15 min in solution B at RT. The slides were then rinsed and were counterstained with Gills II (VWR

code 1.05175.0500) haematoxylin for 20 sec. The slides were then washed using IMS and dehydrated by xylene and then coversliped over 2-3 drops of DPX mountant. A detailed flowchart showing step by step staining procedure is given in the *appendix.3*

2.7 Histomorphometry

Static histomorphometry was done using Leica LEITZ DMRB microscope connected to a Sony colour video camera. Osteomeasure Software (Osteometrics Inc, USA) ver. 4.10 was used to assess the cellular composition of both the trabecular and the endocortical regions. The analysis was done at 10X on a field size of 250 X 250 μm^2. Parameters like osteoclast and osteoblast numbers, the surface occupied by osteoclasts and osteoblasts on the trabecular and endocortical bone, the bone perimeter were measured. Osteoclasts were identified as TRAP stained objects seen occupying the bone surface and osteoblasts were identified morphologically as cuboidal cells seen in groups with an eccentrically placed nucleus having haematoxylin (blue) stain.

Trabecular Analysis and Endocortical Analysis

For analysis of the trabecular region in tibia, a ROI of 250 X 250μm^2 in a 3 X 3 fashion in the metaphyseal region from the growth plate as shown in figure.9A was chosen for analysis. Endocortical analysis was done on 6 consecutive fields on each side having 250 X 250 μm^2 along the upper (antero-medial) and lower (antero-lateral) endocortical surface of the tibia. The ROI was chosen at a distance of 250µm from the intersection of the cortical and trabecular bone on both the side as shown in figure.9B.

Figure 9: ROI for the trabecular and endocortical histomorphometric analysis in the long bones

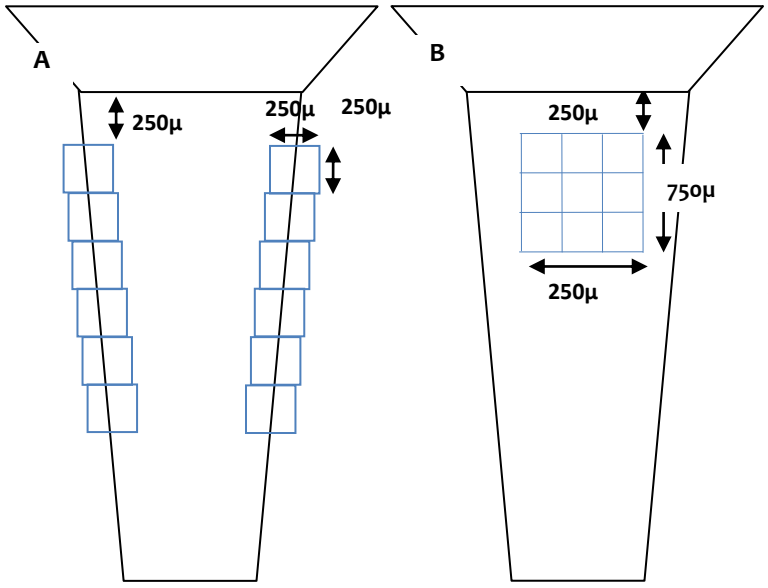

Fig.9A shows the ROI analysed for the endocortical histomorphometric analysis which is 6 consecutive squares each of area 250X250 μm^2 along the endocortical surface of the bone on both the sides at a distance of 250 µm from the intersection of the growth plate and the cortical bone on that side. Fig. 9B shows the ROI for the trabecular histomorphometric analysis in the long bones. The ROI is a square area of 750 X 750 μm^2 (3 X 3 square of 250X250 μm^2) at a distance of 250 µm from the growth plate.

2.8 **Bone Markers**

Elisa for the bone markers Tartrate resistant acid phosphates 5b (TRAP), carboxy terminal telopeptide (CTX), pro-collagen I N terminal peptide (PINP) and osteocalcin was done on the serum samples to assess difference in the bone resorptive activity and bone formation activity between the zol treated and control mice.

Bone resorption Marker Assay

Mouse TRAP Assay™

A Mouse TRAP Assay™ (catalogue no. SB-TR103, Immunodiagnostic systems, UK Ltd) was used to determine the serum levels of the enzyme TRAP5b expressed by bone resorbing osteoclasts. The assay was performed according to the manufacturer's protocol. 100 µl of reconstituted TRAP antibody was added to appropriate wells in an antibody coated microtitre plate and incubated for 1 hr at RT on a shaker (950 RPM). The plate was manually washed 3 times using a wash buffer. 100 µl of calibrators and controls to the well, 75 µl of 0.9% Nacl followed by 25 µl of each sample are added in duplicates. 25 µl of releasing reagent was then added to all wells and incubated for 1 hr at RT on a shaker. The plates were washed 3 times and 100µl of freshly prepared substrate solution was added. The plates were then incubated for 2 hr at 37°C in an incubator. 25 µl of NaOH was used to stop the reaction and the plate was read at 405 nm using a SpectraMax M5^e automated plate reader (*Molecular Devices*).

CTX Assay

A RatLaps™ EIA (catalogue no. AC-06F1, Immunodiagnostic systems, UK Ltd) was used for the quantitative determination of C-terminal telopeptides, a degradation product of type I collagen released during bone resorption. The assay was performed according to the manufacturer's protocol. A streptavidin coated microtitre plate was pre-incubated with 100 µl RatLaps antigen for 30 min. The plate was manually washed 5 times using 300 µl wash buffer. 20 µl of calibrators, controls and samples were added in duplicates to the appropriate wells followed by 100 µl of primary antibody and incubated overnight for 18 hr at 2-8°C. The plates were washed 5 times and incubated with 100 µl of an enzyme conjugate for 60 min at RT. The plates were washed and 100 µl of tetramethylbenzidine (TMB) was added to all wells and incubated for 15 min. 100 µl of H_2SO_4 was used to stop the reaction and the plate was read at 450 nm with a reference range of 650 nm using SpectraMax M5^e automated plate reader (*Molecular Devices*).

Bone formation Marker Assay

PINP Assay

Rat/Mouse PINP EIA (catalogue no. AC-33F1, Immunodiagnostic systems, UK Ltd) was used to measure pro-peptides released from the pro-collagen molecule during collagen synthesis. The assay was performed according to the manufacturer's protocol. 50 µl of calibrators, controls and 5 µl of each sample were added in duplicates. 45 µl of sample diluents was added to wells containing samples. 50 µl of PINP biotin was added to all wells (including calibrators and controls) and the plate was incubated on a shaker for 60min at RT. The plates were washed 3 times in 250 µl of wash buffer. 150 µl of enzyme conjugate was then added to all wells and incubated for 30 min at RT. The plates were washed and 150 µl of TMB was added to all wells and incubated for 30 min. Finally 50 µl of HCl (Stop Solution) was used to stop the reaction. The plate was read at 450 nm with a reference range of 650 nm using SpectraMax M5^e automated plate reader (*Molecular Devices*).

Osteocalcin Assay

Osteocalcin levels in the serum were quantified using Osteocalcin EIA (Biomedical Technologies Inc, BT-470). The standards and controls were prepared according to the manufacturer's instruction. 25 µl of calibrators, controls and samples were added in duplicates to appropriate wells followed by 100 µl of osteocalcin anti-sera wad added to all wells and incubated at 18 hr at 2-8°C. The plate was washed 5 times using 300 µl of wash buffer. 100 µl of horse radish streptavidin peroxidise was added to all wells and incubated at RT for 30 min. 100 µl of TMB-peroxide substrate was added to all wells and incubated in the dark for 15 min. Finally 100 µl of stop solution was added to all wells the absorbance was measured at 450 nm using SpectraMax M5^e automated plate reader (*Molecular Devices*).

2.9 Cryostat Embedding and Sectioning

The right tibiae extracted from mice sacrificed after 18 hr and 72 hr were used for multiphoton microscopic scanning. The femur samples were embedded in OCT before cryosectioning. Embedding of the bone samples was done using a Hexane/methanol freezing bath (HMFB) 20 min prior to embedding (Fig.10). Right tibia completely stripped of soft tissues were placed diagonally in a plastic mould with the knee joint facing upwards. The plastic mould was filled with OCT and placed on the brass chuck inside the metal container until the OCT froze; samples were stored at-80°C until required.

The OCT embedded femur was cut using Cryostat 5030 (Bright Instrument Company, UK) until the BM was exposed over the entire length of the bone (usually 900 µm depth from the surface of the bone). The cut samples were covered in clean foil to prevent contamination of the exposed surface with dirt and to prevent bleaching of the GFP.

Figure 10: Hexane methanol freezing bath

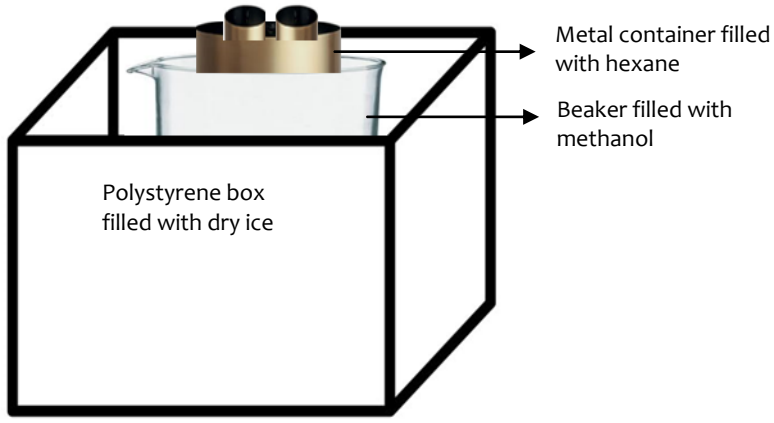

2.10 Multiphoton Microscopy

A Zeiss META 510 inverted microscope, equipped with coherent chameleon laser for multiphoton imaging, was used for scanning the tibia. OCT in the cryosectioned sample was dissolved in sterile PBS (1 X, pH 7.4). The flat cut surface of the tibia was then glued to a small petridish (35 mm glass bottom dishes manufactured by MatTek corporation, USA) using a tissue adhesive (Vetbond) to prevent movement of the bone during scanning. The petridish was filled with sterile (1 X, pH 7.4) to prevent the samples from drying out during the scan (approximately 12 hr).

The bone was focused using a 20X dry piece (Plan-Apochromat) lens and a low resolution pilot image (128 X 128) was taken using 900 nm wavelength with a bandpass filter 435-485 nm (channel-2 also known as CH-T2 or bone channel). This initial pilot scan determined the location of the bone so that the ROI included the entire lower end of the tibia (including the epiphysis) as shown in the figure 12. The ROI is a series of tile scans (size 450 X 450 μm^2) distributed in a 6 X 10 grid fashion over the entire lower end of the femur. Series of high resolution scan (512 X 512) was done on the ROI (on each tile) for a depth of 75 µm inside the bone using 900 nm wavelength with a bandpass filter 435-485 nm for bone (CH-T2) and bandpass filter 500-550 nm (CH-T3) to detect the GFP inside the specimen (Fig. 11).

Figure 11: Principle of Multiphoton Microscopy

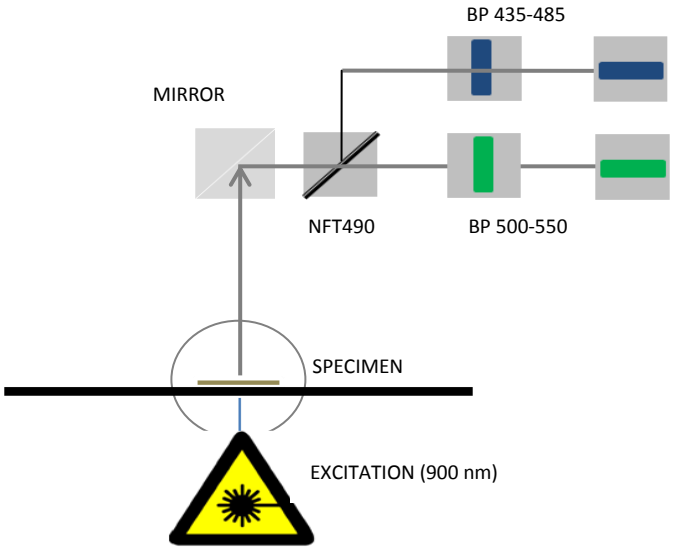

Multiphoton microscopy works on the principle of fluorescence spectroscopy when a high energy laser (900nm wavelength) is used to excite the specimen. As the mice are injected with 5T33MM-GFP cell, the laser excites the GFP. Due the constant colliding of particles at the high energy state slowly loses the energy and decays. During this process it releases a photon which passes through the appropriate green filters (bandpass 500-550nm (CH-T3)) and is picked up by the detectors. Bone is visualised by a second harmonic generation. Collagen is a non-linear material which has the property to combine two high energy photon and release a higher energy photon having double the energy and half the wavelength (Deniset-Besseau *et al.* 2010). Here, as the wavelength used is 900nm the new photon released from the collagen has a wavelength of 450nm which can be passing through blue bandpass filter 435-485nm (CH-T2).

Figure 12: Multiphoton microscopic image of tibia.

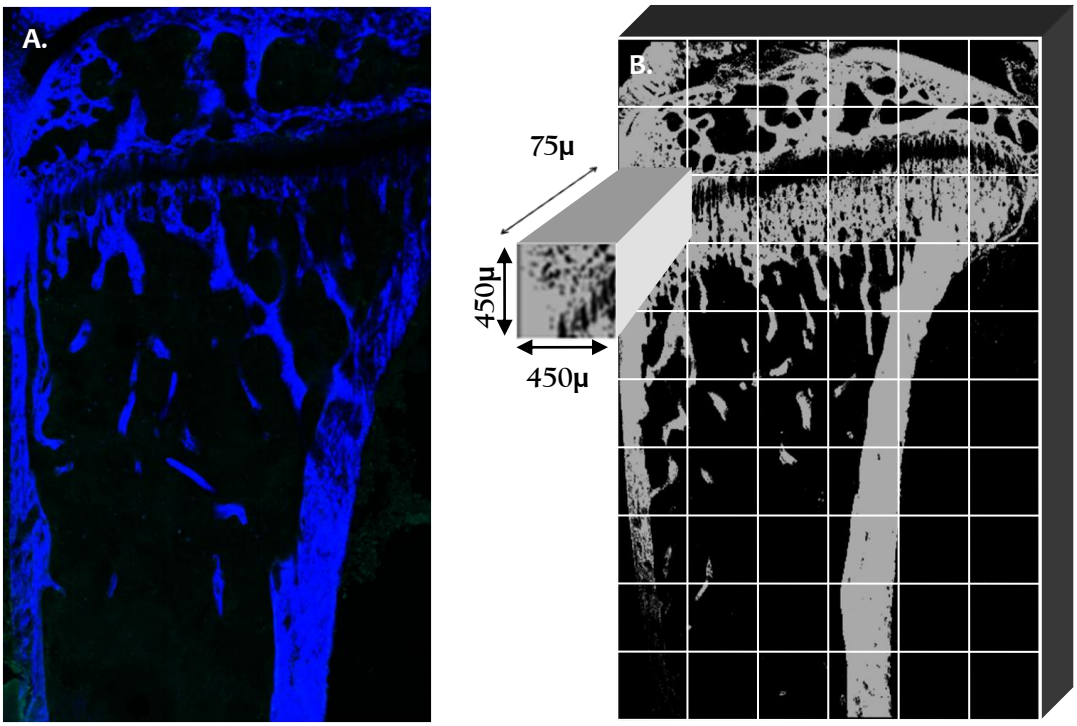

The ROI is a series of tile scans (size 450 X 450 μm^2) distributed in a 6 X 10 grid fashion over the entire lower end of the femur (Fig 12A). Series of high resolution scan (512 X 512) was done on the ROI (on each tile) for a depth of 75 µm inside (Fig. 12B) the bone using 900nm wavelength with a bandpass filter 435-485nm for bone (CH-T2) and bandpass filter 500-550nm (CH-T3) to detect the GFP inside the specimen

2.11 Spectral Finger Printing

Spectral finger printing (Lambda finger printing) was done after completion of each scan. Areas that showed green signals were confirmed to be GFP by lambda finger printing. This was done at a resolution of 256 X 256 over the entire thickness of the Z stack using the same settings with which the scan was done. The images were assessed for the emission spectrum of both bone and the GFP.

Figure 13: Spectral finger printing of green fluorescence spots in the BM

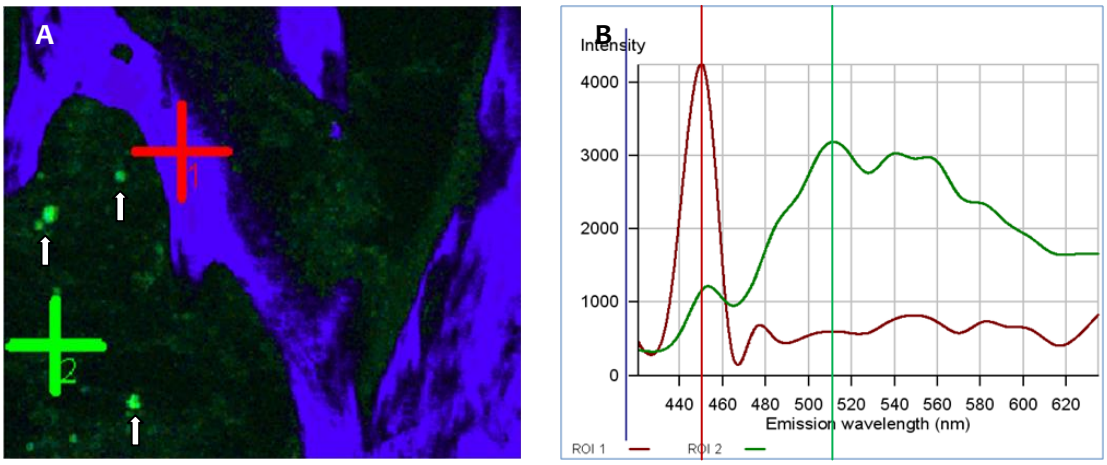

Fig.13A shows the multiphoton microscopic image of the BM in a tibia showing the trabecular architecture generated by SHG in blue. There a few green florescent spots (white arrows) in the field adjacent to the trabeculae. Fig. 13B Graph shows the spectral intensity of the green and blue signals from the multiphoton image. The red line in the graph (corresponding to the red crosshair in the image) shows a peak at 450nm and the green line (corresponding to the green crosshair – a green spot) peaks at 507nm. This confirms that the observed green florescent spot are truly GFP positive.

2.12 Volocity Analysis

Volocity software (Improvision, Perkin Elmer) was used for 3D image reconstruction and analysis. Individual tile Z stacks were analysed for the presence of GFP. The intensity range of normal bone signals detected by CH-T2 were calculated between 500-4095 using a tibia from a naive (not injected with tumour cells) age matched mice. This was used to threshold the bone and thereby calculates the normal bone signals in the test samples. The intensity of GFP was calculated on regions which showed a peak at 507 nm in the lambda finger printing. These were found to be between a intensity of 551-4095 on CH-T3 channel and were used to threshold the GFP signals and calculate the number of object having green signals within this range. Further, the objects less than 500 μm^3 were excluded from the calculation based on previous studies (not published) that showed the normal size of 5T33MM cells were between 500-2000 μm^3. However, object greater than 2000 μm^3 were not excluded from the calculation as tumour cells seen in groups could give a combined volume of more than 2000 μm^3. In such cases these object were individually analysed based on manual judgement. The number of objects with GFP and the volume occupied by these object were computed for assessing the

number of tumour cells in the bone marrow of the tibia between the tumour and tumour-zoledronic acid treated group.

2.13 Experimental protocol to determine the time taken by zoledronic acid to have an effect osteoclastic bone resorption

The aim of this study was to determine the time taken by zoledronic acid at clinical dosage to effectively suppress osteoclastic bone resorption. Groups of 6 weeks old C57BLKalwRij mice (5 mice / group), were injected with of 125 µg / kg X2 /wk of zoledronic acid subcutaneously. Control mice (5 mice / group) were injected with PBS. They were periodically sacrificed at 7, 14 and 21 day after the treatment. The animals were starved without food and water 6 hr prior to sacrifice.

Figure 14: Schematic representation of the study design to determine the time taken by zol to have an effect of osteoclastic bone resorption

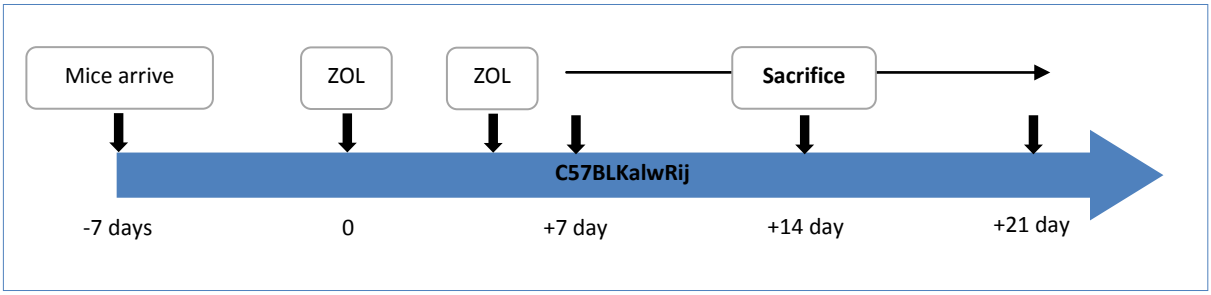

Mice were anaesthetized using 100 µl of pentobarbitone (lethal dosage) and cardiac blood samples were collected. Later death was confirmed by cervical dislocation and samples harvested. Left femur and left tibia (dissected free of soft tissues) was removed from each mouse and preserved in 10% formalin for micro computed tomography imaging and static histomorphometric analysis. The cardiac blood samples were centrifuged at 3000 RPM for 10 min in 4°C for serum extraction. Serum samples were made into suitable aliquots and stored at -80°C for ELISA analysis for bone markers.

2.14 Experimental protocol to determine the effect of zoledronic acid on the 5T33MM cell colonization and survival in bone.

The aim of this study was to investigate whether inhibiting osteoclastic bone resorption using zoledronic acid would affect the immediate homing and colonization of 5T33MM cells in the long bones of C57BL/KaLwRij mice. To achieve effective suppression of osteoclastic resorption, the C57BL/KaLwRij mice were pre-treated with zoledronic acid 7 days before 5T33MM-GFP cells were injection. As the main objective of the study is to determine whether zoledronic acid induced inhibition of bone resorption has any effect on the immediate homing and survival events of tumour cell in the bone, early time points of 18 hr and 72 hr post tumour cell injection were chosen. The 4 week time point in the study was to confirm that the 5T33MM-GFP cell successfully homed and colonised the bone. The early time point was chosen based on the evidence that

5T2MM were present in the BM 18 hr post injection of the tumour cells. In addition 5T2MM and 5T33MM were phenotypically similar and 5T2MM is analogous to human disease (Vanderkerken *et al.* 1997; Vanderkerken *et al.* 2000). The early events of tumour cell homing and colonisation in bone was analysed using multiphoton microscopy. The femurs were scanned for the presence of 5T33MM-GFP cell in the bone marrow after 18 hr and 72 hr after the injection of tumour cell.

Groups of 6wk old C57BL/KaLwRij mice (10 mice / group for 18 hr, 10 mice / group for 72 hr and 5 mice / group for 4 weeks) were pre-treated with zoledronic acid (125µg/kg X2 /wk subcutaneously) 7 days before 5T33MM-GFP cell injection. Equal number of mice (10 mice / group for 18 hrs, 10 mice / group for 72 hr and 5 mice / group for 4 weeks) were given PBS and served as controls for each time point. In addition at each time point 1 naive mouse and 1 zoledronic acid only treated mouse were used as controls. 7 days after treatment with zoledronic acid or PBS, 25 mice / group were injected with 2×10^6 5T33MM-GFP cells via the tail vein. The tail was anaesthetized using a topical anaesthetic agent Emla Cream (Lidocaine 25mg; Prilocaine 25mg) 1 hr prior to injection.

Prior to tumour cell injection GFP and CD11a profiling was done on the 5T33MM-GFP cells by flow cytometry (Methods shown in chapter 2.4). This was to confirm that the injected tumour cells contained adequate GFP expression and CD11a positive cells. Asosingh *et al.* 2003 showed that in vitro 5T33MM (5T33MMvt) cells depends on the expression of CD11a expression for colonisation and tumour development in the C57BLKalwRij mice. An approximate 50% population of CD11a positive 5T33MMvt-GFP was suggested to have a better tumour take rate in C57BL/KaLwRij mice by our collaborators in Belgium (K. Vanderkerken; unpublished data; personal communication).

Figure 15: Schematic representation of the study design to determine the effect of zoledronic acid on the 5T33MM cell colonization and survival in bone

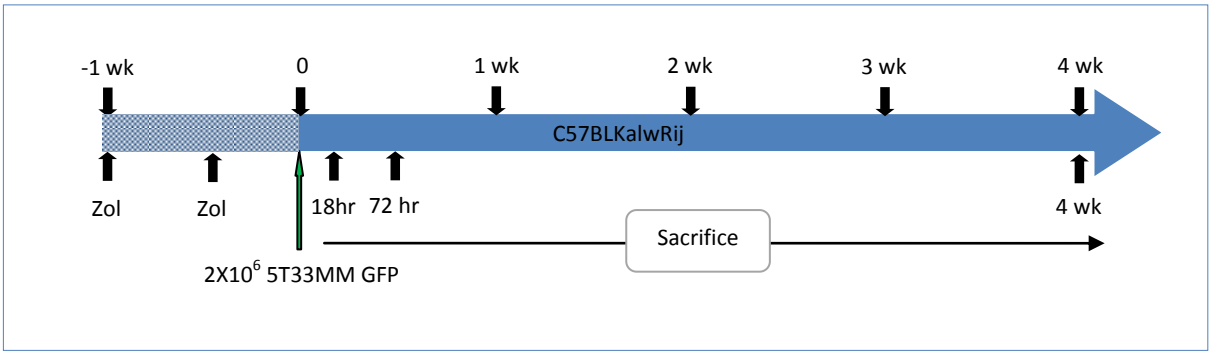

Mice were starved 6hrs prior to sacrifice, and then culled by anaesthetic over dosage followed by cervical dislocation. Cardiac blood samples (via cardiac puncture) were collected for serum extraction. Femur, tibia and lumbar vertebrae were harvested for analysis.

For the 18 hr and 72 hr, samples the left tibiae and femora, L3 lumbar vertebrae from all the mice were stored in 10% formalin for µCT analysis followed by histological sectioning and histomorphometric analysis. Right tibiae and femora, L2 lumbar vertebrae were dipped in dilute optimal cutting temperature solution (OCT), snap frozen in liquid N_2 and stored at -80°C. For the 4 week samples, the right femora, right tibiae and L2 lumbar vertebrae from all the mice were stored in PBS for GFP profiling of the BM to confirm tumour take The left femora and L3 lumbar vertebrae were stored in 10% formalin for µCT and histomorphometric analysis. All the serum samples were stored in -80°C for TRAP and PINP Elisa.

2.15 Statistical Analysis

Statistical analysis was done using *GraphPad Prism* 5. For the first study, to determine the effect of zoledronic acid on the inhibition of osteoclastic bone resorption, a non-parametric, one-tailed unequal variance 'student T test' was used to calculate the statistical difference between the control and the zoledronic acid treated group with a P value ≤ 0.05 as statistically significant. To determine the effect of zoledronic acid treatment on tumour homing and colonisation, a two tailed non-parametric student T test was used with a P value ≤ 0.05 as statistically significant. The graphs are displayed as Mean ± SEM.

Chapter 3

Results

3.1 Zoledronic acid suppressed bone resorption in C57BL/KaLwRij mice

3.1.1 Zoledronic acid treatment is associated with a reduction in osteoclast number

To quantify the effect of zoledronic acid on osteoclasts survival, static histomorphometric examination was done on the TRAP stained slide of the right tibial proximal metaphysis of C57BL/KaLwRij mice treated with zoledronic acid (Fig.16). Treatment with zoledronic acid showed a significant reduction in the number of osteoclasts seen on the surface of the trabecular bone after 7 and 21 day post treatment ($P<0.01$ & $P<0.05$). There was 65.5% and 36.3% reduction in the osteoclast number per mm of trabecular bone compared with age matched controls after 7 and 21 day respectively (Fig.17A). Similar pattern was also observed in the osteoclast surface occupancy with significant reduction in the surface occupied by osteoclast per mm of trabecular bone 7 and 21 day post treatment (Fig.17B).

For endocortical analysis, there was a 68.6% ($P<0.05$) decrease in osteoclast number seen after 21 day following treatment with zoledronic acid. However, no significant difference was observed at earlier time points (7 & 14 day) (Fig.17C). Likewise, a similar pattern was observed in the osteoclast surface occupancy over the endocortical surface of the bone with 72% ($P<0.05$) reduction observed 21 day post treatment with zoledronic acid (Fig.17D). Even though a 46.1% reduction in the osteoclast number and 62.5% reduction in the osteoclast surface occupancy observed after 7 days treatment, there was no statistical significance due to high variance.

Figure 16: Effect of Zoledronic acid treatment on trabecular morphology.

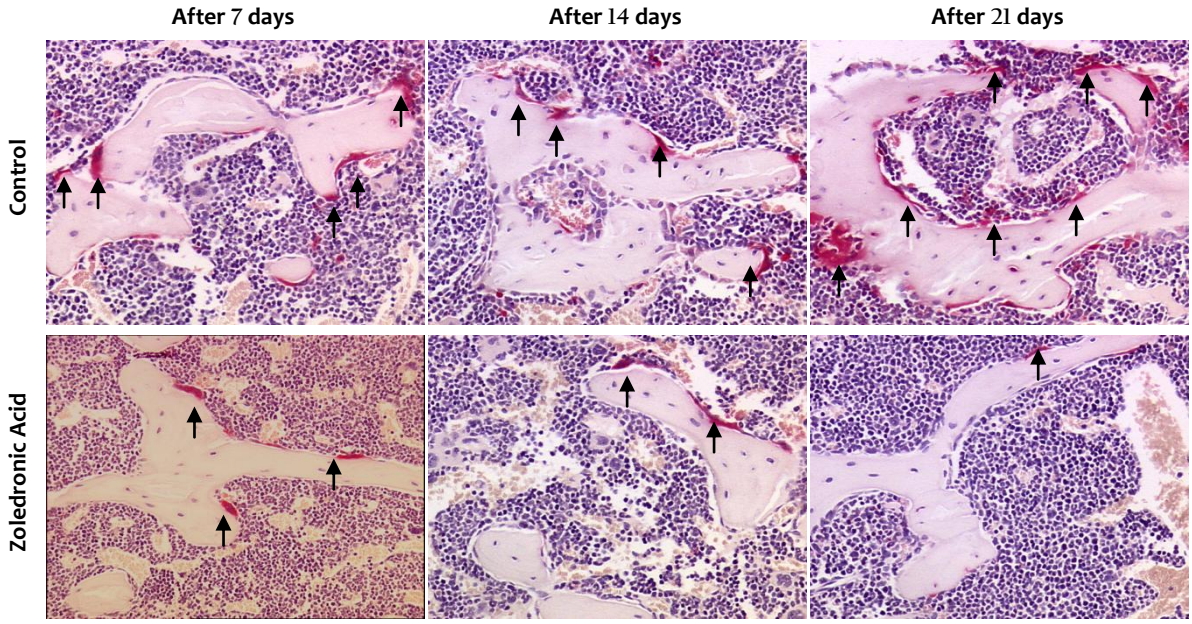

TRAP stained section (10X) of trabecular region (right tibia) showing osteoclast and osteoblast on the surface of the trabecular bone. The is a reduction in the number of osteoclast and osteoblast lining the trabecular bone in the zoledronic acid treated group compared with the untreated control group. Osteoclast are marked in black arrows

Figure 17: Osteoclast histomorphometric analysis of the effect of zoledronic acid treatment in naive C57BL/KalwRij mice

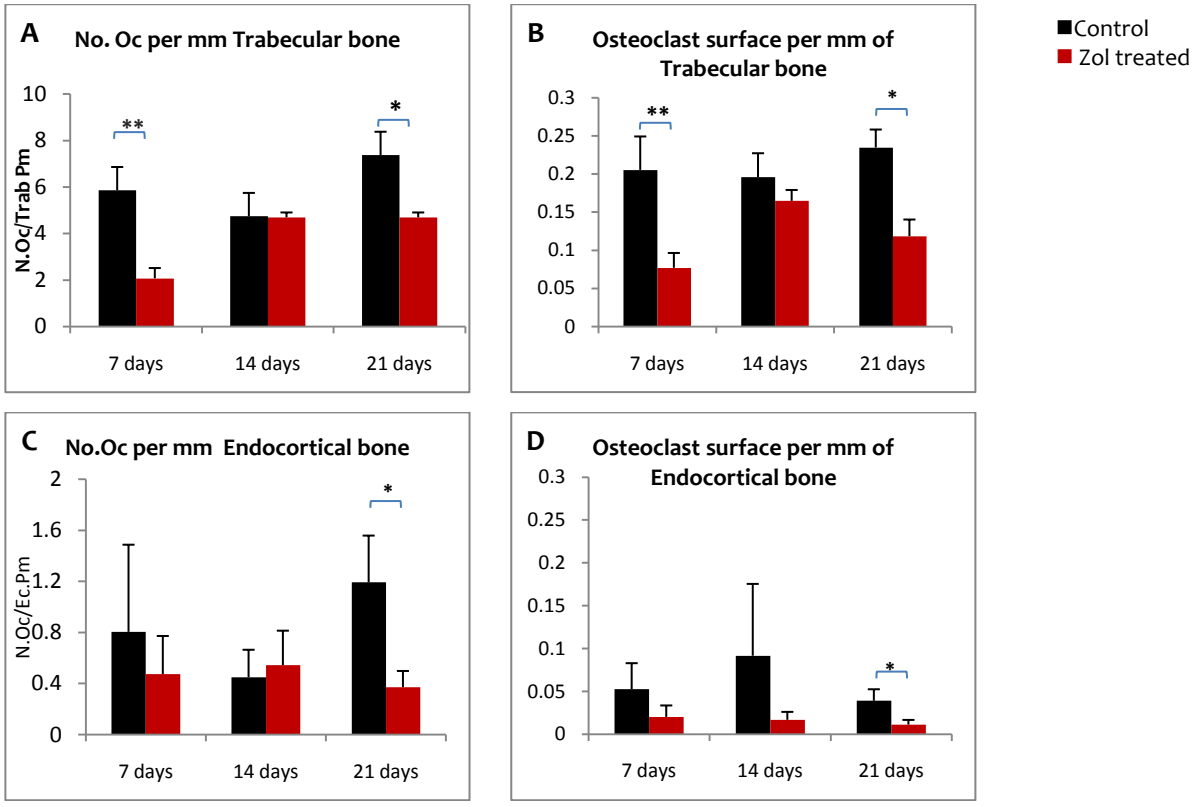

Graph shows the comparison of osteoclast parameters such as osteoclast number and surface occupancy per mm of bone in the trabecular and endocortical region of tibial proximal metaphysis between naive untreated mice and zoledronic acid treated mice.

3.1.2 Zoledronic acid treatment is associated with a reduction in osteoblast number

Histomorphometric analysis for osteoblast parameters on the tibial metaphysis demonstrated that zoledronic acid treatment caused a reduction in osteoblast number and osteoblast surface occupancy on both the trabecular and endocortical bone (Fig.18 A, B, C & D). Zoledronic acid treatment caused a significant 97% ($P<0.05$) and 72% ($P<0.005$) reduction in the number of osteoblasts on the trabecular and endocortical regions respectively, this was observed as early as 7 days after treatment. Although there was significant reduction ($P<0.05$) in the osteoblast number seen with zoledronic acid treatment at later points, the effect was high after 7 days and the effect was gradually reducing with increase in the increase in the time (97% after 7 days to 82.5% after 21 days in the trabecular region; 72% after 7 days to 65.7% after 21 days in the endocortical region).

Figure 18: Osteoblast histomorphometric analysis of the effect of zoledronic acid treatment in naive C57BL/KaLwRij mice

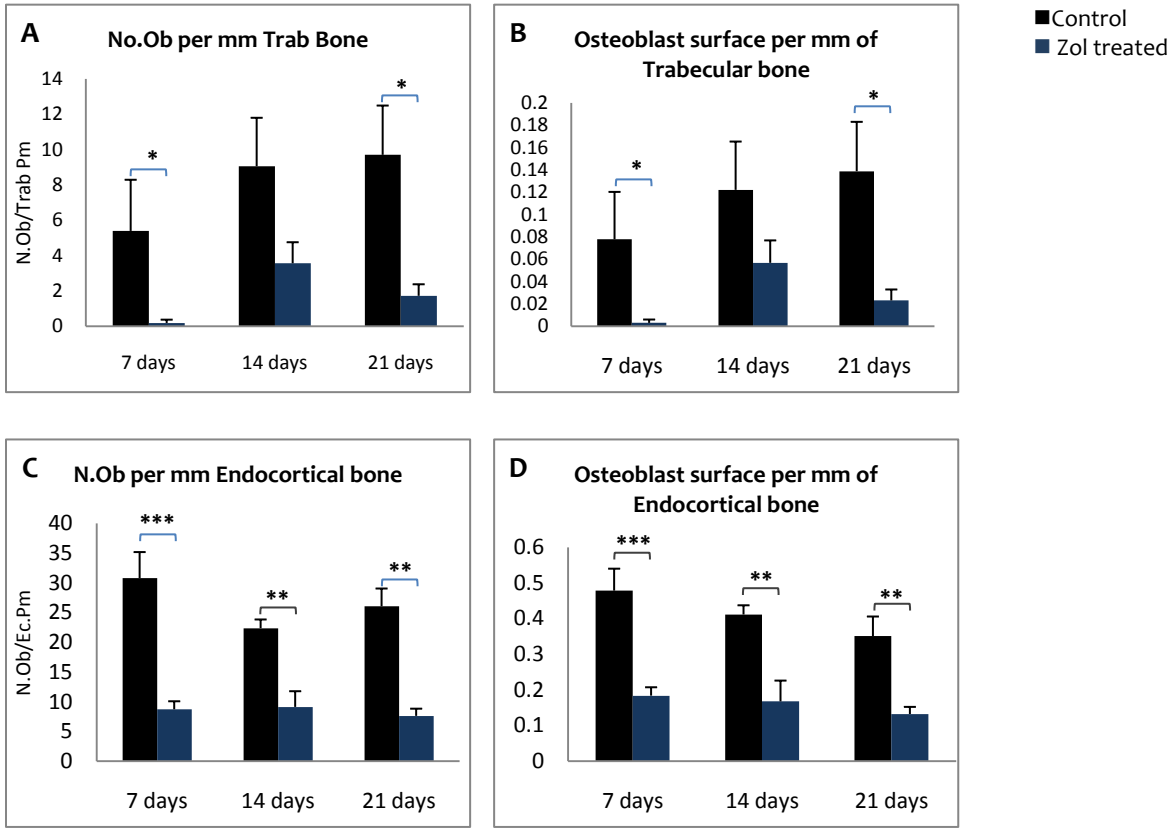

Graph shows the comparison of osteoblast parameters such as osteoblast number and surface occupancy per mm of bone in the trabecular and endocortical region of the proximal tibial metaphysis in untreated naive and zoledronic acid treated mice

3.13 Zoledronic acid treatment reduces osteoclastic and osteoblastic activity

The effect of zoledronic acid treatment on the inhibition of osteoclastic bone resorption activity was observed by measuring serum levels of TRAP5b and CTX. TRAP5b levels were significantly suppressed by approximately 60% after 7 days and by approximately 48% after 14 and 21 days post zoledronic acid treatment. A significant reduction in TRAP5b levels were observed at all the time points with a P value <0.01 (Fig.19A).

Similar to TRAP5b levels, there was a reduction in the levels of CTX observed at all three time points (7, 14 and 21 days). However, a significant difference was observed only until 14 and 21 days post treatment ($P<0.05$ after 14 & $P<0.01$ after 21 day) (Fig.19B). Although there was approximately 55% reduction in the CTX levels observed 7 day post-treatment with zoledronic acid compared to untreated control, it did not reach significance due to high intra-group variation. One possible explanation for this high variance is that the CTX values are extremely sensitive to haemolysed serum.

An interesting observation was the trend of TRAP and CTX with an increase in the age of the mice as observed from the control groups. There was a gradual increase in the TRAP values, while there was a reduction in the CTX values. TRAP5b is an enzyme released from active osteoclasts during the process of bone resorption, while CTX is a bone matrix degradation product released at the end of resorption. Therefore TRAP is released during early events of resorption and CTX is released in later events of resorption, this could account for the difference seen here.

Figure 19: Effect of zoledronic acid on the serum levels of TRAP5b and CTX.

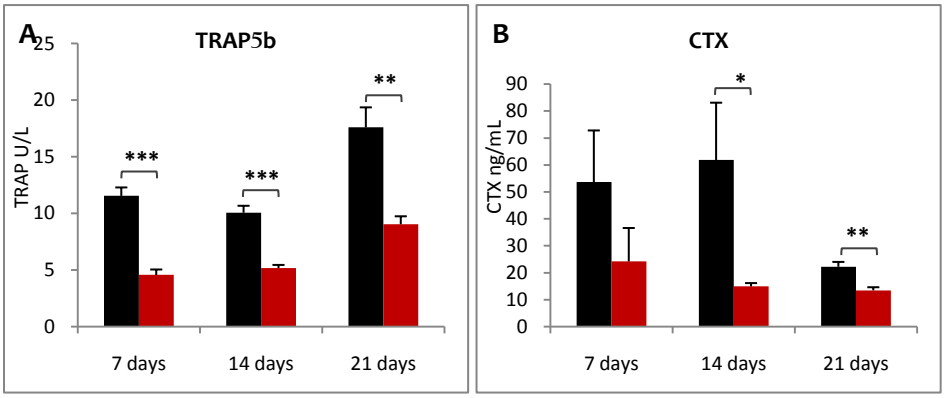

Graph shows the serum levels of bone resorption markers TRAP (A) and CTX (B) after 7, 14 and 21 day following treatment with zol (red) compared with untreated naive control mice (black).

■Control
■Zol treated

The effect of zoledronic acid osteoblastic activity was assessed by measuring serum levels of PINP and osteocalcin. Serum levels of PINP showed significant reduction of 57%, 61% and 50% reduction in the zoledronic acid treated groups after 7, 14 and 21 days with a P<0.01 at all the time points (Fig. 20A). The results reflected the histomorphometric data on the osteoblast number. However, no significant difference was observed with osteocalcin levels at any time point. Although our data showed a reduction in the CTX serum levels after 7 and 14 days, they were not statistically significant. due to high variation. Further, at the 21 day time point there was no difference observed between the treated and the control groups (Fig. 20B).

Figure 20: Effect of Zoledronic acid on the serum levels of PINP and Osteocalcin.

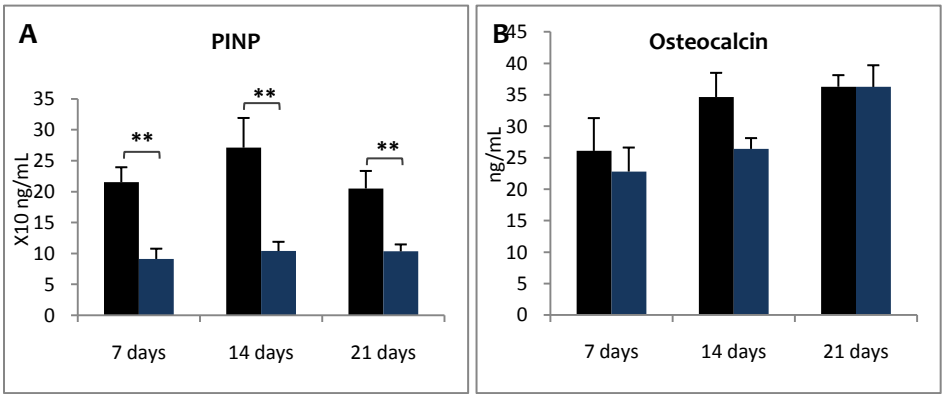

Graph shows the serum levels of bone resorption markers PINP (A) and Osteocalcin (B) after 7, 14 and 21 day following treatment with zoledronic acid treated (blue) compared with untreated naive control mice (black).

■Control
■Zol treated

3.1.4 Zoledronic Acid treatment results in a greater cortical and trabecular bone volume in the tibia

μCT analysis was performed on proximal metaphysis of the right tibiae of both the untreated control and zoledronic acid treated mice to determine the structural consequence of treatment. Zoledronic acid treatment was associated with 68%, 139% and 340% greater trabecular bone volume after 7, 14 and 21 days post treatment respectively (Fig.21). A significant difference between the control and zoledronic cid treated mice was observed at all three time points ($P<0.001$) (Fig.23A). In accordance with a greater bone volume, there was also a significant increase in the trabecular number observed at all three timepoints ($P<0.001$ after 7 and 14 days and $P<0.01$ after 21 days respectively) (Fig.23C). Conversely, there was no difference seen in the mean trabecular thickness between the zoledronic acid treated and untreated control mice at all three timepoints (Fig.23D). There was also significant greater cortical bone volume with a 31%, 14% and 56% increase observed after 7, 14 and 21 days post treatment respectively ($P<0.01$) (Fig.23B).

Structural model index (SMI) is a graphical representation of the micro architecture of the cancellous bone with values between 0 and 3 representing more plate-like or more rod-like structure respectively. Zoledronic acid treatment was associated with a significant decrease in SMI (more plate-like) at all three timepoints. Interestingly, the untreated control mice showed an increase in the SMI values with an increase in age which is due to normal bone resorption converting the plate-like trabeculae into more organized rod-like structure. However, in the zoledronic acid treated group there seemed to show an inverse relationship with decrease in SMI values with an increase in age (Fig.23E). Although each timepoint is an independent experiment with absolutely no influence on the other, it still can be assumed that zoledronic acid treatment drives the trabecular architecture into a more plate-like structure. There was no significant difference in the bone mineral density (BMD) seen after 7 and 14 days post treatment, however a significant 5% reduction was seen after 21 days post treatment ($P<0.05$) (Fig.23F).

Figure 21: Cross sectional images of tibial metaphysis between naive and zoledronic acid treated C57BL/KaLwRij mice

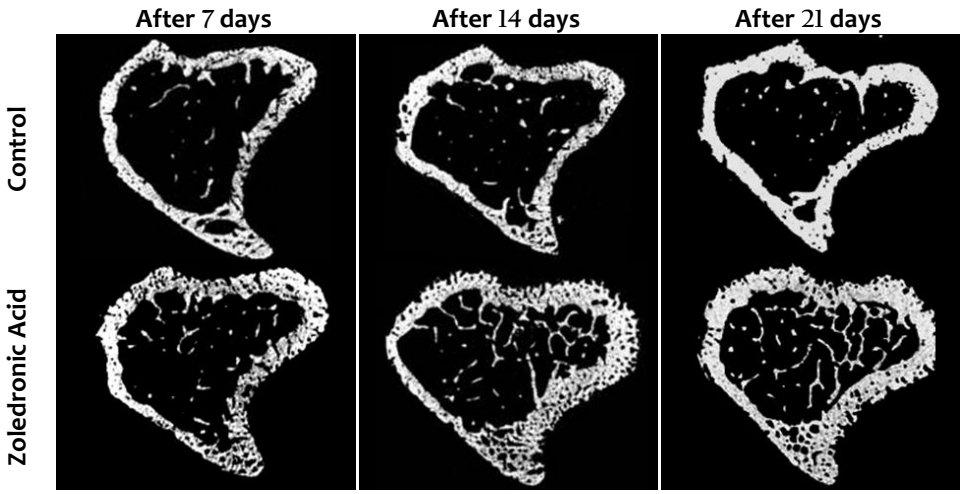

Comparison between μCT cross sectional images of tibial metaphysis taken at a distance of 1 mm from the proximal break in the growth plate showing greater trabecular and cortical bone in the zoledronic acid treated mice compared with naive untreated control after 7, 14 and 21 day following treatment

Figure 22: 3D models (µCT) of proximal tibial metaphysis of naive and zoledronic acid treated C57BL/KaLwRij mice.

Figure 23: Quantitative µCT analysis of the trabecular and cortical parameters in naive and zoledronic acid treated C57BlKalwRij mice

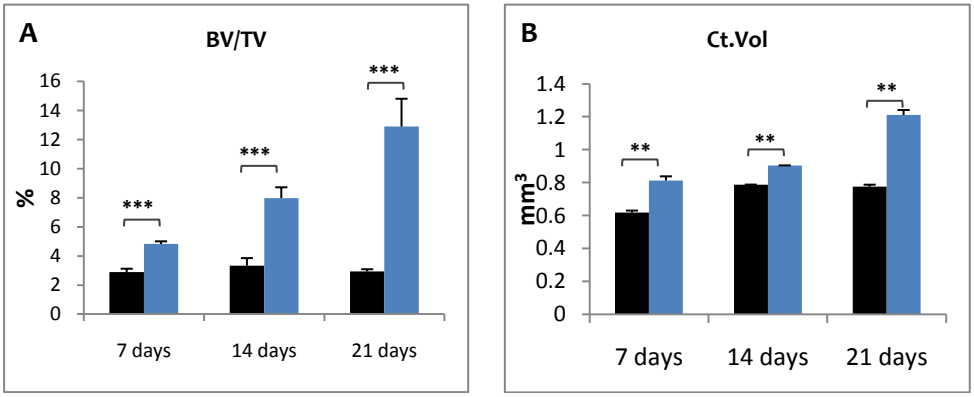

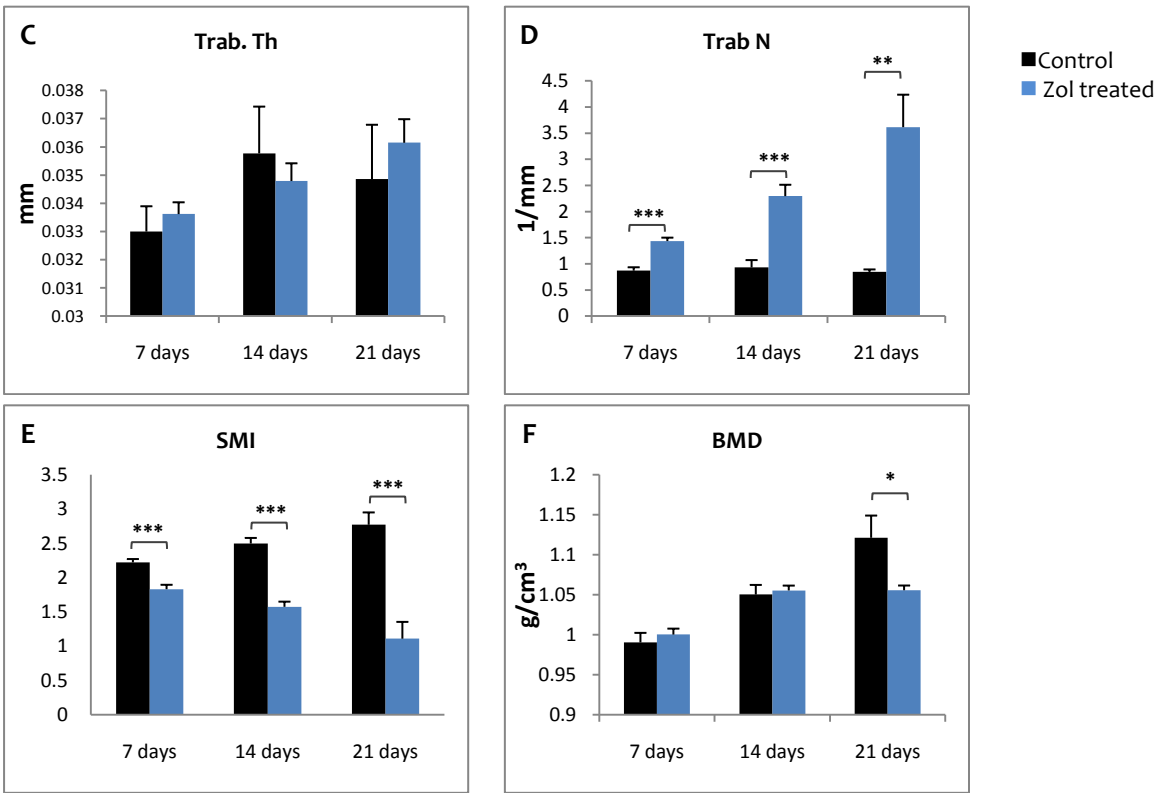

Graph shows quantitative analysis of µCT parameters such as A. percentage trabecular bone volume (BV/TV), B. cortical volume (Ct.V), C. Trabecular thickness (Trab Th), D. Trabecular number (Trab N), E. Structural model index (SMI), F. Bone Mineral Density (BMD) of zoledronic acid treated and control C57BL/KaLwRij mice

3.2 Effect of zoledronic acid on tumour cell homing and colonization in the bone

In this second study C57BL/KaLwRij mice were pre-treated with zoledronic acid 1 week before being injected with 5T33MM-GFP cells via the tail vein. Mice were sacrificed after 18 hr, 72 hr and 4 week post injection. 5T33MM-GFP cells were identified in the BM of tibia by multiphoton microscopy. The effect of zoledronic acid treatment the number of GFP positive tumour cells in the BM was compared between untreated tumour control and zoledronic acid treated mice by volocity analysis. However, initially to confirm whether a 7 day post treatment strategy has effectively inhibited osteoclast mediated bone resorption, as indicated by the previous study the effect of zoledronic acid on the bone was assessed by histomorphometric, TRAP and PINP bone markers and µCT analysis

3.2.1 Zoledronic acid treatment is associated with reduction of osteoclast number in C57BL/KaLwRij mice injected with 5T33MM-GFP cells

A 7 day post treatment strategy with zoledronic acid showed significant reduction in the number of osteoclasts and surface occupancy per mm of the trabecular bone of the femur compared with age matched mice injected with tumour cells alone at 2 time points (Fig. 24) (i.e. 18 & 72 hr). There was a 63% and 53% reduction in the osteoclast number observed at 18 hr ($P<0.001$) and 72 hr ($P<0.01$) post tumour cell injection

respectively (Fig. 25A). A similar pattern of inhibition in the osteoclast surface occupancy per mm of trabecular bone was also observed in the zoledronic acid treated tumour mice compared with untreated tumour controls. The 4 week time point was not analysed due to time constrain.

Zoledronic acid treatment was also associated with a significant reduction in the osteoblast number and surface occupancy per mm trabecular in tumour treated mice compared with untreated control tumour (Fig. 25B).

Figure 24: Effect of zoledronic acid pre treatment mice bearing 5T33MM-GFP cells.

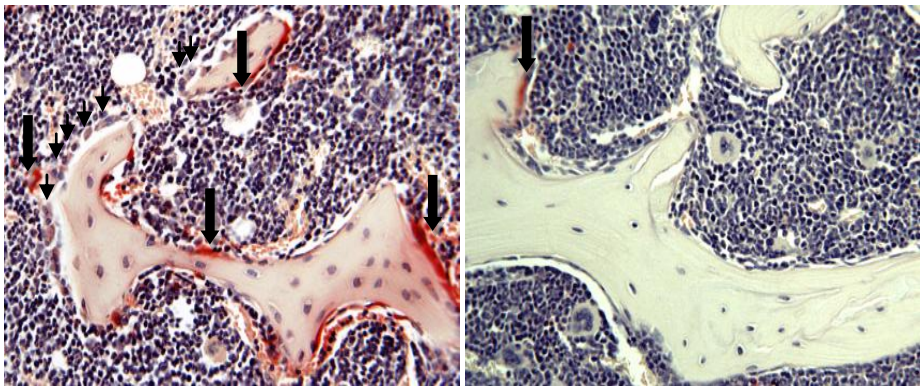

Histological sections of the trabecular region of distal femoral metaphysis from (A) a control PBS treated mice injected with 5T33MM-GFP cells (2 X 10^6) (B) mice pre-treated with zoledronic acid injected with 5T33MM-GFP cells showing a reduction in the number of osteoclast (black bold arrows) and osteoblast (black thin arrows) lining the bone surface, in the zoledronic acid pre-treated animal.

Figure 25: Histomorphometric assessment of zoledronic acid pre-treatment in mice bearing 5T33MM-GFP cells

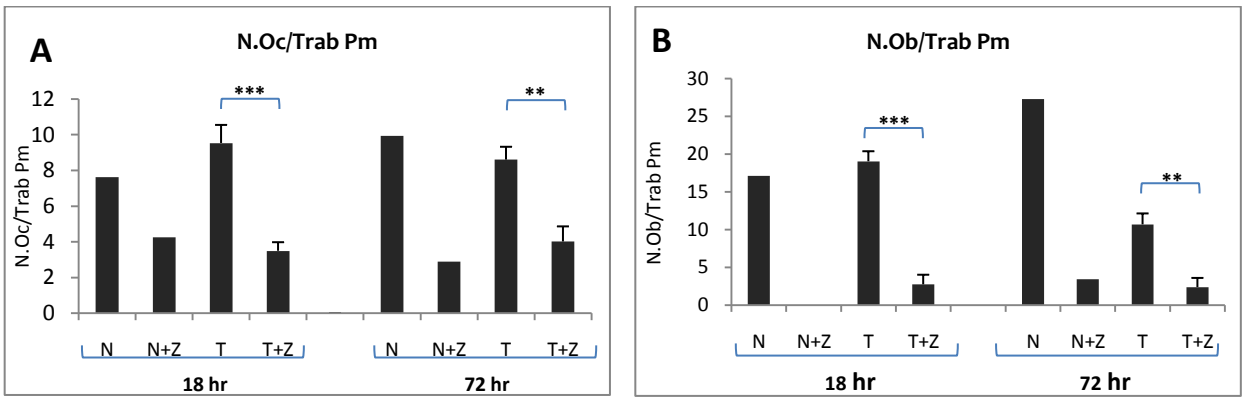

Graph represents the changes in the histomorphometric data such as osteoclast number per mm of trabecular bone (A) and osteoblast number per mm of trabecular bone (B) in the distal femoral metaphysis between zoledronic acid pre-treated 5T33MM-GFP cell bearing mice (T+Z) compared with PBS treated tumour control (T) animal injected with 5T33MM-GFP cell only after 18 and 72 hr post tumour cell injection. Untreated naive (N) and naive treated with zoledronic acid (N+Z) (not injected with tumour cells) age matched mouse served as control for each time point.

3.2.2 Zoledronic Acid treatment is associated with reduction in osteoclastic and osteoblastic activity in C57BL/KaLwRij mice injected with 5T33MM-GFP cells

A significant reduction in serum TRAP5b levels were observed in tumour treated mice compared with untreated tumour mice at all three timepoints (18, 72 and 4 weeks) (Fig. 26A). Absolute serum TRAP5b levels of 5T33MM-GFP mice not treated with zoledronic acid were similar to naive age matched control. Similarly serum TRAP5b levels of zoledronic acid treated mice matched those of non-tumour zoledronic acid treated age matched mice. Over time an increase in the TRAP5b levels among all the groups was observed. These results suggest a reduction in the activity of zoledronic acid over time post treatment (which is observed as a 53% reduction in TRAP levels at 18 hr reducing to 48% and 38% after 72hr and 4 week respectively).

As expected there was also a significant reduction in the serum PINP levels seen in the zoledronic acid treated groups compared with non-treated groups (naive and 5T33MM-GFP) at all time points (P value < 0.001 at 18 hr, 72 hr and 4 week post inoculation) (Fig.26B).

Figure 26: The effect of zoledronic acid treatment on the serum levels of TRAP and PINP on the 5T33MM-GFP tumour cell mice. at 18hr and 74 hr post tumour cell injection

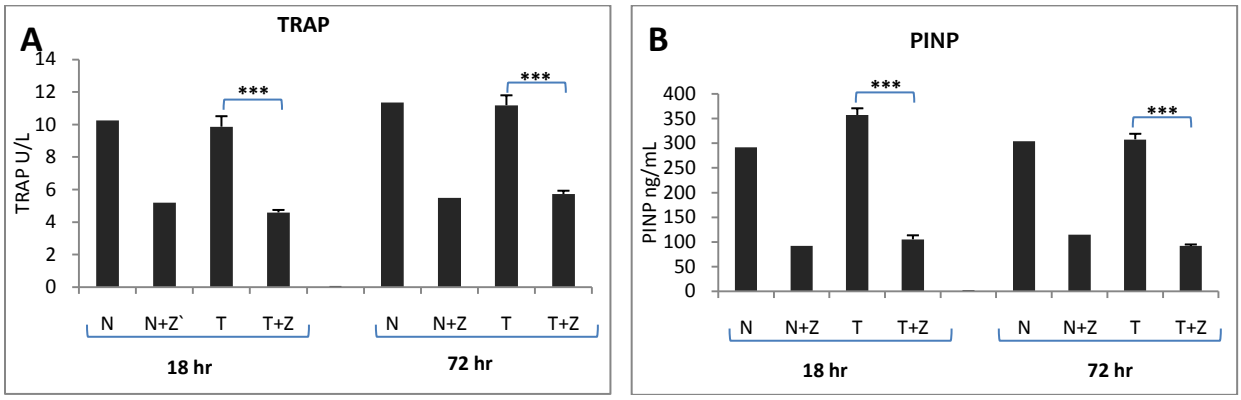

Graphs shows a reduction in the serum levels of TRAP (A) and PINP (B) between the zol treated tumour group (T+Z) when compared with vehicle treated control (T) both after 18 and 72 hr post tumour cell injection. The tumour only group (T) showed values similar to those of naive control (N) and the tumour treated with zol were similar to those of zol treated naive (N+Z) animal. The difference after 4 week was not shown.

3.2.3 Zoledronic acid treatment resulted in greater trabecular bone volume in the vertebrae of C57BL/KaLwRij mice injected with 5T33MM-GFP cells

µCT analysis was done on the trabecular bone of the L3 lumbar vertebrae of all mice. There was significant greater trabecular bone volume (BV/TV) in the tumour mice treated with zoledronic acid compared with the untreated tumour control group (P< 0.001) observed at all time points (Fig. 28A). Unlike the tibia, there was a significant increase in both the trabecular thickness and trabecular number seen at all the time points in the vertebrae, whereas in the tibia there was no evidence of increase in the trabecular thickness with zoledronic acid treatment even after 21 days following treatment. One possible explanation for this variation is the difference in the method used in analysing the trabecular regions in the tibia and vertebrae. In tibia, the

proximal metaphysis is analysed for the trabecular analysis. Here there is an uneven distribution of thicker trabeculae near the growth plate and thinner trabeculae near the diaphysis. However, in the vertebrae the ROI chosen is an isovolumetric cylinder extending between the two growth plates which comprises of both thicker and thinner trabeculae which compensates for the intra-sample variation and hence the intra-group variation.

There was also significant reduction in the trabecular pattern factor (Tr. Pf) and SMI at all the timepoints (Tr. Pf $P< 0.01$; SMI $P<0.05$) (Fig. 28D & E). There was a slight increase of ~3% in the BMD observed in 4 week tumour treated group ($P<0.05$) (Fig. 28F). Taken together these results confirm zoledronic acid is having an effect on bone as previously seen in the initial study on naive mice.

Figure 27: Effect of zoledronic acid treatment in the trabecular architecture of the lumbar vertebrae in 5T33MM-GFP tumour bearing mice

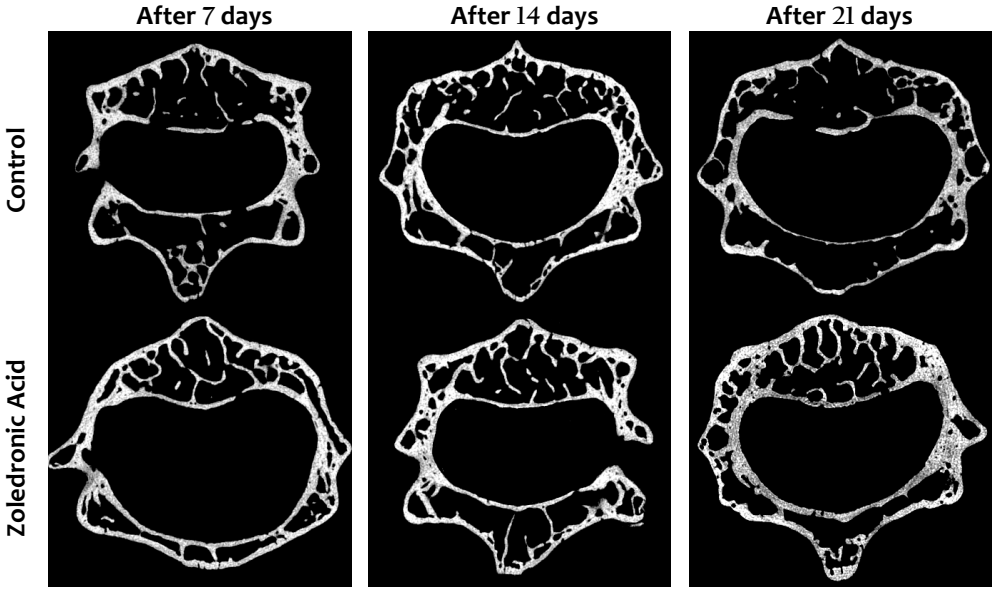

Cross-sectional images of the L4 lumbar vertebrae showing greater trabecular and cortical volume with increase in the trabecular number and thickness in the zoledronic acid pre-treated tumour cell bearing mice compared with vehicle treated tumour control mice.

Figure 28: Quantitative µCT analysis of the trabecular bone in the L3 lumbar vertebrae 5T33MM-GFP tumour bearing and untreated vehicle control mice

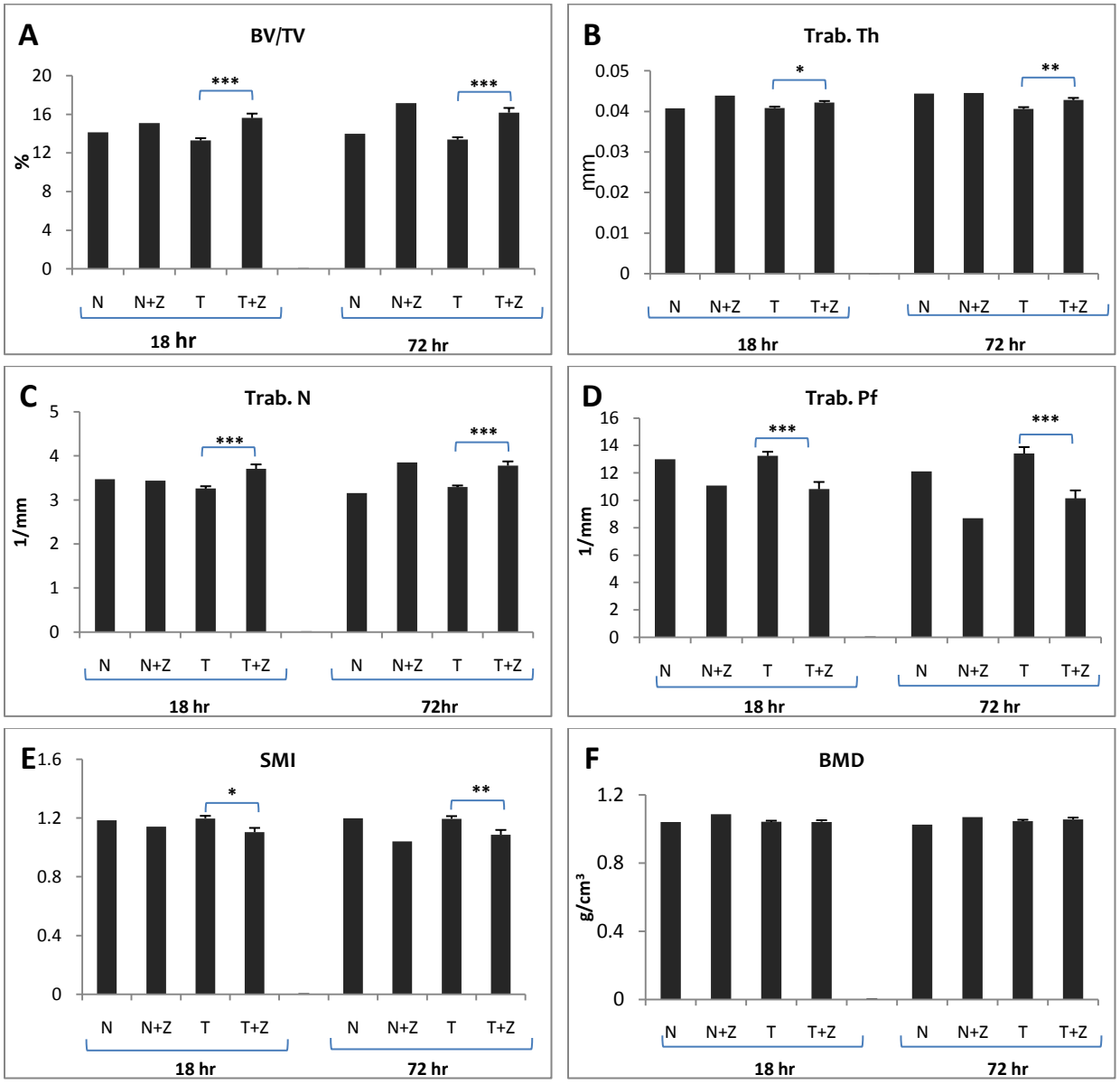

Graph represents the µCT trabecular analysis of L4 lumbar vertebrae between zol treated tumour mice (T+Z) and vehicle treated tumour control mice (T). Changes in trabecular bone volume (A), Trab. Th (B), Trab. N (C), Trab. Pf (D), SMI (E) and BMD (F) are shown in mean ± SEM with a $P < 0.05$ as significant *.The difference in parameters observed at 4 week time point was not shown

3.2.4 GFP profiling

Prior to 5T33MM-GFP cell injection to the mice the percentage of GFP positive cell in the culture were analysed by flow cytometry analysis to confirm whether adequate GFP positive population were present in the culture. 5T33MM-WT cells were used as controls. Results showed that more than 99% of the cell population were positive for GFP (Fig. 29).

Figure 29: GFP profiling of *in vitro* 5T33MM GFP cells in culture by flow cytometry

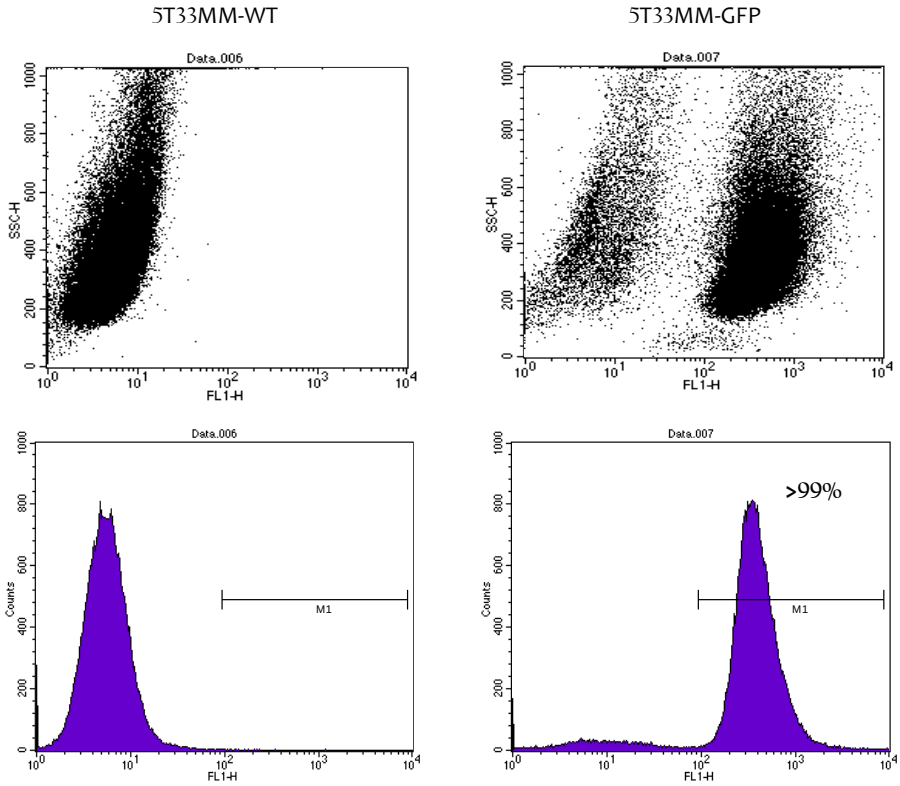

3.2.5 CD11a profiling

Analysis of CD11a profiling was done on the potentially viable cell population by gating the viable cells. Fig 30 shows the CD11a profiling flow cytometry data of the 5T33MM-GFP population used in our study.GFP is seen on the FL1 channel and CD11a on the FL2 channel. For methods refer section 2.4 .Results showed an approximately 90.94% population of cells were positive for GFP, 66.84% of cells were positive for CD11a and 62.88% were positive for both.

Figure 30: CD11a profiling of the *in vitro* 5T33MM-GFP cell in culture by flow cytometry

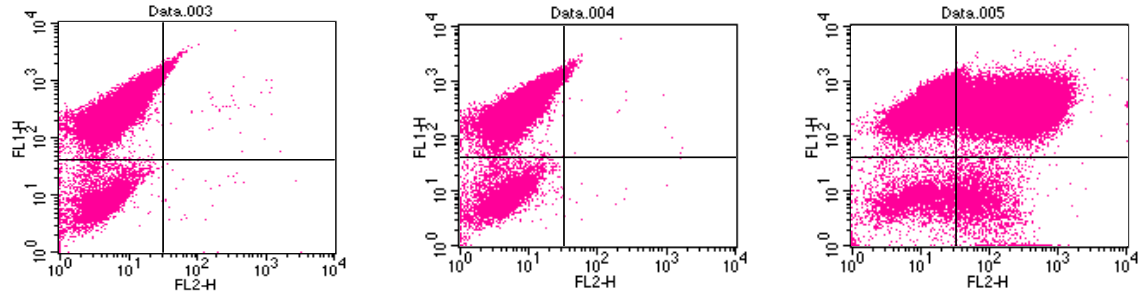

No Antibody | Isotype control | CD11a antibody

3.2.6 5T33MM-GFP cells were seen in the BM of femur, tibia and vertebrae after 4 week post tumour cell injection

In addition, to confirming zol was altering the bone as expected, conformation of tumour take of the 5T33MM-GFP cells was also performed. BM flushes of the femur, tibia and L_2 vertebrae was analysed by FACS. The data shows GFP positive events ranging from 0.01% to 7.42% for every 100,000 events measured by flow cytometry (Fig. 31). Although the percentage of GFP positive events were less, 5/5 mice from both zoledronic acid treated and untreated control groups showed GFP positive events in either of femur, tibia or vertebrae, thus confirming 100% tumour take in this study.

Figure 31: Flow cytometric analysis showing 5T33MM-GFP positive cells in the BM of C57BL/KaLwRij mice injected with *in vitro* 5T33MM-GFP tumour cell after 4 weeks post injection

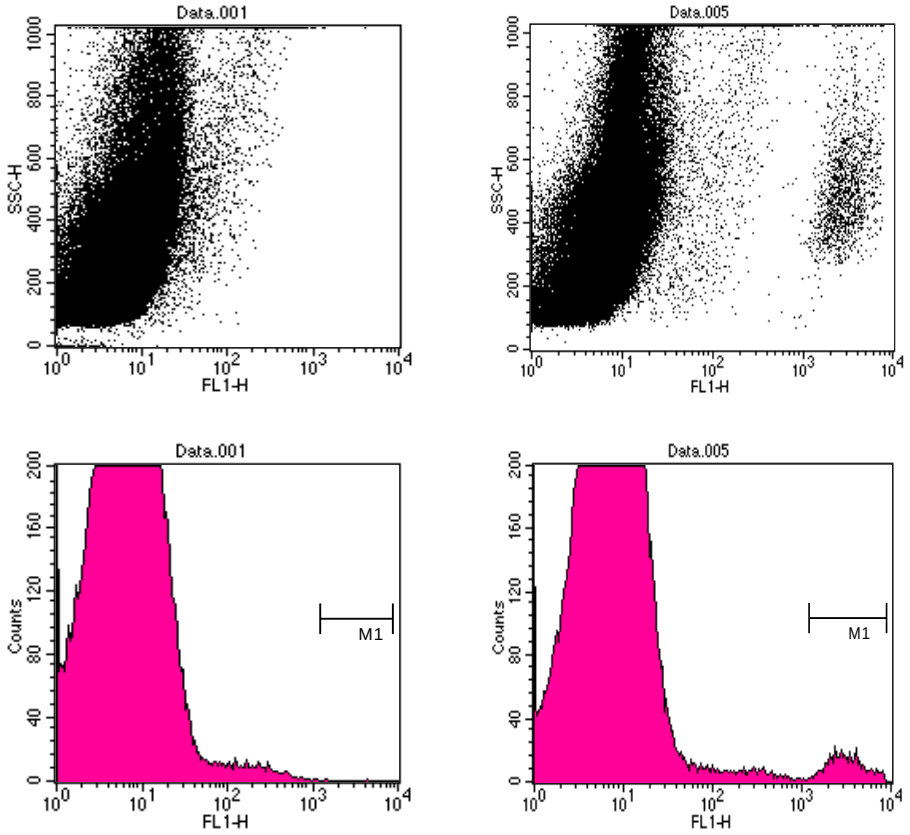

Fig. shows the flow cytometric analysis data of the BM from femur of mice injected with tumour cells (both zol treated and untreated controls). The normal bone marrow contents were gated from the GFP expressing cells by using a femur BM sample from an age matched naive mice without tumour cell injection

3.2.7 Pre-treatment with zoledronic acid does not reduce tumour cell homing and colonizing the tibia after 18 hr post-inoculation

The presence of 5T33MM-GFP cells were established by spectral finger printing as described in section 2.1.1. Comparing the GFP emission spectra *in vitro* of a GFP cell with the emission spectra of the green object seen in the scan confirms that the visualised green object is a true GFP cell (Fig. 32).

Figure 32: Spectral ginger printing of in vitro 5T33MM-GFP cell and comparing with the spectral finger printing of the green florescent object in the bone scan

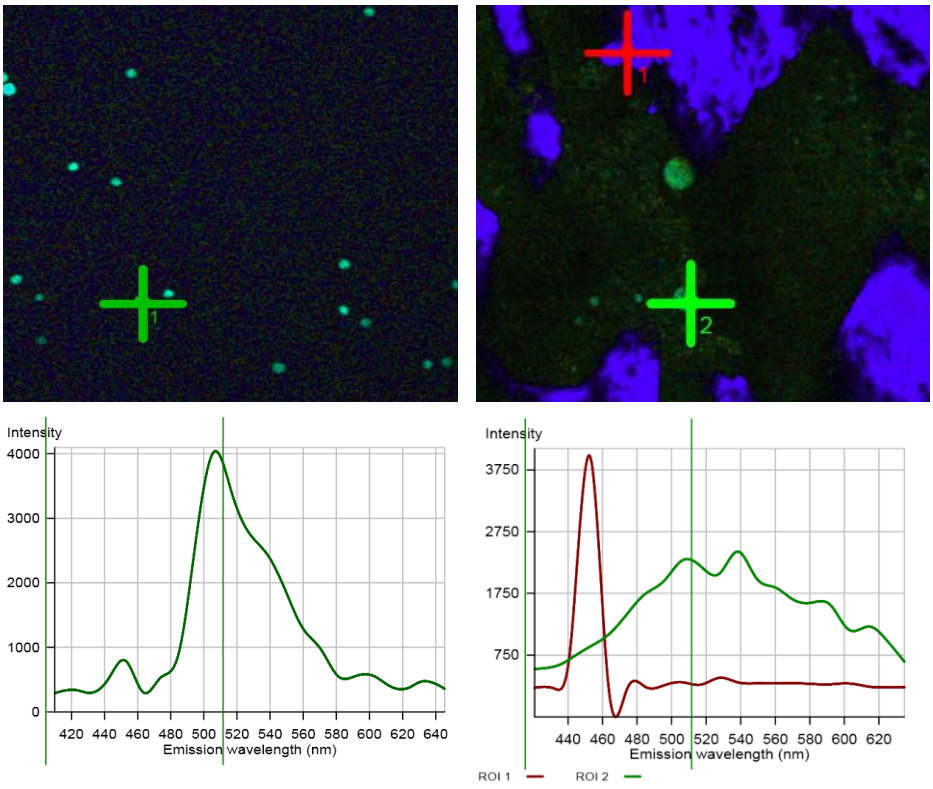

A. In vitro 5T33-GFP finger printing **B. In vivo spectral finger printing**

Figure shows spectral finger printing of *in vitro* 5T33MM-GFP cells and its GFP emission spectrum peaks at 507nm with maximum intensity. Similarly, fig. shows the spectral finger printing data of a GFP positive object seen in the bone marrow. The bone shows a maximum emission at a wavelength of 450nm (red crosshair) whereas the GFP object (green crosshair) shows a maximum intensity at 507nm.

Figure 33: Multiphoton microscopic image of the tibial metaphysis of naive (untreated, no injection of tumour cell) and 5T33MM-GFP cell injected mice.

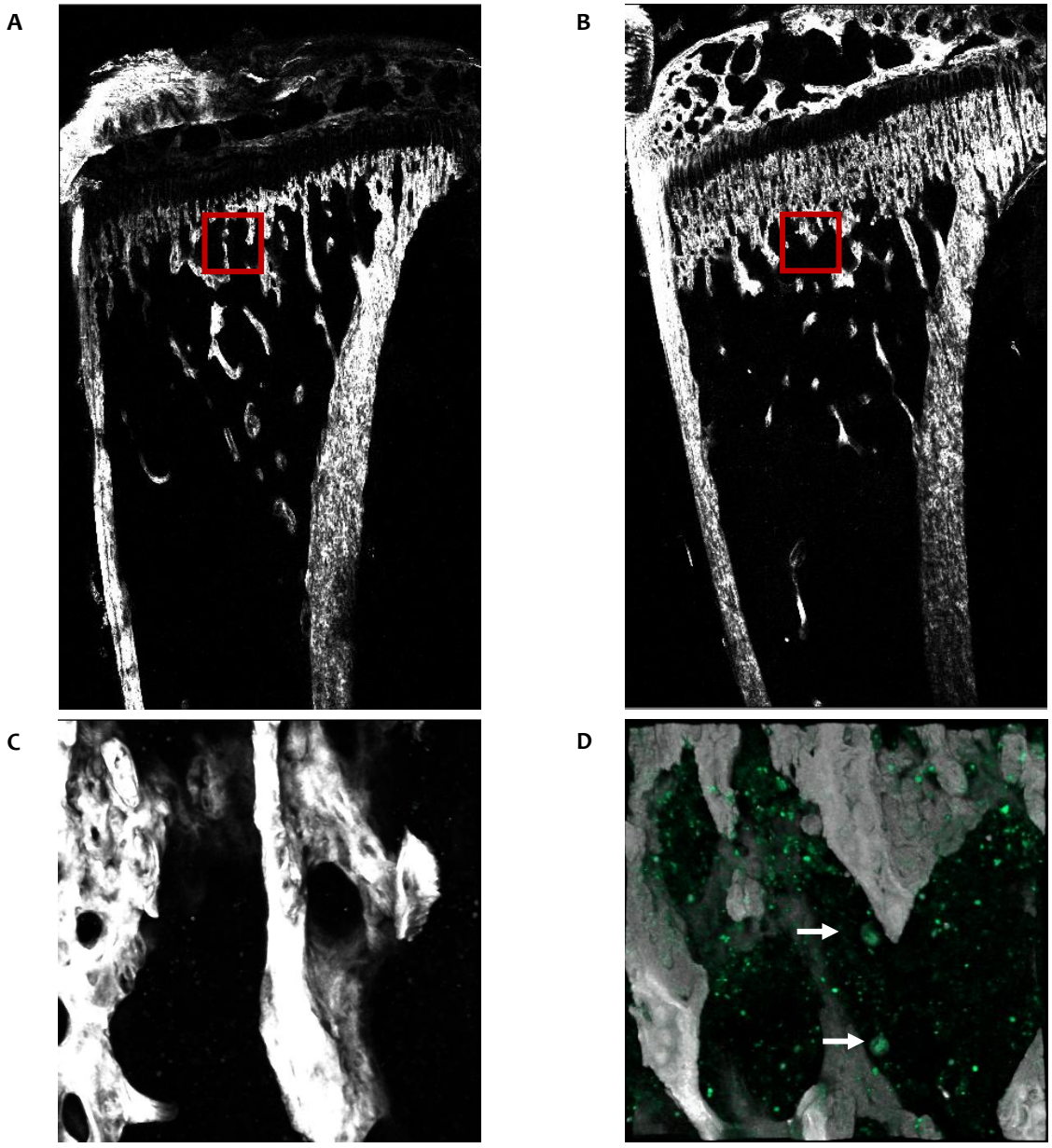

Pilot images on the top (A & B) are multiphoton microscopic image of the proximal end of the tibia including the epiphysis showing trabecular architecture as seen on the multiphoton microscope containing 60 tiles (10 X 6) in a Z stack fashion; each tile measuring 450 X 450 X 75 μm^3. Images on the bottom (C & D) are 'Z' stacks of a single tile showing 3D image of the bone marrow with the bone in grey scale and 5T33MM-GFP cell in green (white arrow)(D only).

Reconstructed 3D images were analysed for quantifying the number of GFP positive object in tibiae of both tumour and tumour treated mice using volocity software. The algorithm was set to measure the number and volume of the GFP positive objects with an intensity between 551-4095 in the green channel (CH-T3). Analysis showed no significant difference in the number of GFP positive tumour cells between the tumour control mice and tumour mice treated with zoledronic acid treatment (Fig 34A). However, there almost a 30%% reduction in the number of tumour cells in the zoledronic acid treated group. Similar to GFP positive cell number, there was a 33% reduction in the mean cell volume occupied by the GFP positive cell in the zol treated group compared with untreated control, but this was not statistically significant (P>0.05) (Fig. 34B). Although there was a reduction in almost one-third of the tumour cell number and tumour cell volume there was no statistical significance due to high intra-group variation. Interestingly there was also a 13% reduction in the mean volume per cell in the zoledronic acid treated group (Fig. 34C).

Figure 34: Effect of zoledronic acid treatment on the number of 5T33MM-GFP cell seen in the BM of tibial metaphysis by multiphoton microscopy

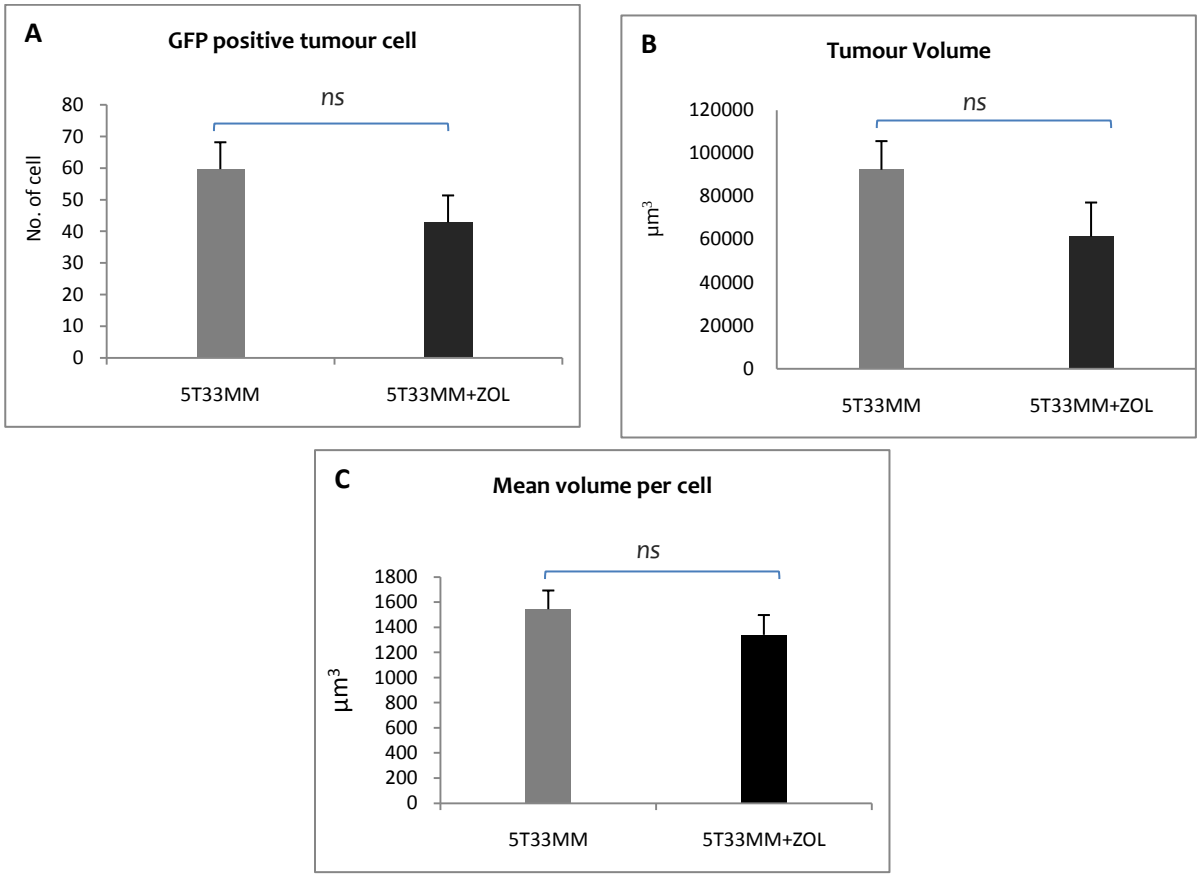

Chapter 4

Discussion

4.1 Discussion

In this report the effect of zoledronic acid treatment on 5T33MM-GFP tumour cell colonisation has been investigated. An initial study was performed to assess the effect of zoledronic acid treatment on the inhibition of osteoclast mediated bone resorption in naive C57BL/KaLwRij mice over time using clinically relevant dosage. To the best of our knowledge this is the first study to investigate the effect of zoledronic acid on naive C57BLKalwRij mice (syngeneic 5TMM model) over a time scale of 3 weeks treatment. Zoledronic acid treatment (125 µg/kg X2 /wk s.c.) showed a reduction in both osteoclast survival and activity evidenced by a reduction in the number of osteoclasts seen in trabecular and endocortical bone by quantitative histomorphometry and a reduction in osteoclast activity seen as a reduction in TRAP5b and CTX levels in the serum of zoledronic acid treated mice. Zoledronic acid caused 65.5% reduction in the osteoclast number soon after 7 days following treatment and the effect persisted even after 21 days with a 36% reduction ($P<0.05$). Similar results were shown by Pozzi and colleagues (2009) when C57BL6 mice were treated with zoledronic acid (single dose 500µg/kg) a reduction in the number of osteoclasts per mm of trabecular bone after 3 weeks post treatment was observed (Pozzi *et al.* 2009). Several preclinical studies have shown that zol treatment is associated with the inhibition of osteoclastic resorption and prevention of bone loss induced by different pathological states like cancer (breast cancer, multiple myeloma), oestrogen deficient rats, and osteoporosis (Croucher *et al.* 2003; Duivenvoorden *et al.* 2007; Mohammad *et al.* 2010). Also, in our study, there was a 60% reduction in the serum TRAP5b levels associated with zoledronic acid treatment which gradually reduced to 48% after 21 days. Our results were similar to the work done by Wiley and colleagues (2010) who showed similar reduction in TRAP5b levels in C57BL6 mice following risedronate treatment. However, there was only a 36% reduction observed after 1 week (Willey *et al.* 2010). The difference in the efficacy between zol and risedronate or the age group of the mice (20 weeks) might account for the difference in the TRAP5b levels (Giovanni Iolascon 2010). Similarly reduction in TRAP levels was also observed with zoledronic acid treatment (Pozzi *et al.* 2009)

Interestingly, in our study there was a significant reduction in the osteoblast number and osteoblast surface occupancy (on both trabecular and endocortical surfaces) accompanied with a significant reduction in PINP and osteocalcin levels in the serum as early as 7 days post treatment (refer results section for statistical significance). These results show that treatment with zoledronic acid, in addition to osteoclast inhibition also affect osteoblasts. This could be either due to a direct cytotoxic effect on the osteoblasts or an indirect effect where a reduction in osteoblasts is relative to a reduction in osteoclasts as bone formation and resorption are a coupled phenomenon. Moreover, there is evidence of a direct cytotoxic effect of zol on osteoblasts *in vitro* (Pozzi *et al.* 2009). Alternatively, in another study done by our group, a similar or even more potent reduction in osteoblast number and serum levels of PINP was observed with FcOPG treatment supporting an indirect mechanism (unpublished data, personal communication). Therefore, the mechanism responsible for this osteoblast inhibitory effect of zoledronic acid is not clear and currently under further investigation.

μCT analysis was undertaken for the qualitative and quantitative assessment of the trabecular and cortical bone architecture to determine the effect of zoledronic acid induced inhibition of bone resorption. There was a significant increase in both cortical and trabecular bone volume of the tibia in the zoledronic acid treated groups. It is interesting to note that the histomorphometric and the bone serum marker data showed a decrease in osteoblasts number and activity with the zoledronic acid treatment. However, there was a continuing increase in the bone volumes in the treated groups as observed in the μCT analysis. It could be argued that the reduction in osteoclasts by zoledronic acid treatment has led to reduced bone resorption and henceforth the normally lost bone normally lost during physiological bone remodelling has halted and led to an increase in the bone volumes. Additionally μCT showed an evidence of increase in trabecular number, but no difference was observed in the trabecular thickness between the treated and control groups which further supports the fact that the usually resorbed thinner trabeculae (usually seen at the diaphysis) are not resorbed with zoledronic acid treatment and accounts for the increased trabecular number. SMI data showed an inverse co-relation between the treated and control groups with increasing age. The trabecular bone in the control group was becoming increasingly rod-like, wherein the treated groups it was becoming increasing plate-like. Here the SMI values in the treated groups showed a declining trend with increase in age. This is intriguing as if the bone resorption is interrupted by zoledronic acid, the SMI values should remain constant unless accompanied by substantial bone formation which shifts the trabecular architecture to even more plate-like (continuously reducing SMI values). Conversely, our data showed a reduction in the osteoblastic activity as well. It is still not clear as what contributes to the increasing plate-like structure formation especially with the reduction in osteoblasts number and activity.

Taken together, this initial study on naive C57BL/KaLwRij has showed that zoledronic acid effectively suppresses osteoclastic bone resorption after 7 days following a single twice weekly regimen. Although the post treatment effect was seen even after 21 days (end-point of our study), the effect seems to be greatest after 7 days compared with 14 and 21 day time points. Therefore, this 7 day post treatment strategy was considered to effectively suppress osteoclastic bone resorption and was used in our study to investigate the effect of zoledronic acid on tumour cell homing and colonisation. However although osteoclastic bone resorption is suppressed so is osteoblastic bone formation. Therefore zoledronic acid treatment is effectively suppressing bone remodelling and the effect of this on tumour cell homing and colonisation was observed in a further study

As already discussed, several preclinical and clinical studies have shown that treatment with zoledronic acid postpones the development of bone metastasis in myeloma and other solid tumours and also prolongs the progression free survival and overall survival (Croucher *et al.* 2003; Mystakidou *et al.* 2005; Avilés *et al.* 2007; Guenther *et al.* 2010). Recently, there has been increasing recommendations for the early inclusion of zoledronic acid into the standard anti-cancer chemotherapy regimens for the treatment of multiple myeloma.

Although there are several paradigms to explain the anti-tumour effect, the underlying mechanism is not clearly understood. In this study zoledronic acid was used to suppress bone remodelling and what effect this has on the myeloma cell homing and colonisation of the bone. Vanderkerken *et al.* (2000) showed that 5T2MM cells home to BM as early as 18 hr post inoculation in C57BL/KalwRij mice. Furthermore, previous work done by our group has also demonstrated that 5T33MM cells are seen in the BM of long bones in C57BL/KaLwRij mice as early as 18 hr post inoculation (unpublished data). Therefore an 18 hr time point was chosen to study zoledronic acid effect on the homing of 5T33MM cells in the bone. In addition a 72 hr time point was chosen as after 48 hrs 5T2MM cells could not be detected in the BM (Vanderkerken *et al.* 2000). A 4 week time point was also chosen to confirm the presence of tumour in the bone (Manning *et al.* 1992). In our study mice were pre-treated with zoledronic acid (125µg/kg X2 /wk s.c.) and after 7 days tumour cells were injected via the tail vein

The effect of zoledronic acid treatment on the 5T33MM-GFP mice were confirmed by histomorphometric analysis (osteoclast and osteoblast numbers and surface occupancy per mm of bone), serum levels of bone markers (TRAP and PINP) and µCT analysis on comparison with the untreated tumour control mice As expected there was a significant reduction of all the above parameters in the tumour zoledronic acid treated group compared with untreated tumour control group. Further, the values in the untreated tumour group were similar to the naive mouse and tumour mice treated with zoledronic acid were similar to non-tumour zoledronic acid treated mouse at each time point. Although in this study there was only one naive and one naive + zoledronic acid mice at each timepoint and it is not possible to conclude without statistical evidence.

The effect of zoledronic acid treatment on tumour cell homing showed no significant difference in the number of tumour cells seen in the proximal tibial metaphysis after 18 hrs post tumour cell injection between the untreated tumour mice and zoledronic acid treated mice. However, there was almost a 30% reduction seen in the zoledronic acid treated mice group, but this did not reach statistical significance due to high intra group variation observed within both groups. One possible reason for this indifference in the number of tumour cells seen between the treated and untreated group is that we counted the number of GFP positive tumour cells seen in the tibial metaphysis irrespective of their location inside the bone. The protocol used for this study did not have the ability to distinguish whether the tumour cells were located inside the bone marrow space or in the bone marrow vasculature. So the number of 5T33MM-GFP cells counted includes both the cells that have homed to the BMM and also the cells binding the BMEC inside the BM blood vessels. Homing of myeloma cell to the BM is a multistep process which involves adhesion of the myeloma cell to the BMEC (Vacca *et al.* 2003; Vanderkerken *et al.* 2003). This initial study was an attempt to visualise the 5T33MM-GFP cell inside the BMM and design an algorithm to measure the number of 5T33MM-GFP cell in the BMM. In the future defining the BM vasculature could further refine our data to include only the 5T33MM-GFP cells that have homed to the bone marrow.

Further, in our study we used the *in vitro* 5T33MM-GFP cell line (5T33MMvt-GFP) for tumour cell injection which is independent of BMSC in culture for survival and proliferation (Refer section 2.1) (Caers *et al.* 2008). In contrast, the 5T2MM myeloma model cell which resembles the human disease condition, where the cells are stromal dependant for *in vitro* culture, and the growth is restricted to the bone and spleen (at sites of haematopoiesis). This is not the case with 5T33MMvt cells where in the latter stages of the disease cell growth is seen at extra osseous sites other than the spleen (Manning *et al.* 1992; Vanderkerken *et al.* 1997). Perhaps the bone marrow independency nature of the 5T33MMvt cell was responsible for not seeing an effect with zoledronic acid, as zoledronic acid treatment did not affect the 5T33MMvt cell growth and proliferation in the bone. Similar result was previously reported by Dallas and colleagues (1999) using an environment independent cell line 5TGM1 (variant of 5T33MM) bearing mice on treatment by ibandronate (Dallas *et al.* 1999).Vanderkerken *et al.* (2003) showed anti-tumour effect in *in vivo* models of 5T33MM using osteoclast inhibitor FcOPG. Here, they used 5T33MMvv cell line for tumour injection which is dependent on the local environment for survival. Therefore, the observed effect with no difference might possibly be due to the environment independent cell line used in our study. Future studies will address this question using environment dependent cell lines like 5T33MMvv or 5T2MM or tumour homing and survival is not dependent on bone remodelling.

Several preclinical animal studies have demonstrated zoledronic acid to have an anti-myeloma effect and cause a reduction in the tumour burden (Yaccoby *et al.* 2002; Croucher *et al.* 2003; Libouban *et al.* 2003). So far all these studies have looked into the late effects of zoledronic acid treatment on the myeloma tumour burden. Furthermore, the tumour burden in these studies was a measure of serum monoclonal paraprotein levels. These parameters are less reliable due to their long plasma half life and are potentially ambiguous in interpreting drug efficacy over short periods (Hobbs 1969; Oyajobi *et al.* 2007). However, using multiphoton microscopy the number of tumour cells can be measured with an absolute quantification of the extent and activity of the tumour burden. Moreover, it also offers the advantage of visualising individual tumour cells in their native microenvironment and measure its proximity to other cellular structures which they might possibly interact with (Lawson *et al.* 2009). One potential downside in our study was the cross talk between the SHG from the collagen in the bone (which is half the wavelength of the laser used for excitation - 450nm) and the auto-florescence from the GFP (wider wavelength interval between 560–490 nm) which overlaps with the SHG (Stroh *et al.* 2005). Moreover spectral changes observed in the emission pattern of GFP make it difficult to distinguish true GFP positive cell to auto-florescence. The close proximity of more than one GFP positive cell and the interference from the BMM might explain this altered emission pattern (De Angelis *et al.* 1998). As the analysis is made on the basis of the differences in the intensity of the emitted light from bone and GFP, the spectral overlapping and florescence cross talks gives false positive data (Thews *et al.* 2005). In order to overcome this drawback in future studies we have planned to use red fluorescent protein (RFP) tagged to tumour cell which avoids cross talk due to its narrow wavelength interval (700–635 nm) (Stroh *et al.* 2005).

4.2 Conclusion & Future direction

Firstly, we have shown that zoledronic acid treatment was effective in suppressing the osteoclast mediated bone resorption in the 5T33MM murine myeloma model and this effect was seen after 7 days following treatment. So this 7 day post treatment strategy was adopted to achieve effective suppression in bone resorption for future experiments. Moreover our data also suggests that zoledronic acid treatment was associated with an inhibition of bone formation, the mechanism for which is not clearly understood yet. Further we have also shown that it is possible to visualise and measure fluorescently labelled myeloma cells in the bone microenvironment using multiphoton microscopy. So far, we have established a protocol to visualise and count the number of 5T33MM-GFP cell in the bone using multiphoton microscopy and our data shows no significant difference in the number of tumour cell homing the bone after 18 hr post tumour cell injection.

Our future works will be aimed at completing the analysis for the 72 hr time point in the current study. We also aim to develop tools in multiphoton microscopy to distinguish between the tumour cells present in blood vessels and those extravasated to the bone microenvironment. Furthermore, in future animal experiments will be conducted using stromal dependent models such as 5T33MM*vv* or 5T2MM. Also, imaging studies will be undertaken using other osteoclast inhibitors like FcOPG to investigate their effect on tumour cell homing in bone and compare the effects with zoledronic acid.

The direct cytotoxic effects of BPs on myeloma cell will be addressed in independent experiments using multiphoton microscopy and fluorophore tagged BPs to see whether myeloma cell can take up BPs *in vivo*.

Reference

Abe, M., K. Hiura, J. Wilde, *et al.* (2004). "Osteoclasts enhance myeloma cell growth and survival via cell-cell contact: a vicious cycle between bone destruction and myeloma expansion." *Blood* **104**(8): 2484-2491.

Abe, M., S. Kido, M. Hiasa, *et al.* (2006). "BAFF and APRIL as osteoclast-derived survival factors for myeloma cells: a rationale for TACI-Fc treatment in patients with multiple myeloma." *Leukemia* **20**(7): 1313-1315.

Aiuti, A., I. J. Webb, C. Bleul, *et al.* (1997). "The chemokine SDF-1 is a chemoattractant for human CD34+ hematopoietic progenitor cells and provides a new mechanism to explain the mobilization of CD34+ progenitors to peripheral blood." *J Exp Med* **185**(1): 111-120.

Alsayed, Y., H. Ngo, J. Runnels, *et al.* (2007). "Mechanisms of regulation of CXCR4/SDF-1 (CXCL12)-dependent migration and homing in multiple myeloma." *Blood* **109**(7): 2708-2717.

Amin, D., S. Cornell, S. Gustafson, *et al.* (1992). "Bisphosphonates used for the treatment of bone disorders inhibit squalene synthase and cholesterol biosynthesis." *J. Lipid Res.* **33**(11): 1657-1663.

Aparicio, A., A. Gardner, Y. Tu, *et al.* (1998). "In vitro cytoreductive effects on multiple myeloma cells induced by bisphosphonates." *Leukemia* **12**(2): 220-229.

Asosingh, K., U. Gunthert, H. De Raeve, *et al.* (2001). "A unique pathway in the homing of murine multiple myeloma cells: CD44v10 mediates binding to bone marrow endothelium." *Cancer Res* **61**(7): 2862-2865.

Avet-Loiseau, H., T. Facon, B. Grosbois, *et al.* (2002). "Oncogenesis of multiple myeloma: 14q32 and 13q chromosomal abnormalities are not randomly distributed, but correlate with natural history, immunological features, and clinical presentation." *Blood* **99**(6): 2185-2191.

Avilés, A., M. Nambo, N. Neri, *et al.* (2007). "Antitumor effect of zoledronic acid in previously untreated patients with multiple myeloma." *Medical Oncology* **24**(2): 227-230.

Barille, S., C. Akhoundi, M. Collette, *et al.* (1997). "Metalloproteinases in multiple myeloma: production of matrix metalloproteinase-9 (MMP-9), activation of proMMP-2, and induction of MMP-1 by myeloma cells." *Blood* **90**(4): 1649-1655.

Barille, S., M. Collette, R. Bataille, *et al.* (1995). "Myeloma cells upregulate interleukin-6 secretion in osteoblastic cells through cell-to-cell contact but downregulate osteocalcin." *Blood* **86**(8): 3151-3159.

Bataille, R., D. Chappard, C. Marcelli, *et al.* (1991). "Recruitment of new osteoblasts and osteoclasts is the earliest critical event in the pathogenesis of human multiple myeloma." *J Clin Invest* **88**(1): 62-66.

Baulch-Brown, C., T. J. Molloy, S. L. Yeh, *et al.* (2007). "Inhibitors of the mevalonate pathway as potential therapeutic agents in multiple myeloma." *Leuk Res* **31**(3): 341-352.

Benford, H. L., N. W. A. McGowan, M. H. Helfrich, *et al.* (2001). "Visualization of bisphosphonate-induced caspase-3 activity in apoptotic osteoclasts in vitro." *Bone* **28**(5): 465-473.

Bergstrom, J. D., R. G. Bostedor, P. J. Masarachia, *et al.* (2000). "Alendronate is a specific, nanomolar inhibitor of farnesyl diphosphate synthase." *Arch Biochem Biophys* **373**(1): 231-241.

Brocke-Heidrich, K., A. K. Kretzschmar, G. Pfeifer, *et al.* (2004). "Interleukin-6-dependent gene expression profiles in multiple myeloma INA-6 cells reveal a Bcl-2 family-independent survival pathway closely associated with Stat3 activation." *Blood* **103**(1): 242-251.

Caers, J., E. Menu, H. De Raeve, *et al.* (2008). "Antitumour and antiangiogenic effects of Aplidin[reg] in the 5TMM syngeneic models of multiple myeloma." *Br J Cancer* **98**(12): 1966-1974.

Carmeliet, P., L. Moons, R. Lijnen, *et al.* (1997). "Urokinase-generated plasmin activates matrix metalloproteinases during aneurysm formation." *Nat Genet* **17**(4): 439-444.

Chatterjee, M., T. Stuhmer, P. Herrmann, *et al.* (2004). "Combined disruption of both the MEK/ERK and the IL-6R/STAT3 pathways is required to induce apoptosis of multiple myeloma cells in the presence of bone marrow stromal cells." *Blood* **104**(12): 3712-3721.

Chauhan, D., H. Uchiyama, Y. Akbarali, *et al.* (1996). "Multiple myeloma cell adhesion-induced interleukin-6 expression in bone marrow stromal cells involves activation of NF-kappa B." *Blood* **87**(3): 1104-1112.

Chen, T., J. Berenson, R. Vescio, *et al.* (2002). "Pharmacokinetics and pharmacodynamics of zoledronic acid in cancer patients with bone metastases." *J Clin Pharmacol* **42**(11): 1228-1236.

Chim, C. S., R. Pang, T. K. Fung, *et al.* (2007). "Epigenetic dysregulation of Wnt signaling pathway in multiple myeloma." *Leukemia* **21**(12): 2527-2536.

Choi, S. J., J. C. Cruz, F. Craig, *et al.* (2000). "Macrophage inflammatory protein 1-alpha is a potential osteoclast stimulatory factor in multiple myeloma." *Blood* **96**(2): 671-675.

Choi, S. J., Y. Oba, Y. Gazitt, *et al.* (2001). "Antisense inhibition of macrophage inflammatory protein 1-α blocks bone destruction in a model of myeloma bone disease." *The Journal of Clinical Investigation* **108**(12): 1833-1841.

Clezardin, P. (2005). "Anti-tumour activity of zoledronic acid." *Cancer Treat Rev* **31 Suppl 3**: 1-8.

Clezardin, P., F. H. Ebetino and P. G. J. Fournier (2005). "Bisphosphonates and Cancer-Induced Bone Disease: Beyond Their Antiresorptive Activity." *Cancer Res* **65**(12): 4971-4974.

Croucher, P., S. Jagdev and R. Coleman (2003). "The anti-tumor potential of zoledronic acid." *Breast* **12 Suppl 2**: S30-36.

Croucher, P. I., R. De Hendrik, M. J. Perry, *et al.* (2003). "Zoledronic acid treatment of 5T2MM-bearing mice inhibits the development of myeloma bone disease: evidence for decreased osteolysis, tumor burden and angiogenesis, and increased survival." *J Bone Miner Res* **18**(3): 482-492.

Croucher, P. I., H. De Raeve, M. J. Perry, *et al.* (2003). "Zoledronic Acid Treatment of 5T2MM-Bearing Mice Inhibits the Development of Myeloma Bone Disease: Evidence for Decreased Osteolysis, Tumor Burden and Angiogenesis, and Increased Survival." *Journal of Bone and Mineral Research* **18**(3): 482-492.

Croucher, P. I., C. M. Shipman, J. Lippitt, *et al.* (2001). "Osteoprotegerin inhibits the development of osteolytic bone disease in multiple myeloma." *Blood* **98**(13): 3534-3540.

Dabaja, B., F. L. Nasr, G. Y. Chahine, *et al.* (2004). "Estramustine, zoledronic acid and weekly docetaxel in metastatic androgen independent prostate cancer (MAIP)." *J Clin Oncol (Meeting Abstracts)* **22**(14_suppl): 4706-.

Dallas, S. L., I. R. Garrett, B. O. Oyajobi, *et al.* (1999). "Ibandronate Reduces Osteolytic Lesions but not Tumor Burden in a Murine Model of Myeloma Bone Disease." *Blood* **93**(5): 1697-1706.

Damaj, G., M. Mohty, N. Vey, *et al.* (2004). "Features of extramedullary and extraosseous multiple myeloma: a report of 19 patients from a single center." *European Journal Of Haematology* **73**(6): 402-406.

De Angelis, D. A., G. Miesenböck, B. V. Zemelman, *et al.* (1998). "PRIM: Proximity imaging of green fluorescent protein-tagged polypeptides." *Proceedings of the National Academy of Sciences of the United States of America* **95**(21): 12312-12316.

Deniset-Besseau, A., P. D. S. Peixoto, J. Duboisset, *et al.* (2010). Nonlinear optical response of the collagen triple helix and second harmonic microscopy of collagen liquid crystals, SPIE.

Derenne, S., M. Amiot, S. Barille, *et al.* (1999). "Zoledronate is a potent inhibitor of myeloma cell growth and secretion of IL-6 and MMP-1 by the tumoral environment." *J Bone Miner Res* **14**(12): 2048-2056.

Diel, I. J. (2000). "Antitumour effects of bisphosphonates: first evidence and possible mechanisms." *Drugs* **59**(3): 391-399.

Dittel, B., J. McCarthy, E. Wayner, *et al.* (1993). "Regulation of human B-cell precursor adhesion to bone marrow stromal cells by cytokines that exert opposing effects on the expression of vascular cell adhesion molecule-1 (VCAM-1)." *Blood* **81**(9): 2272-2282.

Drach, J., J. Angerler, J. Schuster, *et al.* (1995). "Interphase fluorescence in situ hybridization identifies chromosomal abnormalities in plasma cells from patients with monoclonal gammopathy of undetermined significance." *Blood* **86**(10): 3915-3921.

Duivenvoorden, W. C. M., S. Vukmirovic-Popovic, M. Kalina, *et al.* (2007). "Effect of zoledronic acid on the doxycycline-induced decrease in tumour burden in a bone metastasis model of human breast cancer." *Br J Cancer* **96**(10): 1526-1531.

Dunford, J. E., K. Thompson, F. P. Coxon, *et al.* (2001). "Structure-activity relationships for inhibition of farnesyl diphosphate synthase in vitro and inhibition of bone resorption in vivo by nitrogen-containing bisphosphonates." *J Pharmacol Exp Ther* **296**(2): 235-242.

Durie, B. G. M. (1988). "The biology of multiple myeloma." *Hematological Oncology* **6**(2): 77-81.

Erickson, L. D., L. L. Lin, B. Duan, *et al.* (2003). "A genetic lesion that arrests plasma cell homing to the bone marrow." *Proc Natl Acad Sci U S A* **100**(22): 12905-12910.

Ferlin, M., N. Noraz, C. Hertogh, *et al.* (2000). "Insulin-like growth factor induces the survival and proliferation of myeloma cells through an interleukin-6-independent transduction pathway." *British Journal of Haematology* **111**(2): 626-634.

Fooksman, D. R., T. A. Schwickert, G. D. Victora, *et al.* (2010). "Development and Migration of Plasma Cells in the Mouse Lymph Node." **33**(1): 118-127.

Franchimont, N., S. Rydziel and E. Canalis (2000). "Transforming growth factor-[beta] increases interleukin-6 transcripts in osteoblasts." *Bone* **26**(3): 249-253.

Fuller, K., C. Murphy, B. Kirstein, *et al.* (2002). "TNF{alpha} Potently Activates Osteoclasts, through a Direct Action Independent of and Strongly Synergistic with RANKL." *Endocrinology* **143**(3): 1108-1118.

Giovanni Iolascon, F. S., Alberto Ferrante, Raffaele Gimigliano, and Francesca Gimigliano (2010). "Risedronate's efficacy: from randomized clinical trials to real clinical practice." *Clin Cases Miner Bone Metab.* **7**(1): 19-22.

Giuliani, N., R. Bataille, C. Mancini, *et al.* (2001). "Myeloma cells induce imbalance in the osteoprotegerin/osteoprotegerin ligand system in the human bone marrow environment." *Blood* **98**(13): 3527-3533.

Giuliani, N., S. Colla, F. Morandi, *et al.* (2005). "Myeloma cells block RUNX2/CBFA1 activity in human bone marrow osteoblast progenitors and inhibit osteoblast formation and differentiation." *Blood* **106**(7): 2472-2483.

Giuliani, N., F. Morandi, S. Tagliaferri, *et al.* (2006). "Interleukin-3 (IL-3) is overexpressed by T lymphocytes in multiple myeloma patients." *Blood* **107**(2): 841-842.

Giuliani, N., V. Rizzoli and G. D. Roodman (2006). "Multiple myeloma bone disease: pathophysiology of osteoblast inhibition." *Blood* **108**(13): 3992-3996.

Glass Ii, D. A., P. Bialek, J. D. Ahn, *et al.* (2005). "Canonical Wnt Signaling in Differentiated Osteoblasts Controls Osteoclast Differentiation." *Developmental Cell* **8**(5): 751-764.

Gnant, M., B. Mlineritsch, H. Stoeger, *et al.* (2010). "Mature results from ABCSG-12: Adjuvant ovarian suppression combined with tamoxifen or anastrozole, alone or in combination with zoledronic acid, in premenopausal women with endocrine-responsive early breast cancer." *J Clin Oncol (Meeting Abstracts)* **28**(15_suppl): 533-.

Green, J. R. (2003). "Antitumor effects of bisphosphonates." *Cancer* **97**(S3): 840-847.

Green, J. R. (2005). "Zoledronic acid: pharmacologic profile of a potent bisphosphonate." *Journal of Organometallic Chemistry* **690**(10): 2439-2448.

Green, J. R. and P. Clezardin (2002). "Mechanisms of bisphosphonate effects on osteoclasts, tumor cell growth, and metastasis." *Am J Clin Oncol* **25**(6 Suppl 1): S3-9.

Guenther, A., S. Gordon, M. Tiemann, *et al.* (2010). "The bisphosphonate zoledronic acid has antimyeloma activity in vivo by inhibition of protein prenylation." *International Journal of Cancer* **126**(1): 239-246.

Guenther, A., S. Gordon, M. Tiemann, *et al.* (2010). "The bisphosphonate zoledronic acid has antimyeloma activity in vivo by inhibition of protein prenylation." *Int J Cancer* **126**(1): 239-246.

Gupta, D., S. P. Treon, Y. Shima, *et al.* (2001). "Adherence of multiple myeloma cells to bone marrow stromal cells upregulates vascular endothelial growth factor secretion: therapeutic applications." *Leukemia* **15**(12): 1950-1961.

Hallek, M., P. Leif Bergsagel and K. C. Anderson (1998). "Multiple Myeloma: Increasing Evidence for a Multistep Transformation Process." *Blood* **91**(1): 3-21.

Heider, U., I. Zavrski, C. Jakob, *et al.* (2004). "Expression of receptor activator of NF-?B ligand (RANKL) mRNA in human multiple myeloma cells." *Journal of Cancer Research and Clinical Oncology* **130**(8): 469-474.

Henriksen, K., M. Karsdal, J.-M. Delaissé, *et al.* (2003). "RANKL and Vascular Endothelial Growth Factor (VEGF) Induce Osteoclast Chemotaxis through an ERK1/2-dependent Mechanism." *Journal of Biological Chemistry* **278**(49): 48745-48753.

Hideshima, T., C. Mitsiades, G. Tonon, *et al.* (2007). "Understanding multiple myeloma pathogenesis in the bone marrow to identify new therapeutic targets." *Nat Rev Cancer* **7**(8): 585-598.

Hideshima, T., N. Nakamura, D. Chauhan, *et al.* (2001). "Biologic sequelae of interleukin-6 induced PI3-K/Akt signaling in multiple myeloma." *Oncogene* **20**(42): 5991-6000.

Hjertner, Ö., G. Qvigstad, H. Hjorth-Hansen, *et al.* (2000). "Expression of urokinase plasminogen activator and the urokinase plasminogen activator receptor in myeloma cells." *British Journal of Haematology* **109**(4): 815-822.

Hobbs, J. R. (1969). "Immunochemical Classes of Myelomatosis. INCLUDING DATA FROM A THERAPEUTIC TRIAL CONDUCTED BY A MEDICAL RESEARCH COUNCIL WORKING PARTY*." *British Journal of Haematology* **16**(6): 599-606.

Iguchi, T., Y. Miyakawa, K. Yamamoto, *et al.* (2003). "Nitrogen-containing bisphosphonates induce S-phase cell cycle arrest and apoptosis of myeloma cells by activating MAPK pathway and inhibiting mevalonate pathway." *Cell Signal* **15**(7): 719-727.

Kaisho, T., J. Ishikawa, K. Oritani, *et al.* (1994). "BST-1, a surface molecule of bone marrow stromal cell lines that facilitates pre-B-cell growth." *Proc Natl Acad Sci U S A* **91**(12): 5325-5329.

Kawabata, K., M. Ujikawa, T. Egawa, *et al.* (1999). "A cell-autonomous requirement for CXCR4 in long-term lymphoid and myeloid reconstitution." *Proc Natl Acad Sci U S A* **96**(10): 5663-5667.

Koenig, J., C. Ballantyne, A. Kumar, *et al.* (2002). "Vascular cell adhesion molecule-1 expression and hematopoietic supportive capacity of immortalized murine stromal cell lines derived from fetal liver and adult bone marrow." *In Vitro Cellular & Developmental Biology - Animal* **38**(9): 538-543.

Komori, T. (2010). Regulation of Osteoblast Differentiation by Runx2. Osteoimmunology. Y. Choi, Springer US. **658:** 43-49.

Kong, Y.-Y., H. Yoshida, I. Sarosi, *et al.* (1999). "OPGL is a key regulator of osteoclastogenesis, lymphocyte development and lymph-node organogenesis." *Nature* **397**(6717): 315-323.

Kubagawa, H., L. B. Vogler, J. D. Capra, *et al.* (1979). "Studies on the clonal origin of multiple myeloma. Use of individually specific (idiotype) antibodies to trace the oncogenic event to its earliest point of expression in B-cell differentiation." *The Journal of Experimental Medicine* **150**(4): 792-807.

Lacey, D. L., E. Timms, H. L. Tan, *et al.* (1998). "Osteoprotegerin Ligand Is a Cytokine that Regulates Osteoclast Differentiation and Activation." *Cell* **93**(2): 165-176.

Lawson, M. A., L. Coulton, F. H. Ebetino, *et al.* (2008). "Geranylgeranyl transferase type II inhibition prevents myeloma bone disease." *Biochemical and Biophysical Research Communications* **377**(2): 453-457.

Lawson, M. A., A. J. Williams, T. Bos, *et al.* (2009). "Localising individual myeloma cells to the myeloma [`]niche' in bone using multiphoton microscopy." *Bone* **44**(Supplement 1): S164-S164.

Lee, J. W., H. Y. Chung, L. A. Ehrlich, *et al.* (2004). "IL-3 expression by myeloma cells increases both osteoclast formation and growth of myeloma cells." *Blood* **103**(6): 2308-2315.

Libouban, H., M.-F. Moreau, M. F. Baslé, *et al.* (2003). "Increased bone remodeling due to ovariectomy dramatically increases tumoral growth in the 5T2 multiple myeloma mouse model." *Bone* **33**(3): 283-292.

Lijnen, H. R., B. Van Hoef, F. Lupu, *et al.* (1998). "Function of the Plasminogen/Plasmin and Matrix Metalloproteinase Systems After Vascular Injury in Mice With Targeted Inactivation of Fibrinolytic System Genes." *Arterioscler Thromb Vasc Biol* **18**(7): 1035-1045.

Luckman, S. P., D. E. Hughes, F. P. Coxon, *et al.* (1998). "Nitrogen-containing bisphosphonates inhibit the mevalonate pathway and prevent post-translational prenylation of GTP-binding proteins, including Ras." *J Bone Miner Res* **13**(4): 581-589.

Manning, L. S., J. D. Berger, H. L. O'Donoghue, *et al.* (1992). "A model of multiple myeloma: culture of 5T33 murine myeloma cells and evaluation of tumorigenicity in the C57BL/KaLwRij mouse." *Br J Cancer* **66**(6): 1088-1093.

Masarachia, P., M. Weinreb, R. Balena, *et al.* (1996). "Comparison of the distribution of 3H-alendronate and 3H-Etidronate in rat and mouse bones." *Bone* **19**(3): 281-290.

Menu, E., K. Asosingh, I. Van Riet, *et al.* (2004). "Myeloma cells (5TMM) and their interactions with the marrow microenvironment." *Blood Cells, Molecules, and Diseases* **33**(2): 111-119.

Mitsiades, C. S., D. W. McMillin, S. Klippel, *et al.* (2007). "The Role of the Bone Marrow Microenvironment in the Pathophysiology of Myeloma and Its Significance in the Development of More Effective Therapies." *Hematology/Oncology Clinics of North America* **21**(6): 1007-1034.

Mohammad, S., Y. Wei, D. WeiWei, *et al.* (2010). "Higher doses of bisphosphonates further improve bone mass, architecture, and strength but not the tissue material properties in aged rats." *Bone* **46**(5): 1267-1274.

Mohan, S. and D. J. Baylink (1991). "Bone growth factors." *Clin Orthop Relat Res*(263): 30-48.

Monkkonen, H., S. Auriola, P. Lehenkari, *et al.* (2006). "A new endogenous ATP analog (ApppI) inhibits the mitochondrial adenine nucleotide translocase (ANT) and is responsible for the apoptosis induced by nitrogen-containing bisphosphonates." *Br J Pharmacol* **147**(4): 437-445.

Mönkkönen, H., P. D. Ottewell, J. Kuokkanen, *et al.* (2007). "Zoledronic acid-induced IPP/ApppI production in vivo." *Life Sciences* **81**(13): 1066-1070.

Moreaux, J., E. Legouffe, E. Jourdan, *et al.* (2004). "BAFF and APRIL protect myeloma cells from apoptosis induced by interleukin 6 deprivation and dexamethasone." *Blood* **103**(8): 3148-3157.

Morgan, G., F. Davies, W. Gregory, *et al.* (2010). "Evaluating the effects of zoledronic acid (ZOL) on overall survival (OS) in patients (Pts) with multiple myeloma (MM): Results of the Medical Research Council (MRC) Myeloma IX study." *J Clin Oncol (Meeting Abstracts)* **28**(15_suppl): 8021-.

Mystakidou, K., E. Katsouda, E. Parpa, *et al.* (2005). "Randomized, open label, prospective study on the effect of zoledronic acid on the prevention of bone metastases in patients with recurrent solid tumors that did not present with bone metastases at baseline." *Medical Oncology* **22**(2): 195-201.

Noel, A., C. Gilles, K. Bajou, *et al.* (1997). "Emerging roles for proteinases in cancer." *Invasion Metastasis* **17**(5): 221-239.

Ogata, A., D. Chauhan, G. Teoh, *et al.* (1997). "IL-6 triggers cell growth via the Ras-dependent mitogen-activated protein kinase cascade." *J Immunol* **159**(5): 2212-2221.

Oshima, T., M. Abe, J. Asano, *et al.* (2005). "Myeloma cells suppress bone formation by secreting a soluble Wnt inhibitor, sFRP-2." *Blood* **106**(9): 3160-3165.

Oyajobi, B. O., S. Muñoz, R. Kakonen, *et al.* (2007). "Detection of myeloma in skeleton of mice by whole-body optical fluorescence imaging." *Molecular Cancer Therapeutics* **6**(6): 1701-1708.

Papapoulos, S. E. (2006). "Bisphosphonate actions: Physical chemistry revisited." *Bone* **38**(5): 613-616.

Parmo-Cabañas, M., R. A. Bartolomé, N. Wright, *et al.* (2004). "Integrin [alpha]4[beta]1 involvement in stromal cell-derived factor-1[alpha]-promoted myeloma cell transendothelial migration and adhesion: role of cAMP and the actin cytoskeleton in adhesion." *Experimental Cell Research* **294**(2): 571-580.

Parmo-Cabañas, M., I. Molina-Ortiz, S. Matías-Román, *et al.* (2006). "Role of metalloproteinases MMP-9 and MT1-MMP in CXCL12-promoted myeloma cell invasion across basement membranes." *The Journal of Pathology* **208**(1): 108-118.

Pearse, R. N., E. M. Sordillo, S. Yaccoby, *et al.* (2001). "Multiple myeloma disrupts the TRANCE/ osteoprotegerin cytokine axis to trigger bone destruction and promote tumor progression." *Proceedings of the National Academy of Sciences of the United States of America* **98**(20): 11581-11586.

Pozzi, S., S. Vallet, S. Mukherjee, *et al.* (2009). "High-Dose Zoledronic Acid Impacts Bone Remodeling with Effects on Osteoblastic Lineage and Bone Mechanical Properties." *Clinical Cancer Research* **15**(18): 5829-5839.

Reszka, A. A. and G. A. Rodan (2003). "Mechanism of action of bisphosphonates." *Curr Osteoporos Rep* **1**(2): 45-52.

Ria, R., A. M. Roccaro, F. Merchionne, *et al.* (2003). "Vascular endothelial growth factor and its receptors in multiple myeloma." *Leukemia* **17**(10): 1961-1966.

Rogers, M. J., J. C. Frith, S. P. Luckman, *et al.* (1999). "Molecular mechanisms of action of bisphosphonates." *Bone* **24**(5, Supplement 1): 73S-79S.

Rogers, M. J., S. Gordon, H. L. Benford, *et al.* (2000). "Cellular and molecular mechanisms of action of bisphosphonates." *Cancer* **88**(S12): 2961-2978.

Russell, R. G., N. B. Watts, F. H. Ebetino, *et al.* (2008). "Mechanisms of action of bisphosphonates: similarities and differences and their potential influence on clinical efficacy." *Osteoporos Int* **19**(6): 733-759.

Saad, F. (2008). "New research findings on zoledronic acid: survival, pain, and anti-tumour effects." *Cancer Treat Rev* **34**(2): 183-192.

Sanz-Rodriguez, F., A. Hidalgo and J. Teixido (2001). "Chemokine stromal cell-derived factor-1{alpha} modulates VLA-4 integrin-mediated multiple myeloma cell adhesion to CS-1/fibronectin and VCAM-1." *Blood* **97**(2): 346-351.

Sato, M., W. Grasser, N. Endo, *et al.* (1991). "Bisphosphonate action. Alendronate localization in rat bone and effects on osteoclast ultrastructure." *J Clin Invest* **88**(6): 2095-2105.

Senaratne, S. G., J. L. Mansi and K. W. Colston (2002). "The bisphosphonate zoledronic acid impairs Ras membrane [correction of impairs membrane] localisation and induces cytochrome c release in breast cancer cells." *Br J Cancer* **86**(9): 1479-1486.

Shipman, C. M., P. I. Croucher, R. G. Russell, *et al.* (1998). "The bisphosphonate incadronate (YM175) causes apoptosis of human myeloma cells in vitro by inhibiting the mevalonate pathway." *Cancer Res* **58**(23): 5294-5297.

Shipman, C. M., M. J. Rogers, J. F. Apperley, *et al.* (1997). "Bisphosphonates induce apoptosis in human myeloma cell lines: a novel anti-tumour activity." *Br J Haematol* **98**(3): 665-672.

Smith, M. R. (2003). "Antitumor Activity of Bisphosphonates." *Clinical Cancer Research* **9**(15): 5433-5434.

Sordillo, E. M. and R. N. Pearse (2003). "RANK-Fc: a therapeutic antagonist for RANK-L in myeloma." *Cancer* **97**(3 Suppl): 802-812.

Spencer, G. J., J. C. Utting, S. L. Etheridge, *et al.* (2006). "Wnt signalling in osteoblasts regulates expression of the receptor activator of NF{kappa}B ligand and inhibits osteoclastogenesis in vitro." *J Cell Sci* **119**(7): 1283-1296.

Standal, T., C. Seidel, O. Hjertner, *et al.* (2002). "Osteoprotegerin is bound, internalized, and degraded by multiple myeloma cells." *Blood* **100**(8): 3002-3007.

Stauder, R., M. Van Driel, C. Schwarzler, *et al.* (1996). "Different CD44 splicing patterns define prognostic subgroups in multiple myeloma." *Blood* **88**(8): 3101-3108.

Stroh, M., J. P. Zimmer, D. G. Duda, *et al.* (2005). "Quantum dots spectrally distinguish multiple species within the tumor milieu in vivo." *Nat Med* **11**(6): 678-682.

Taube, T., M. N. Beneton, E. V. McCloskey, *et al.* (1992). "Abnormal bone remodelling in patients with myelomatosis and normal biochemical indices of bone resorption." *Eur J Haematol* **49**(4): 192-198.

Terpos, E., M. Politou, R. Szydlo, *et al.* (2003). "Serum levels of macrophage inflammatory protein-1 alpha (MIP-1α) correlate with the extent of bone disease and survival in patients with multiple myeloma." *British Journal of Haematology* **123**(1): 106-109.

Thews, E., M. Gerken, R. Eckert, *et al.* (2005). "Cross Talk Free Fluorescence Cross Correlation Spectroscopy in Live Cells." *Biophysical journal* **89**(3): 2069-2076.

Thomas, D. M., S. A. Johnson, N. A. Sims, *et al.* (2004). "Terminal osteoblast differentiation, mediated by runx2 and p27KIP1, is disrupted in osteosarcoma." *The Journal of Cell Biology* **167**(5): 925-934.

Thompson, K., M. J. Rogers, F. P. Coxon, *et al.* (2006). "Cytosolic Entry of Bisphosphonate Drugs Requires Acidification of Vesicles after Fluid-Phase Endocytosis." *Molecular Pharmacology* **69**(5): 1624-1632.

Tian, E., F. Zhan, R. Walker, *et al.* (2003). "The role of the Wnt-signaling antagonist DKK1 in the development of osteolytic lesions in multiple myeloma." *N Engl J Med* **349**(26): 2483-2494.

Trikha, M., R. Corringham, B. Klein, *et al.* (2003). "Targeted Anti-Interleukin-6 Monoclonal Antibody Therapy for Cancer." *Clinical Cancer Research* **9**(13): 4653-4665.

Uchiyama, H., B. A. Barut, D. Chauhan, *et al.* (1992). "Characterization of adhesion molecules on human myeloma cell lines." *Blood* **80**(9): 2306-2314.

Uchiyama, H., B. A. Barut, A. F. Mohrbacher, *et al.* (1993). "Adhesion of human myeloma-derived cell lines to bone marrow stromal cells stimulates interleukin-6 secretion." *Blood* **82**(12): 3712-3720.

Vacca, A., R. Ria, F. Semeraro, *et al.* (2003). "Endothelial cells in the bone marrow of patients with multiple myeloma." *Blood* **102**(9): 3340-3348.

Vacca, A., D. Ribatti, M. Presta, *et al.* (1999). "Bone Marrow Neovascularization, Plasma Cell Angiogenic Potential, and Matrix Metalloproteinase-2 Secretion Parallel Progression of Human Multiple Myeloma." *Blood* **93**(9): 3064-3073.

van Beek, E., E. Pieterman, L. Cohen, *et al.* (1999). "Farnesyl pyrophosphate synthase is the molecular target of nitrogen-containing bisphosphonates." *Biochem Biophys Res Commun* **264**(1): 108-111.

van Beek, E. R., C. W. G. M. Löwik, F. H. Ebetino, *et al.* (1998). "Binding and antiresorptive properties of heterocycle-containing bisphosphonate analogs: structure-activity relationships." *Bone* **23**(5): 437-442.

van de Donk, N. W. C. J., H. M. Lokhorst and A. C. Bloem (2005). "Growth factors and antiapoptotic signaling pathways in multiple myeloma." *Leukemia* **19**(12): 2177-2185.

Van Driel, M., U. Gunthert, A. C. Van Kessel, *et al.* (2002). CD44 variant isoforms are involved in plasma cell adhesion to bone marrow stromal cells. London, ROYAUME-UNI, Nature Publishing.

Van Riet, I., K. Vanderkerken, C. de Greef, *et al.* (1998). "Homing behaviour of the malignant cell clone in multiple myeloma." *Med Oncol* **15**(3): 154-164.

Van Valckenborgh, E., M. Bakkus, C. Munaut, *et al.* (2002). "Upregulation of matrix metalloproteinase-9 in murine 5T33 multiple myeloma cells by interaction with bone marrow endothelial cells." *Int J Cancer* **101**(6): 512-518.

Vande Broek, I., K. Asosingh, V. Allegaert, *et al.* (2004). "Bone marrow endothelial cells increase the invasiveness of human multiple myeloma cells through upregulation of MMP-9: evidence for a role of hepatocyte growth factor." *Leukemia* **18**(5): 976-982.

Vanderkerken, K., K. Asosingh, P. Croucher, *et al.* (2003). "Multiple myeloma biology: lessons from the 5TMM models." *Immunological Reviews* **194**(1): 196-206.

Vanderkerken, K., C. De Greef, K. Asosingh, *et al.* (2000). "Selective initial in vivo homing pattern of 5T2 multiple myeloma cells in the C57BL/KalwRij mouse." *Br J Cancer* **82**(4): 953-959.

Vanderkerken, K., E. De Leenheer, C. Shipman, *et al.* (2003). "Recombinant Osteoprotegerin Decreases Tumor Burden and Increases Survival in a Murine Model of Multiple Myeloma." *Cancer Research* **63**(2): 287-289.

Vanderkerken, K., E. De Leenheer, C. Shipman, *et al.* (2003). "Recombinant Osteoprotegerin Decreases Tumor Burden and Increases Survival in a Murine Model of Multiple Myeloma." *Cancer Res* **63**(2): 287-289.

Vanderkerken, K., H. De Raeve, E. Goes, *et al.* (1997). "Organ involvement and phenotypic adhesion profile of 5T2 and 5T33 myeloma cells in the C57BL/KaLwRij mouse." *Br J Cancer* **76**(4): 451-460.

Vanderkerken, K., I. Vande Broek, D. L. Eizirik, *et al.* (2002). "Monocyte chemoattractant protein-1 (MCP-1), secreted by bone marrow endothelial cells, induces chemoattraction of 5T multiple myeloma cells." *Clin Exp Metastasis* **19**(1): 87-90.

Vescio, R., J. Cao, C. Hong, *et al.* (1995). "Myeloma Ig heavy chain V region sequences reveal prior antigenic selection and marked somatic mutation but no intraclonal diversity." *J Immunol* **155**(5): 2487-2497.

Vordos, D., B. Paule, F. Vacherot, *et al.* (2004). "Docetaxel and zoledronic acid in patients with metastatic hormone-refractory prostate cancer." *BJU International* **94**(4): 524-527.

Wahlgren, J., P. Maisi, T. Sorsa, *et al.* (2001). "Expression and induction of collagenases (MMP-8 and -13) in plasma cells associated with bone-destructive lesions." *The Journal of Pathology* **194**(2): 217-224.

Willey, J. S., E. W. Livingston, M. E. Robbins, *et al.* (2010). "Risedronate prevents early radiation-induced osteoporosis in mice at multiple skeletal locations." *Bone* **46**(1): 101-111.

Wong, A. P., S. L. Cortez and W. H. Baricos (1992). "Role of plasmin and gelatinase in extracellular matrix degradation by cultured rat mesangial cells." *Am J Physiol* **263**(6 Pt 2): F1112-1118.

Yaccoby, S., R. N. Pearse, C. L. Johnson, *et al.* (2002). "Myeloma interacts with the bone marrow microenvironment to induce osteoclastogenesis and is dependent on osteoclast activity." *British Journal of Haematology* **116**(2): 278-290.

Yamaguchi, T., M. Yamauchi, T. Sugimoto, *et al.* (2002). "The extracellular calcium (Ca2+o)-sensing receptor is expressed in myeloma cells and modulates cell proliferation." *Biochemical and Biophysical Research Communications* **299**(4): 532-538.

Yang, Q., K. P. McHugh, S. Patntirapong, *et al.* (2008). "VEGF enhancement of osteoclast survival and bone resorption involves VEGF receptor-2 signaling and [beta]3-integrin." *Matrix Biology* **27**(7): 589-599.

Yoneda, T. and T. Hiraga (2005). "Crosstalk between cancer cells and bone microenvironment in bone metastasis." *Biochemical and Biophysical Research Communications* **328**(3): 679-687.

Zandecki, M., V. Obein, F. Bernardi, *et al.* (1995). "Monoclonal gammopathy of undetermined significance: chromosome changes are a common finding within bone marrow plasma cells." *Br J Haematol* **90**(3): 693-696.

Appendix

Appendix: 1

Flow cytometry Instrument setting for GFP (FACS Calibur Flow Cytometer)

Detector/Amps:

Parameters	Detectors	Voltage	AmpGain	Mode
P1	FSC	E-1	8.51	Lin
P2	SSC	471	1.00	Lin
P3	FL1	566	1.00	Log
P4	FL2	561	1.00	Lin
P5	FL3	650	1.00	Lin
P6	FL2-A		1.00	Lin
P7	FL4	716	1.00	Lin

Threshold:

Primary Paramter: FSC

Value 52

Secondary Parameter: None

Appendix: 2

Flow cytometry Instrument setting for CD11a and GFP (FACS Calibur Flow Cytometer)

Detector/Amps:

Parameters	Detectors	Voltage	AmpGain	Mode
P1	FSC	E-1	8.51	Lin
P2	SSC	427	1.00	Lin
P3	FL1	470	1.00	Log
P4	FL2	420	1.00	Log
P5	FL3	650	1.00	Lin
P6	FL2-A		1.00	Lin
P7	FL4	704	1.00	Log

Threshold:

Primary Paramter: FSC

Value 52

Secondary Parameter: None

Compensation	
FL1	4.0% FL2
FL2	14.0% FL1
FL2	0.0% FL2
FL3	0.0% FL3
FL3	0.0% FL3
FL4	0.0% FL4

Appendix: 3

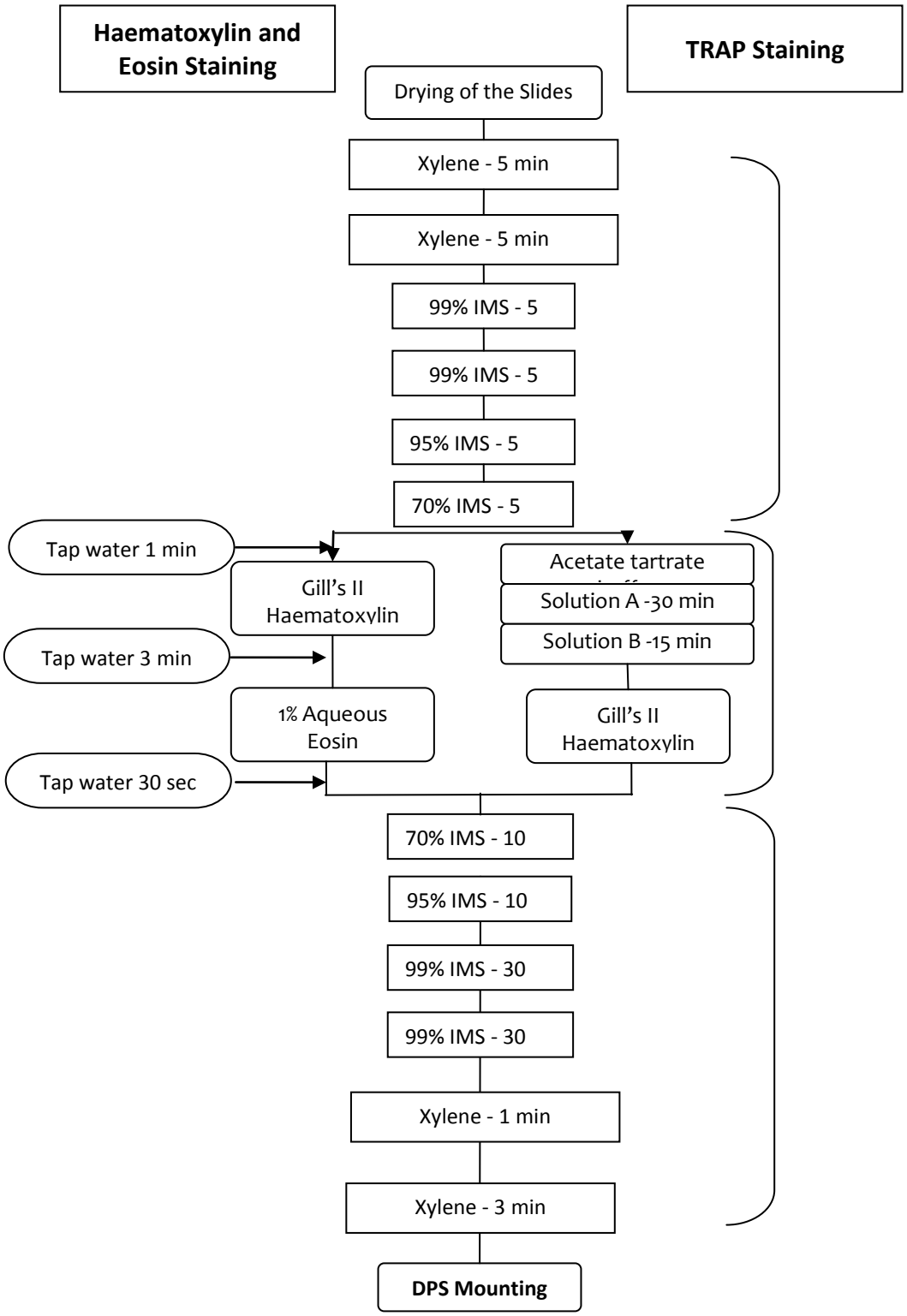

Adopted from Gurubalan J (2009) "NOD SCID mice as a model of Prostate Cancer Metastasis to the Bone" M.Sc., Thesis submitted to The University of Sheffield.